Shaped Casting of Aluminum Wrought Alloys by Controlled Diffusion Solidification (CDS) in a Tilt-Pour Gravity Casting process

Shaped Casting of Aluminum Wrought Alloys by Controlled Diffusion Solidification (CDS) in a Tilt-Pour Gravity Casting process

By
Gabriel Birsan

A Thesis
Submitted to the School of Graduate Studies
in Partial Fulfillment of the Requirements
for the Degree
Master of Applied Science

McMaster University

MASTER OF APPLIED SCIENCE (2009) McMaster University
(Mechanical Engineering) Hamilton, Ontario

TITLE: Controlled Diffusion Solidification for Tilt Pouring casting process

AUTHOR: Gabriel Birsan,
B.E- Mechanical Engineering (Dunarea de Jos University,Galati, Romania)

SUPERVISOR: Dr. Sumanth Shankar
Department of Mechanical Engineering

NUMBER OF PAGES: xiii , 80

ABSTRACT

Increased efforts have been undertaken to develop advanced casting (near-net shaped) processes and materials to attain high-integrity cast components with improved mechanical properties and performances. Semi-Solid Metal (SSM) process is one such process route where in typical binary eutectic alloys with suitable alloying additions could be cast from a two phase (solid and liquid) state into a near net shaped component. The SSM technology has been feverishly developed globally via two fundamental processing routes, namely, thixocasting and rheocasting. The use of the former process has been diminishing in recent years due to economic disadvantages inherent to the process and the development of rheocasting route has been dominant. In this process the new SSM processing route in Controlled Diffusion Solidification (CDS) has been validated by carrying out shaped casting in a tilt-pour casting process. Additionally, the project has shown for the first time that it is viable to shape cast Al wrought alloys which have been traditionally impossible to do so. In CDS technology two pre-cursor alloys with specific chemical composition and melt temperatures are mixed in a controlled manner and subsequently cast into a shaped component. The process yields components with a non-dendritic morphology of the primary phase during solidification in the resultant microstructure. Further, CDS circumvents the problems of hot tearing during casting which has been the primary deterrent in casting Al wrought alloys into shaped castings. The project has shown that CDS technology can be used for commercial casting of sound components with Al wrought alloys by using three alloys, namely, 2024, 6082, 7075 Al alloys. The objectives of the project were achieved by designing, manufacturing and validating a tilt-pour casting equipment along with a standard metal mould to shape cast test bars for tensile and fatigue properties assessment. Alloy compositions, melt temperatures and several process conditions were optimized by laboratory experiments and industrial tilt-pour casting trials. The project was successful in establishing a viable method to shape cast Al wrought alloys, specifically the three example alloys considered and it has been shown that the shaped casting of these alloys were visually sound with good casting integrity, heat treatable and showed reasonable tensile properties. Further, a viable scrap recycling methodology for shape casting Al wrought alloys by CDS has been formulated and validated in this project with 2024 Al alloy.

ACKNOWLEDGEMENTS

I thank Dr. Sumanth Shankar for his help, guidance and financial support. We had various interesting discussions regarding the present project along the last two years that significantly contributed to removing all the technical road blocks and helped in shaping the path of achieving the goals of the present research activity related to CDS.

I thank National Science and Engineering Research Council (NSERC) for their financial support.

I extend my sincere thanks to the technicians, machinist and non-teaching staff in the department of mechanical engineering for their help and support. I thank Joe Verhaeghe, JP Talon, Mark MacKenzie, Jim McLaren and Ron Lodewyks for their intensive support in machining and welding various components for the tilt equipment during manufacturing and assembly. My thanks go to Rob Lemmon of the Department of Materials Science and Engineering for his patient assistant in evaluating the tensile properties of several cast samples.

I would also like to thank my colleagues at the Light Metal Casting Research Centre (LMCRC) for all their help and insightful discussions as well as providing a peaceful environment for study and growth. Special thanks go to my colleagues in the CDS research team Dr Peyman Ashtari and PhD Candidate Abbas Khalaf for their support in theoretical and experimental research.

I thank Mr. David Knowles (Operations Manager), Grant Panchyson (Customer Service), Jim Misener (Engineering) Dave Davies (Tooling Coordinator), Don Sheppard (D/C Process Control), Roy Simmons (Maintenance DC Supervisor), and all the maintenance employees at Orlick Industries Limited, Hamilton, ON, Canada for all the support in carrying out the industrial experiments.

I thank my family members for being patient throughout my research period and supporting me.

TABLE OF CONTENTS

LIST OF FIGURES

Chapter 1 Introduction and Motivation

1.1. Introduction

Aluminum (Al) is the second most widely used metal behind Iron with increasing usage each year in the form of various Al based alloys. A high strength to weight ratio of components cast by aluminum alloys had enabled a wide-spread and increasing usage of these materials in casting technology. Canada is one of the key global players in Al industry [1]. Al alloy based cast products are extensively used in aerospace, automotive, domestic and military applications. This has lead to an increasing industrial demand for cast components with these alloys. The recent road map for the Aluminum technology developed by the Canadian government has outlined the following as the focus for research in this field of study.

- Development of newer aluminum alloys with superior mechanical properties and performances.
- Novel casting processes to increase the efficiency, productivity and reduce waste.
- Develop novel semi-solid casting technologies to enhance properties and performance of the cast components.

To maintain a competitive edge in the global automotive Al industry, various Research and Development (R & D) projects were initiated by the Canadian government in line with the above-mentioned strategic objectives. This project is one such effort and is a collaborative work between Light Metal Casting Research Center (LMCRC) at the Department of Mechanical Engineering, McMaster University, ON, and Natural Sciences and Engineering Research Council (NSERC) of Canada to understand and develop a novel casting process using the Controlled Diffusion Solidification (CDS) technology [2,3] to produce high-integrity shaped cast components with improved properties and performances. Specifically, the project aims to use the CDS technology to enable shaped casting of Al based wrought alloys which would be a global novel concept.

CDS is an innovative casting technology [2,4] which enables casting shaped components from certain Al based wrought and casting alloys [5] with a microstructure akin to those obtained in Semi-solid casting processes [6] wherein the primary Al phase has a non-dendritic morphology. Although, Al wrought alloys are envisioned to have superior properties in cast components [7, 8] than the casting alloys, the shaped casting of these alloys has always eluded researchers due the severity of hot-tearing tendencies in the cast components [9]. Due to the low levels of alloying elements in the wrought alloys, the dendrite arm spacing is much larger and the dendritic network is more complicated in cast components than in those obtained from Al casting alloys [10]. Due to the complexities involved in feeding the mushy zone during solidification of Al wrought alloys, weak non-filled regions in the castings develop into large

tears and cracks which render the cast component useless [4, 11]. A non-dendritic morphology of the primary solidifying phase in a cast component can circumvent the hot-tearing tendencies and render a sound shaped casting. CDS technology presents such a solution to enable sound shaped casting of Al based wrought and cast alloys with a non-dendritic morphology of the primary solidifying phase.

This work aims to develop a viable process route to cast three commercially popular aluminum wrought alloys, namely the 2024, 6082 and 7075 alloys, using the CDS technology and the tilt-pour casting process. The critical process variables were identified and optimized. A laboratory based tilt-pour casting apparatus was designed, developed and validated along with a suitable standard mould to cast tensile and fatigue test bars for property assessments.

In subsequent sections of this chapter, an introduction to conventional casting processes, semi-solid casting technology and processes, and CDS technology are presented and discussed. Further a hypothesis [4] for the mechanism of the CDS technology is also highlighted along with the critical process variables to enable a successful CDS process [4].

1.2 Conventional Shaped Casting process

Conventional shaped casting is a manufacturing process wherein using molten metal is introduced into a mould cavity (negative of the final desired shape) and then allowed to solidify by releasing heat from the molten alloy to the atmosphere via the mould walls [12]. Typically sand and ferrous alloys are used as mould materials. The various shaped casting processes [13] can be classified as shown in Figure 1-1,**Error! Reference source not found.** by the mould type, use of pressure to fill the mould and microstructure of the final product. Figure 1-1 also illustrates the competitive edge of each casting processes in the industry as of the year 2006.

In a typical sand casting process, a combination of sand with specialized high heat resistant additives or thermosetting resins is used to create the mould cavity. After the part is produced the mould is broken and the sand is mostly reused to create a new mould. This process achieves high integrity castings but at the expense of cycle time due to slow solidification time achieved with sand walls. Additional operations such as machining and surface modifications are necessary to achieve precision. In permanent mould casting processes, the cavity is produced from steel or cast iron to allow a high rate of heat transfer from the molten aluminum to the atmosphere providing faster castings cycles compared to sand castings. Tighter tolerances and a good surface finish are achieved in this process and hence, reduced post treatment is necessary for precision. There is a combination of the two casting processes (sand and permanent mould) and this is called the semi-permanent mould process. In this process, the exterior shell of the casting is made in a steel mould and the interior of the casting is made from sand cores that are later broken and the sand is reused. With this method

undercuts and complicated internal shapes are achieved. The draw back for this process is that high pressure on the molten metal cannot be applied since the sand cores cannot sustain it and the cycle times are relatively slow.

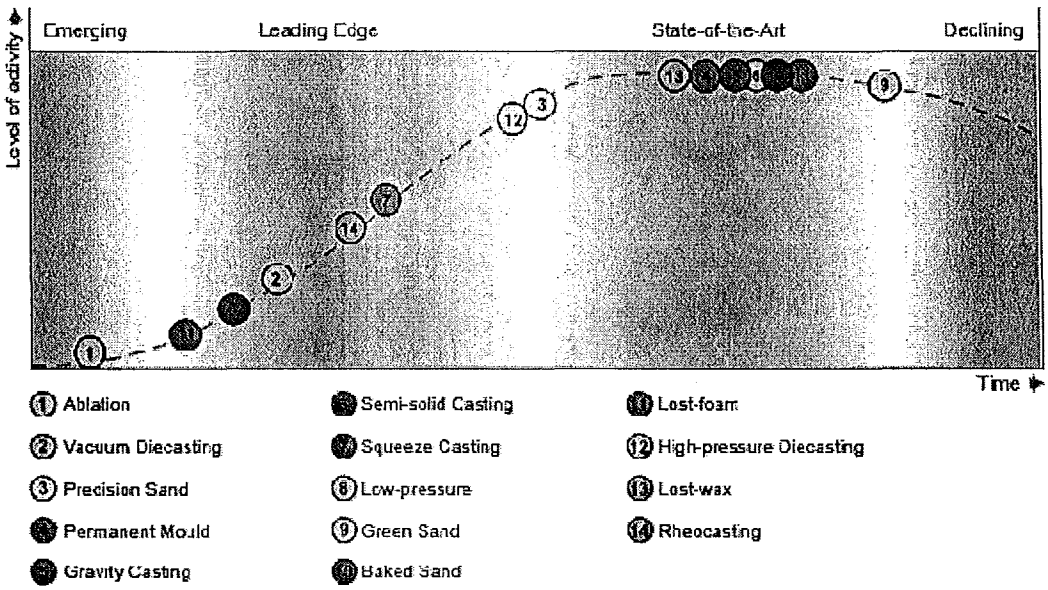

Figure 1-1: Life Cycle of Technology in the Shaped Casting Industry [1].

Figure 1-2 shows the classification of various metal mould casting processes based on the velocity and pressure induced on molten metal filling the mould [14]. In Figure 1-2 the quality of casting is high at low velocities and decreases at higher values. Pressure is used in casting processes depending on the type and mould, casting equipment and desired final microstructure in the component.

In terms of feeding methods; there also two main casting processes:

- Low Pressure (Gravity Casting, Tilt Casting, Low Pressure Die Casting), and
- High Pressure (High pressure Die Casting and Squeeze Castings).

Gravity pouring can be performed on sand moulds or metal moulds. The mould is stationary and the molten metal is introduced from the top of the mould through a "sprue" (conical funnel). Feeding method and risers are critical for this process in order to maintain a laminar flow of molten metal by avoiding turbulence in the runners and achieve directional solidification. Tilt-pour casting process was developed to eliminate the issues of turbulence in the cavity, by rotating the moulds 90 degree after molten metal is poured into a cup attached to the mould. Molten metal is always in contact with the steel walls in the feeding channel and velocity in the runner is controlled by the rotation speed of the mould. In Low Pressure die casting, the molten metal is fed into a cavity from the bottom of a steel mould by applying a low pressure (typical 0.8-1.0 psi) on top of the melt in the furnace placed directly below the steel mould, forcing the molten metal to rise through a feeding channel (runner system) into

the mould. This process is popular in the wheel manufacturing foundries since quality of the castings produced by this method meets the stringent requirements set for safety. Disadvantage in this case is a relatively low cycle time.

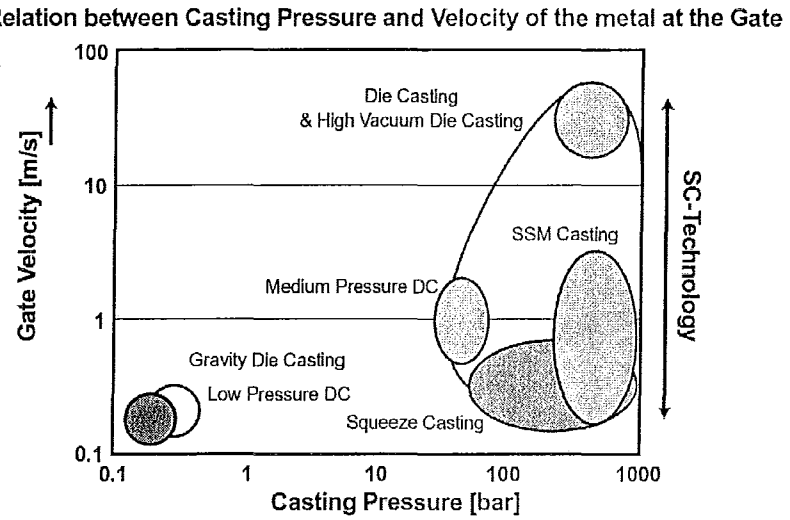

Figure 1-2. Classification of metal mould casting processes based on inlet gate velocities and casting pressures [14]

The High Pressure Die Casting (HPDC) is the most popular manufacturing process since it offers a significant cost advantage over all the other casting processes due to a very short cycle time (typical shot rates of about 50 to 200 shots/hour based on the casting weight) required to produce a viable casting. Disadvantage of the HPDC process are the high porosity in the cast component caused by high levels of air entrapment coupled with high solidification rates. This lack of casting integrity does not let these components to be heat treated to enable further property improvements. To improve the integrity of the HPDC, new processes were developed called High Integrity High Pressure (HIHP) processes and vacuum assisted HPDC. According to North American Die Cast Association (NADCA) [14], two of the main route of the HIHP process was developed: Squeeze Casting process and Semi-Solid Material process (SSM). HIHP castings typically have superior mechanical performance because of the combination of fine-scale microstructures and lack of micro-porosity [14]

In squeeze casting, the molten metal is introduced into the cavity with slow gate velocities (typical 3-8 inch/sec) at very high pressures (typical around 1,000bar or 14,500psi). The high pressure combined with a fast solidification rate results in a high integrity cast component caused by better feeding of the inter-dendritic spaces during solidification. Squeeze cast component, typically have improved mechanical properties [14].

Another development in the HIHP process is the Semi-Solid Metal (SSM) processing [15]. There are many manufacturing routes to attain a SSM casting by either Low Pressure or High Pressure

casting technologies. CDS is one such technological route to shape cast SSM components of Al alloys. The subsequent section presents a detailed overview of the SSM casting technologies.

1.3 Semi-Solid Metal (SSM) Casting Technology

In 1971, Spencer et al [16] found that it was possible to obtain a non-dendritic morphology of the primary phase during solidification for a binary alloy by applying a shear stress to the alloy during solidification in the semi-solid state. This phenomenon was named "Thixotropy". This discovery was the fundamental work for the SSM processes and alloys. Semi-solid Metal or Semi-solid Metallurgy (SSM) according to NADCA [14] is "a casting process employing relatively slow ingate flow velocities, minimum flow turbulence and high pressure applied throughout solidification to consistently produce high integrity castings capable of solution heat treatment without blistering". Typically, Al casting alloys solidify from the liquid phase to the solid phase through a range of temperatures wherein the two phases co-exist called the semi-solid region. When the input alloy into the casting mould is in the semi-solid region, the process is termed SSM casting. There are two main types of SSM processes, namely, Rheocasting and Thixocasting. The schematic shown in Figure 1-3 shows the salient differences between the SSM casting processes (Figure 1-3 (a) and (b)) and the conventional casting processes (Figure 1-3 (c)).

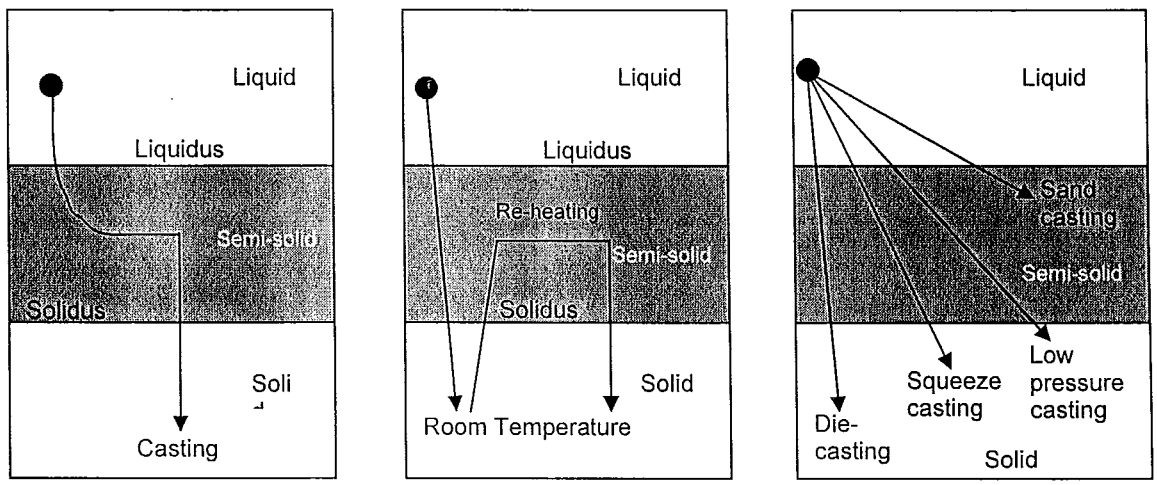

Figure 1-3. Comparison among rheocasting, thixoforming (thixocasting) and conventional casting processes showing the temperature variation at each stage of the processes. (a) Rheocasting, (b) Thixocasting and (c) Conventional casting process.

The main characteristic of the SSM process is that the input alloy used in this process contains both the solid and liquid phases. SSM materials can be classified into two types, slurry and mush. A *Slurry* is when the solid fraction is less than 0.25 in the two phase mixture and a *Mush*

is when the solid fraction is more than 0.6 [9]. The primary phase morphology in a SSM castings is non-dendritic (globular or rosettes).

The specific advantages of the SSM process are low gas porosity, low pouring temperature, longer metal mould life and improved properties and performance of the cast part. Figure 1-4 shows a comparison between rheocasting and thixoforming routes [17]. In rheocasting, the liquid metal is cooled to a specific temperature in the semi-solid region (fraction solid less than 0.30) and subsequently held for a while for homogenization of thermal and solute fields in the mixture before casting into a shaped component by a pressure induced process. The fundamental mechanism underlying rheocasting is the copious nucleation event combined with forced convection in the mixture to evenly spread the nuclei during solidification to the prescribed semi-solid temperature regime to enable a non-dendritic microstructure [18]. Figure 1-5 shows typical micrographs of conventional cast and SSM (rheocasting) cast sample showing the dendritic and non-dendritic morphology of the primary phase in them, respectively.

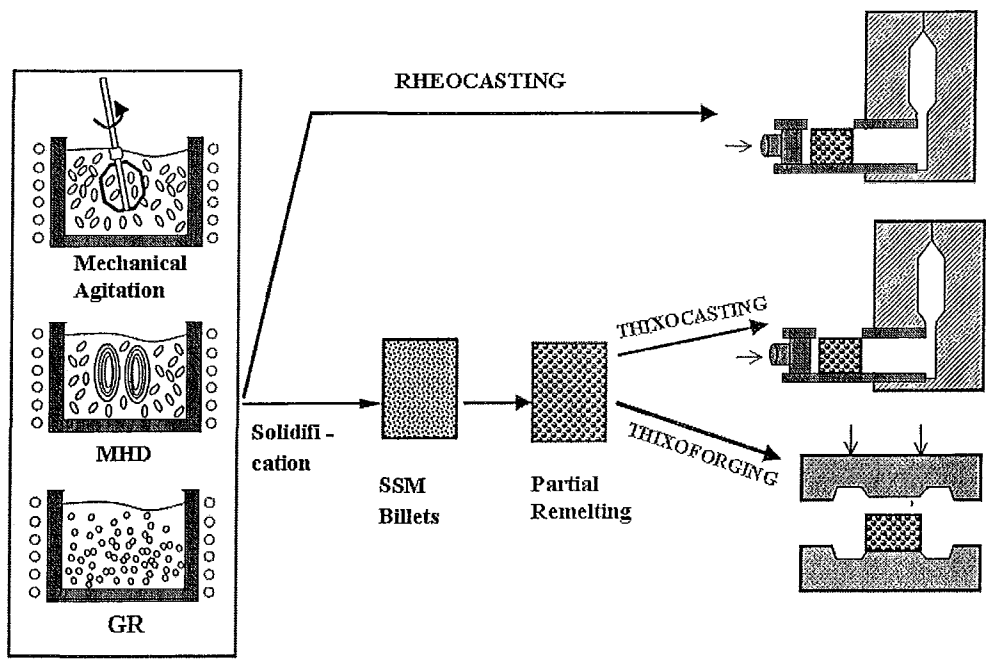

Figure 1-4. Semi-Solid Metal (SSM) processing routes showing both Rheocasting and Thixocasting/Thixoforming [17].

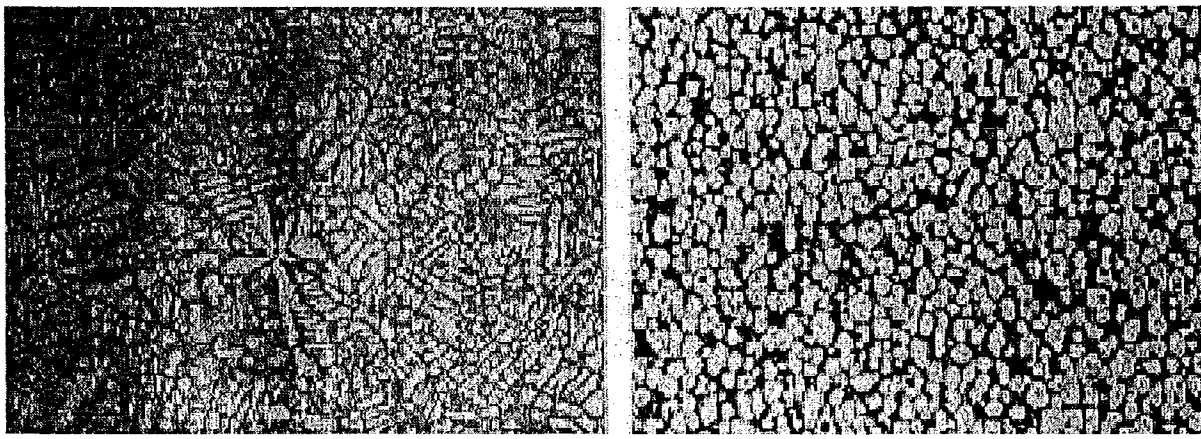

(a) (b)

Figure 1-5. Typical microstructures of (a) conventional cast alloy showing dendritic morphology of the primary phase and (b) SSM (rheocasting) cast alloy components showing a non-dendritic morphology of the primary phase

In thixocasting or thixoforming route (Figure 1-4), the liquid is solidified as billets with a small grain size of the primary phase caused by a grain refiner, applied strain fields or mechanical stirring of the melt by mechanical or electromagnetic forces during solidification. These billets are subsequently reheated to a suitable temperature in the semi-solid region and held for a period of time until the temperature and the microstructure are homogenized. The homogenized semi-solid billet is cast into shaped components using a pressure assisted process. The conventional process yields a dendritic morphology (Figure 1-5 (a)), whereas, SSM processes yield a non-dendritic morphology of the primary Al phase (Figure 1-5(b)).

An important difference between the microstructures of the rheocasting and thixocasting processes is the existence of entrapped inter-dendritic liquid inside the primary Al phase in the latter as shown in Figure 1-6 [19].

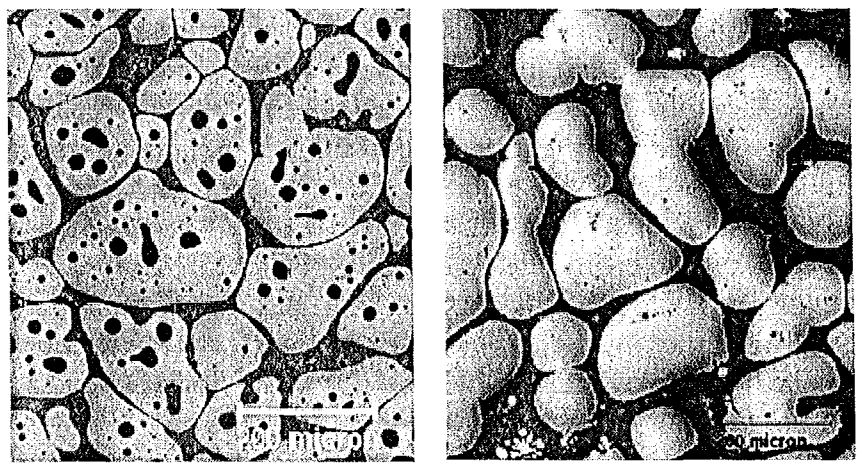

(a) (b)

Figure 1-6. Thixocasting and rheocasting microstructures showing non-dendritic morphology of the primary Al phase. (a) microstructure of a Thixocast component showing entrapped liquid inside the primary Al phase and (b) microstructure of a rheocast component with no entrapped liquid in the primary Al phase [19].

The entrapped liquid contributes to the deterioration of the cast property and performance of the thixocast components compared to those rheocast. Moreover, the thixocasting process involves a number of additional processing steps which make the process energy inefficient and expensive.

Figure 1-7 shows a schematic of the steps involves in thixocasting processing. The main disadvantage of the thixocasting process is the premium price casters have to pay for the special material (billets) and the scrap handle technique. Scrap from castings cannot be re-used in-house.

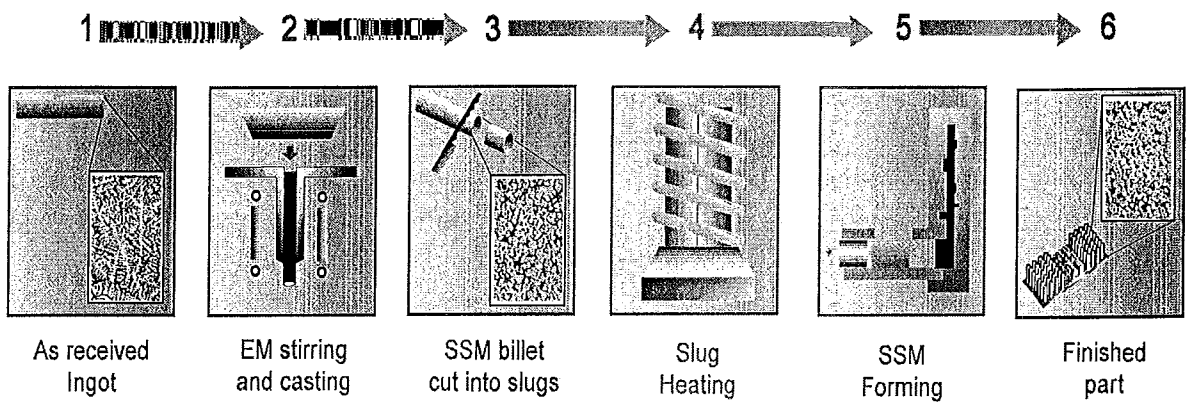

Figure 1-7. Thixocasting processing of billets obtained by Electromagnetic (EM) stirring.

Rheocasting alleviated the economic disadvantages of thixocasting by directly processing the liquid alloy melt into a semi-solid cast product with specialized capital equipment in addition to a casting machine. Recently, there have been various commercial processes developed for rheocasting Al alloys. The common feature in all of them is that during solidification, copious nucleation of primary phase is enabled by introducing inoculants or heat sinks inside the melt and simultaneously creating forced convection fields in the liquid generated by techniques such as Magneto Hydro Dynamics (MHD), mechanical stirring and/or stirring with electromagnetic forces. Few examples of commercial rheocasting processes are shown in Figure 1-8 to Figure 1-12. The holding period at the semi-solid stage to create a billet for casting in currently available commercial rheocasting processes can take several minutes (8 to 10 minutes) for the temperature and the microstructure to homogenize. The time and energy spent to perform this important step in addition to the high capital cost of the rheocasting equipment is proving to be economically prohibitive to most casting companies. Further, only the New Rheocasting Process (NRP) shown in Figure 1-8 has been commercially implemented. The other processes

are still in development various stages of development due to the complexities of various problems such as cast part quality, capital equipment, repeatability of process and optimization of cast part properties.

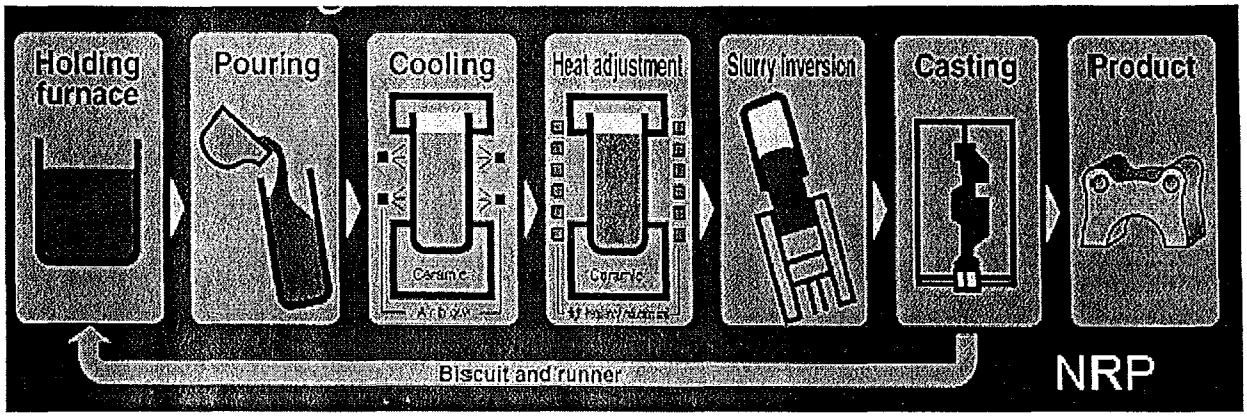

Figure 1-8. Rheocast processing route (or Slurry-on-Demand) showing the New Rheocasting Process (NRP) [6].

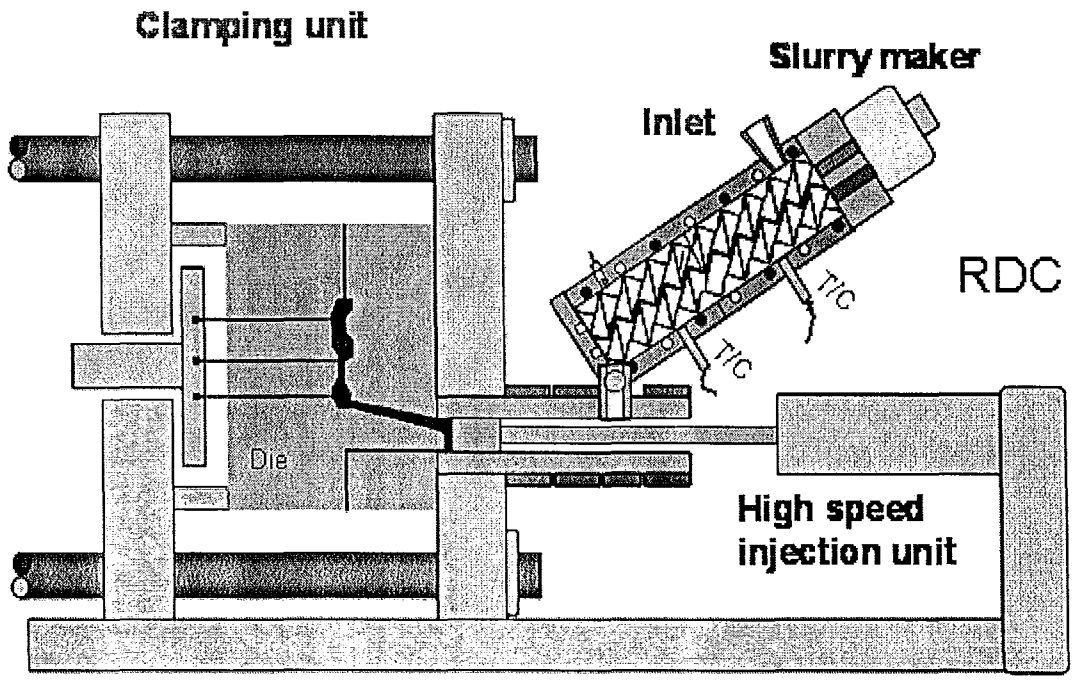

Figure 1-9. Rheo-Diecasting(RDC) Process [6].

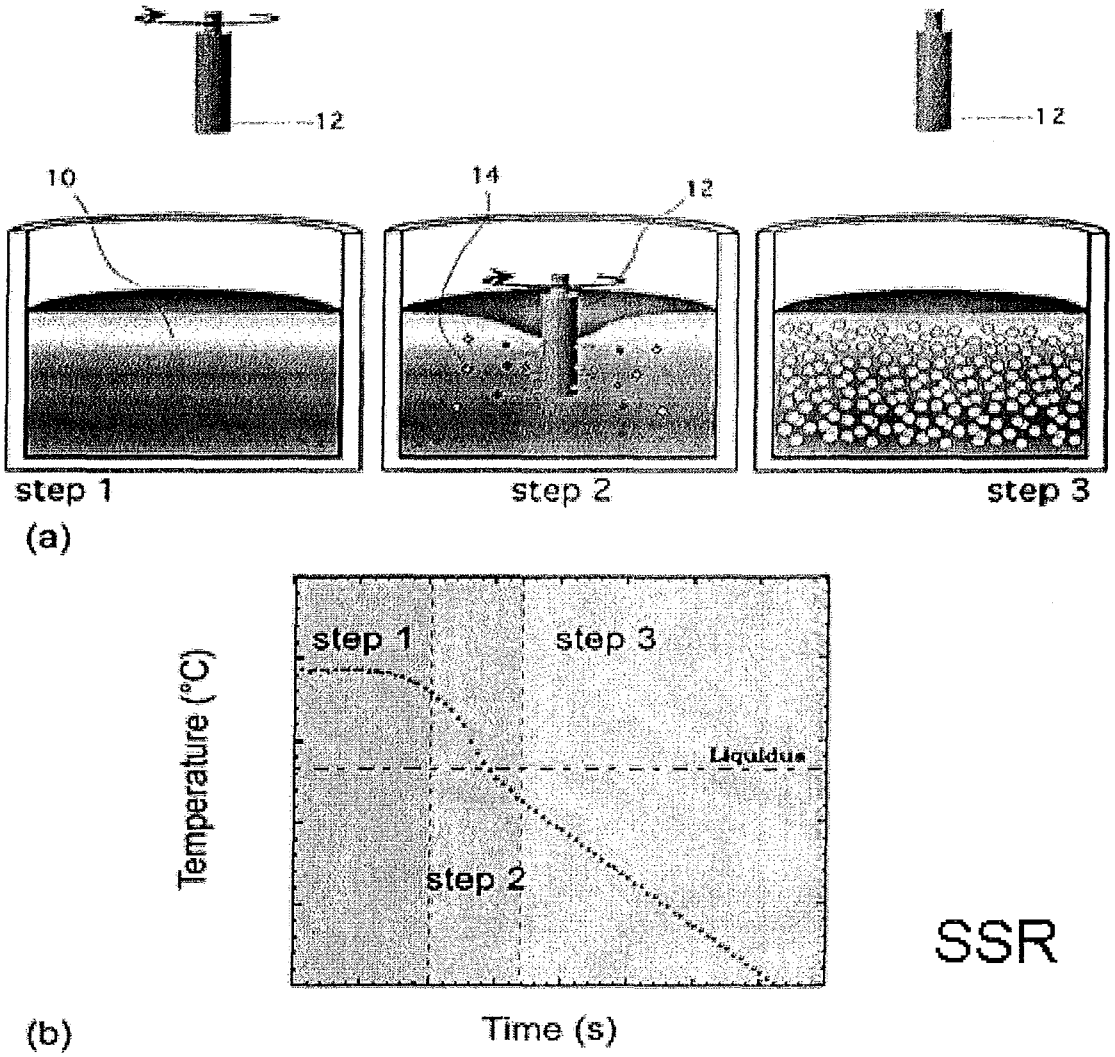

Figure 1-10. Semi Solid Rheocasting (SSR) [6].

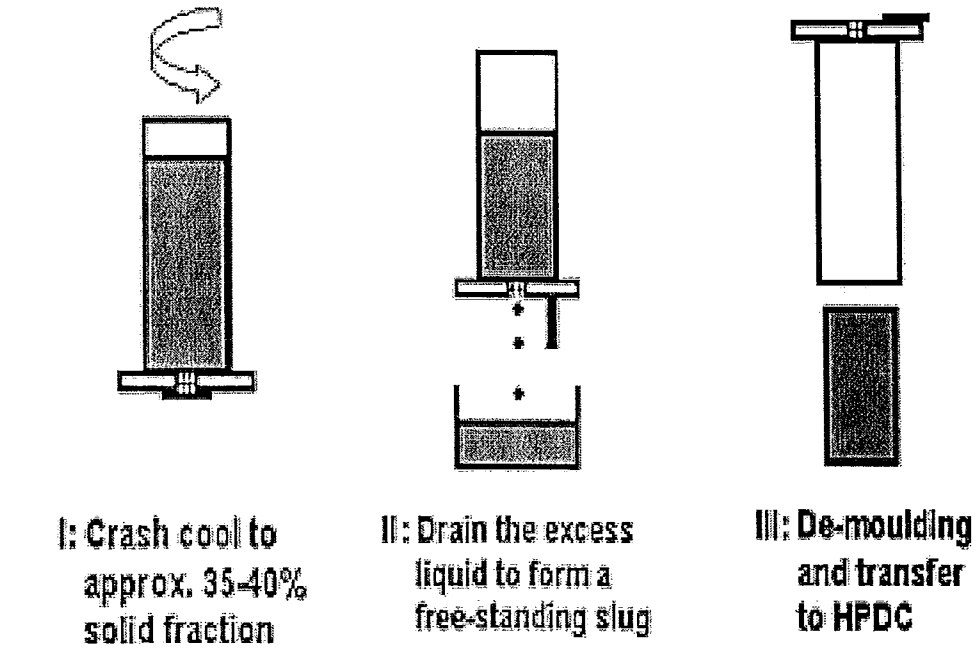

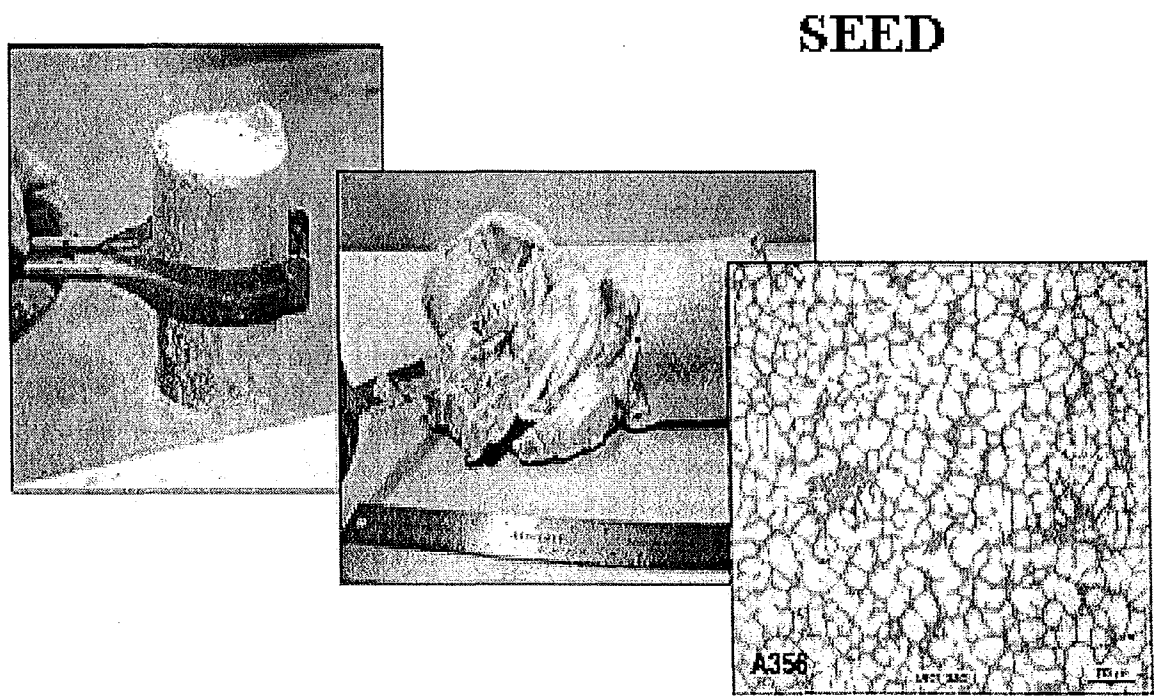

Figure 1-11. Swirled Enthalpy Equilibration Device (SEED). [6]

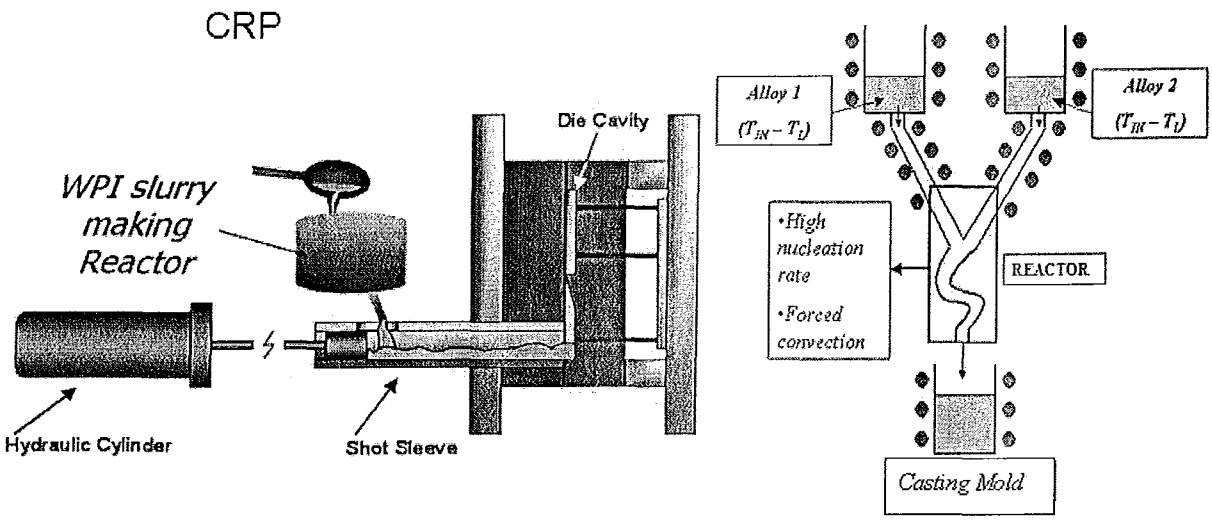

Figure 1-12. Continuous Rheocasting Process (CRP). [6]

The advantage of rheocasting process is that currently existing horizontal die cast machines can be easily modified to use along with the respective capital equipment for the individual processes. CDS technology circumvents the two main disadvantages of the existing rheocasting technologies: long homogenization time, high capital equipment cost and provides a fairly simple and easy to adopt casting process enabling SSM cast components [3,4,20].

1.4 Controlled Diffusion Solidification (CDS) – Motivation for this Project

CDS is an SSM processing route akin to the rheocasting technology wherein two pre-cursor alloys of specific temperature and compositions are mixed to form the final desired alloy composition at a specific temperature at or near the liquidus temperature of the desired alloy [3,4,20]. The alloy with the higher thermal mass (mass and temperature combined) is mixed into the alloy with a lower thermal mass to effect complete mixing of the alloys to form the desired alloy sample. The simplicity of the process lies in the near instantaneous mixing of the thermal fields to attain the desired homogeneity of temperature in the final desired alloy mixture. The alloy with the lower thermal mass acts as a heat sink to enable copious nucleation of the primary phase from the alloy with the higher thermal mass and the turbulent dissipation energy caused by the mixing causes an even spreading of the nuclei. Adaptation for the CDS technology into a viable commercial process would not be complicated and economically viable because the only capital cost associated is the addition of another holding furnace near the casting equipment. The CDS process has been repeatedly proved viable to carry out SSM casting [3,4,20,21]. The following are the main differences between CDS technology and conventional rheocasting technologies:

- The fraction solid prior in the slurry prior to casting is less than 5% in CDS as compared to less than 30% in conventional rheocasting processes [4,18].
- Both pressure and pressure-less metal injection can be adopted for CDS castings where as conventional rheocasting can only be pressure-assisted processes.
- CDS technology enables shaped casting of Al based wrought alloys which could only achieved by thixoforming techniques [7,8] and never achieved by any shaped casting process including rheocasting.

An example of the CDS process is shown in Figure 1-13 where the Al-Cu binary phase diagram is used as an example to cast Al-4.5wt%Cu alloy. The two pre-cursor alloys, in this case, are pure Al and Al-33wt% Cu eutectic alloy taken at around 5 °C superheat above the liquidus temperature, respectively. The pure Al with the higher thermal mass is poured into the eutectic alloy melt with the lower thermal mass and the resultant mixture is subsequently cast in a component. Figure 1-14 is a schematic of a typical thermal curve showing the various stages involved in CDS [4].

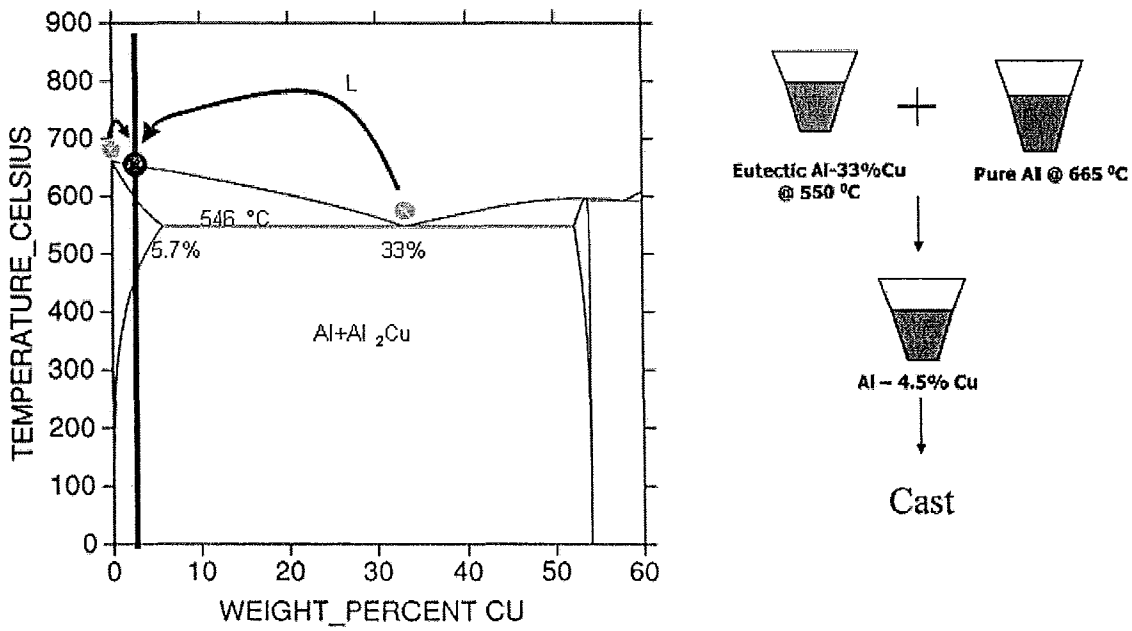

Figure 1-13. Schematic of typical CDS casting process [3]

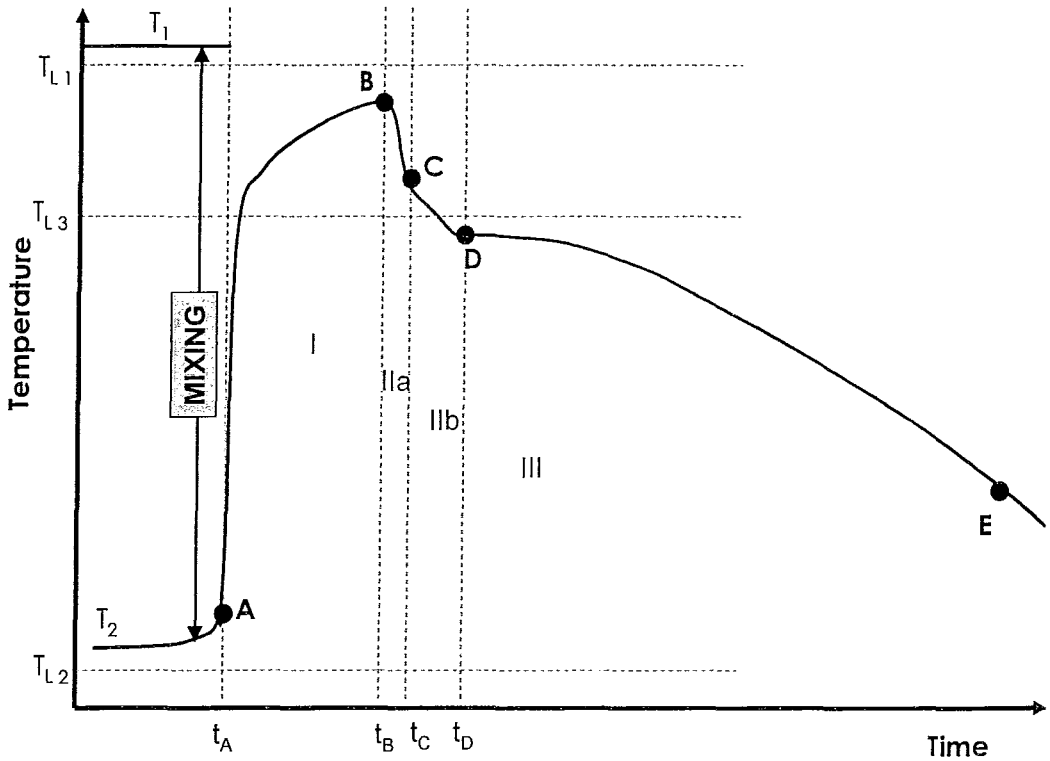

Figure 1-14. Schematic of thermal data for a successful CDS process [4].

The following are the brief details of the various stages involved in CDS process (Figure 1-14) starting from the mixing of two pre-cursor alloys as written by Khalaf et al [20].

Stage I → Segment AB

In this stage, the Alloy 1 is mixed into Alloy 2. The following are the events occurring in Stage I

1. The mechanical mixing starts at A and ends at point B.
2. Nucleation of primary Al phase begins from pre-cursor Alloy 1. Nucleation is higher at bottom of the crucible and decreases towards the top.
3. Heat added to the system until a maximum temperature of mixing is reached at B is as follows:-
    - Enthalpy of pre-cursor Alloy 1.
    - Enthalpy of Mixing pre-cursor Alloy 1 and Alloy 2.
    - Enthalpy of fusion from nucleation.
4. The temperature and solute fields in the mixture do not fully equalize between times t_A and t_B. Further, the temperature at the bottom of the crucible is highest and there is a temperature gradient from the bottom to the top of the crucible where the temperature is lowest.
5. At B, pockets of Alloy 1 and Alloy 2 exist.

Stage II → Segment BCD

1. Equalization of all temperature fields in the melt, especially the gradient from the bottom to the top of the mixture as described in event 4 of Stage I. The temperature equalization takes place in the segment BC and denoted as Stage IIa in Figure 1.
2. Simultaneous heat loss from the mixture due to ambient conditions.
3. Growth of the nuclei of primary Al phase from Alloy 1 formed in Stage 1. Figure 1-15(a) shows the compositional and temperature fields ahead of a growing nucleus at the end of stage I at point B. Figure 1-15(b) is the compositional and temperature fields observed ahead of a growing nucleus in a conventional casting process. In Figure 1-15, the notation C denotes average solute concentration, the notation T denotes temperature, the subscripts 1 and 2 are for the two pre-cursor alloys, respectively, the subscript 3 is for the final desired alloy, the subscript L denotes liquidus temperature and the subscript o denotes average bulk solute concentration in conventional casting process.

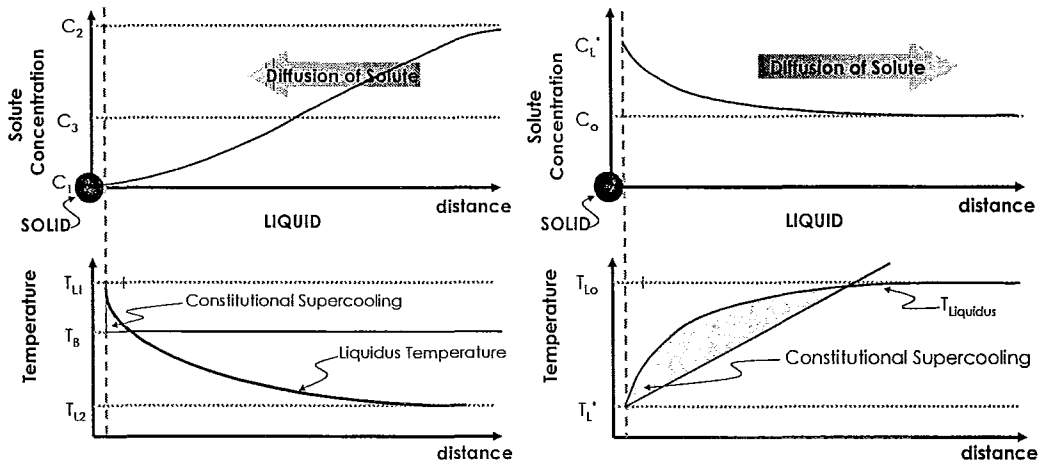

Figure 1-15. Solidification conditions in the liquid ahead of the growing primary Al phase in CDS and conventional casting process at the beginning of solidification. The solute concentration and temperature profiles are presented for (a) CDS and (b) conventional casting. The constitutional supercooling for CDS is negligible compared to conventional casting process. The critical difference lies in the direction of solute diffusion at the beginning of solidification [20].

Khalaf et al [20] formulated a set of mathematical inequalities as presented in Equations 1 to 3 which define the morphology of the primary phase during solidification by CDS technology.

$$\frac{d(T_L)_\xi}{dt} \leq \frac{d(T)_\xi}{dt} \qquad \text{Globular Morphology of Primary Phase} \qquad (1)$$

$$\frac{d(T_L)_\xi}{dt} \overset{\text{(Marginally)}}{>} \frac{d(T)_\xi}{dt} \qquad \text{Rossete Morphology of Primary Phase} \qquad (2)$$

$$\frac{d(T_L)_\xi}{dt} >> \frac{d(T)_\xi}{dt}$$ **Dendritic Morphology of Primary Phase** **(3)**

Stage III → Segment DE

At point D, there are innumerable nuclei and non-dendritic solid phase distributed evenly in the liquid (if Equations (1) and (2) are in effect), a nearly constant solute field and a low to negligible temperature gradient in the liquid ahead of the S/L interface. This scenario is similar to that found in conventional rheocasting process and will yield a non-dendritic primary phase morphology in the cast microstructure [18,22].

The significant advantages of the CDS technology have been motivating factor to carry out this project and write this M.A.Sc. thesis. This thesis aims at initiating the development of a viable commercial process to shape cast Al wrought alloys using the CDS technology. The specific objectives of the project have been elaborated in the next chapter of this thesis.

Chapter 2 Objectives and project plan

This section of the thesis presents the research objectives of this project and the plan adopted to obtain the deliverables fulfilling the objectives.

2.1 Objectives

The research objectives for this project are listed below in chronological order:

1. Design and manufacture a new Tilt-Pour Casting Equipment for laboratory scale operations.
2. Design, manufacture and validate a new metal mould in to enable casting of test bars (ASTM B557) to assess mechanical properties of castings manufactures in a tilt-pour setup.
3. Develop and validate a methodology to enable casting of aluminum wrought alloys by CDS process.
4. Optimize casting process parameters for shaped casting aluminum wrought alloys: 2024, 6082 and 7075 by CDS process via laboratory and industrial experiments.
    - Pre-cursor alloy compositions.
    - Pre-cursor alloy temperatures.
    - Pre-heat temperatures of mould and pouring cup in the tilt-pour equipment.
    - Tilt-pour process (tilt velocity and filling time).
5. Evaluation of soundness of castings, cast microstructure, material properties and fractography of broken tensile test bars under as-cast and heat treated conditions.
6. Design and optimize a scrap handling technique for shape casting with CDS technology.

2.2 Project Plan

The project was carried out in three phases as listed below:

1. Design, Development, Manufacturing, Optimization and Validation of the metal mould and tilt-pour casting equipment to hold the metal mould to cast test bars for tensile and fatigue properties assessments.

2. Laboratory scale CDS experiments to optimize the alloy designs and melt superheat temperatures above the respective liquidus temperatures for shape casting.
3. Tilt-pour casting process optimization to shape cast 2024, 6082 and 7075 Al wrought alloys.

Figure 2-1 presents an overview of the project plan showing the three phases adopted to fulfill the objectives mentioned above.

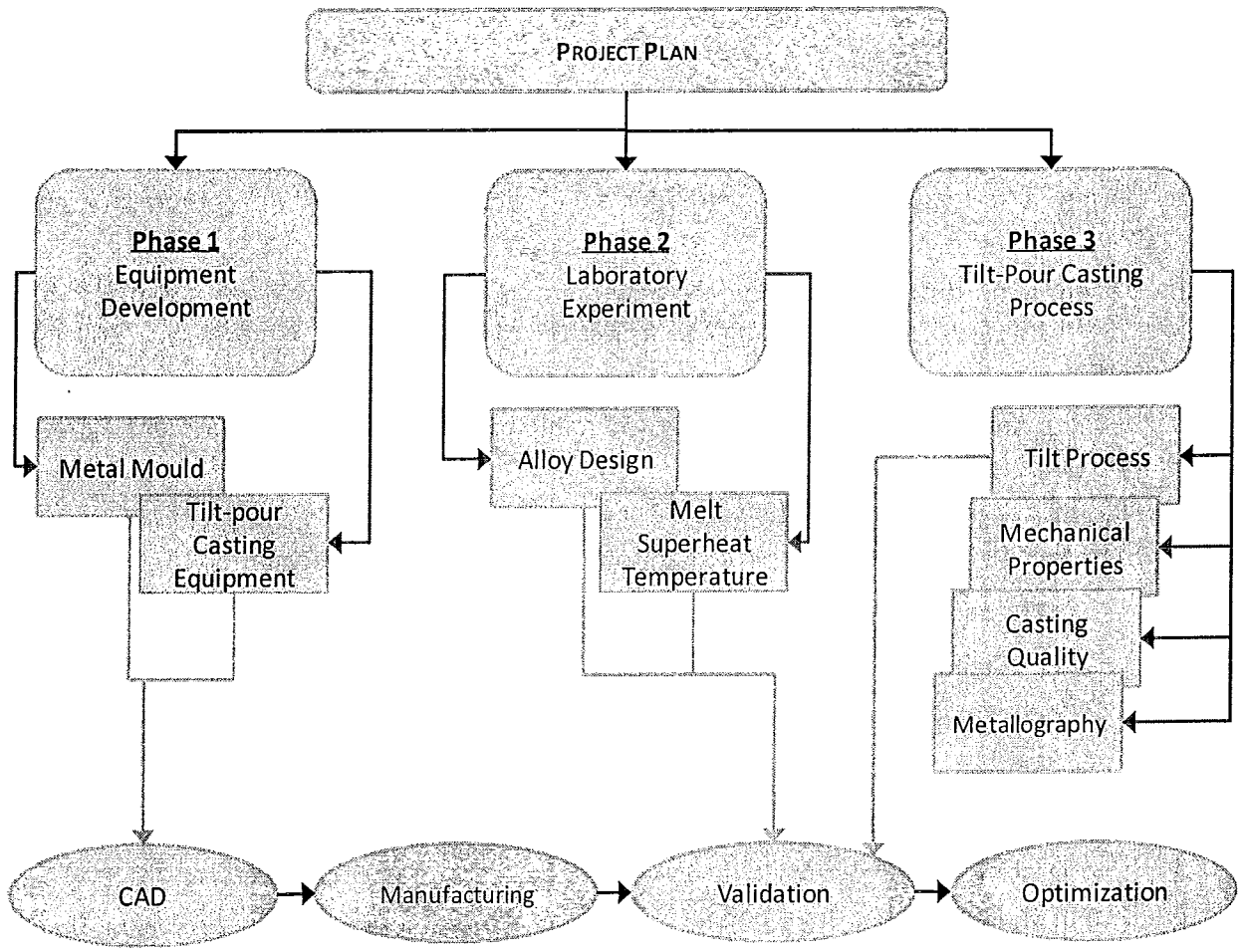

Figure 2-1. Overview of the project plan adopted in this study.

2.3 CONTRIBUTIONS OF PERSONNEL IN THIS PROJECT

The overall activities related to this thesis were the result of an intensive and carefully planned team work among various researchers at the Light Metal Casting Research Centre (LMCRC) in McMaster University.

- The work related to the mechanism of CDS (Theory and Experiments) were primarily carried out by Mr. Abbas Khalaf and assisted by me and Dr. Peyman Ashtari.

- I had solely carried out the design, development, manufacturing of the tilt-pour casting equipment and the metal mould on this equipment that cast the test bars.

- Dr. Ashtari and I had jointly planned all the laboratory experiments in Phase 2 of this project and the experiments were carried out by Dr.Peyman Ashtari and assisted by me. Dr. Ashtari and I jointly analyzed the experiment results in Phase 2.

- Tilt pour casting experiments were jointly planed by Dr. Ashtari and myself. The experiments were carried out by me with assistance from Dr. Ashtari.

- Heat treatment, microstructure analysis and tensile test data analysis were designed and carried out by me and Dr. Ashtari with assistance from various summer students.

- The analysis with the Scanning Electron Microscope (SEM) was carried out by me and Dr. Ashtari with Mr. Anton Gorny assisting us in operating the microscope.

Chapter 3 Materials and Equipment

This section lists the various materials and equipment used in the three phases of this project. Unless otherwise mentioned in this thesis, all material percentages are in weight percent.

3.1 Raw materials

Raw material	Purpose
Pure aluminum (Al)	First alloy composition
Al-50%Mg	Second alloy of 6082
Al-28%Cu	Second alloy of 2024
Pure Zn, Al-20%Cr,Al-25% Mn	Second alloy of 7075 and 2024

3.2 Computer Software

Software	Purpose
Unigraphics[a] NX2- NX6	Computer Aided Design (CAD)
Flow3d [b] version 9.3.2	CFD software for gate and riser optimization
FactSage 6.5 [c]	Alloy design by phase diagrams simulation
LabView 7.5 [d]	Data acquisition

3.3 Metallography

Equipment	Purpose
Leco PR-25	Metallographic sample mounting

[a] Unigraphics, Copyright © 2009 Siemens Product Lifecycle Management Software Inc.
[b] Flow-3D is a registered trademark of Flow Science, Inc., Santa Fe, NM, USA 87505.
[c] FactSage © CRCT 2006-2009 - www.factsage.com
[d] Labview © 2009 National Instruments Corporation. All rights reserved.

Automatic Polishing Equipment Struers [e] model RotoPol-31 and Struers LaboPol-21	Metallographic sample preparation
Nikon [f]Optical Microscope	Optical Microscopy
Scanning Electron Microscope Model JEOL [g] 7000	Metallography, Phase analysis and Fractorgraphy

3.4 Data Acquisition

Equipment	Purpose
National Instrument SCXI 1100 data acquisition box	Thermal data acquisition
Labview 7.5	Interface to control thermal data acquisition.
K-type thermocouples with	Temperature measurements

3.5 Melting, Handling and Casting

Equipment	Purpose
Paragon electric furnace	Melting and holding molten aluminum alloys
Custom ladles	Transfer of molten alloys at pre-calculated volumes
Custom built degasser	Degassing melt to eliminate Hydrogen
Custom Tilt Pour Equipment	Hold die mould, heater and pouring cup. Variable tilt function during casting

[e] Stuers © 2009 Struers A/S. All rights reserved.
[f] Nikon © 2009 Nikon Corporation
[g] JEOL Copyright 2006-2009 JEOL Ltd.

Custom Heaters	Maintain a preset preheat temperature for die mould and pouring cup
K Type Thermocouples (Omega) Ø 0.040" and Ø 0.25"	Measure temperature
Foseco Dycote Coatings: Dycote39, Dycote36	Protect and create a thermal barrier on mould surface in contact with solidifying alloy.

3.6 MATERIAL PROPERTIES TESTING EQUIPMENT

Equipment	Purpose
Instron 8800 Universal Testing machine	Measure Ultimate Tensile Strength UTS (MPa), Yield Strength YS (MPa) and Elongation (%) at 1mm/min strain rate.
Instron Data acquision software	
250 kN Model 312 MTS Load cell	
On-line Extensometer – 2 in gage length and 10% maximum elongation.	

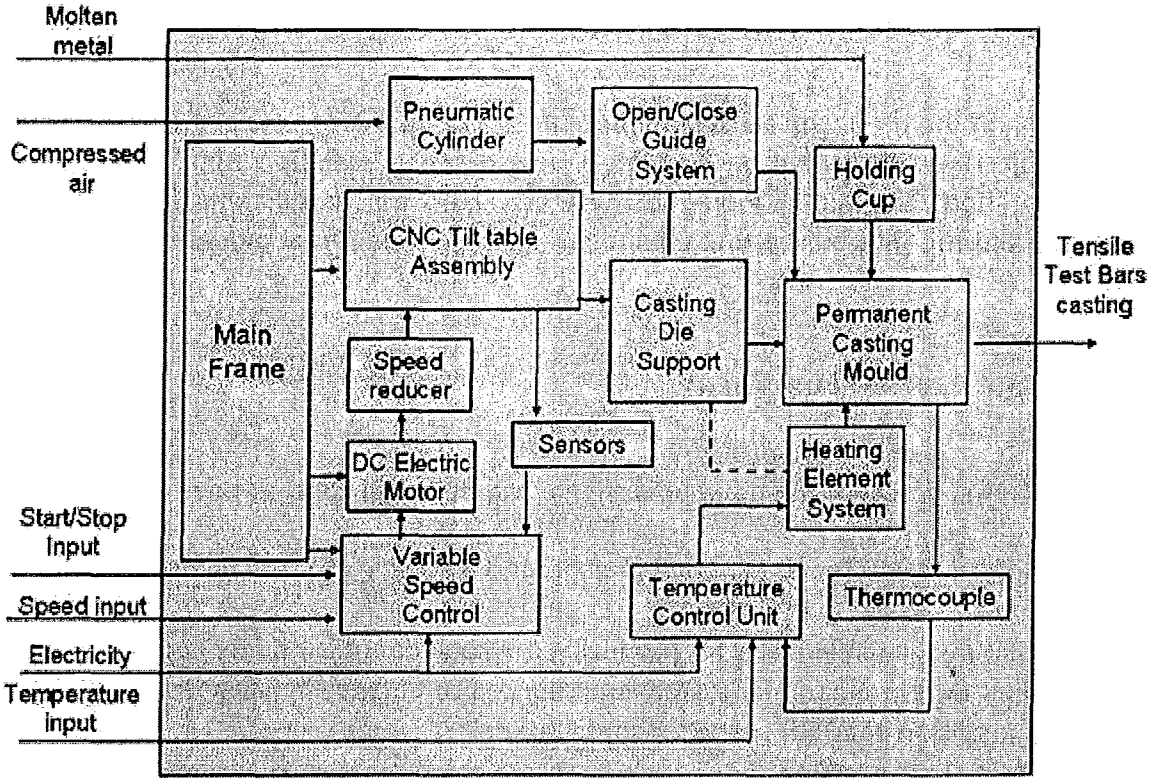

Figure 4-1. Functional Analysis Diagram for Tilt-pour Casting Equipment

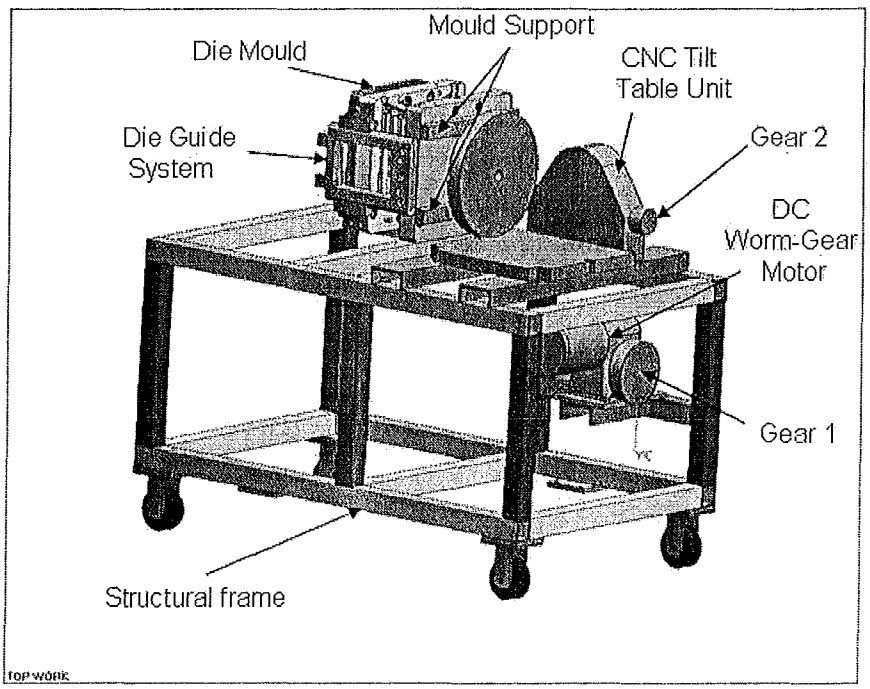

Figure 4-2. Tilt Casting Equipment CAD design

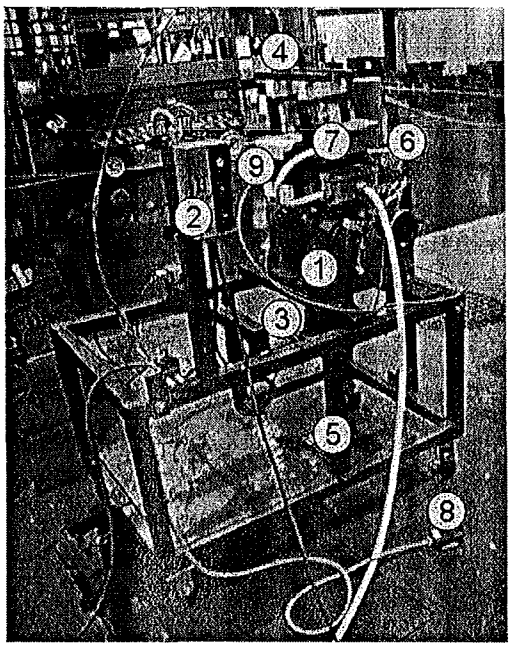

KEY	
1	CNC Tilt Table
2	Variable Speed Control Unit
3	DC Motor and Timing Gears
4	Open-Close Guide System Pneumatic
5	Frame Support
6	Custom Pouring Cup
7	Custom Die Heating System
8	Foot pedal operating switch
9	Metal die mould Support

Figure 4-3. Prototype Tilt Equipment

Table 4-1 presents a detailed description of the various components in the tilt-pour casting equipment shown in Figure 4-3.

Table 4-1. Description of various components in the tilt-pour casting equipment.

Component Number	Description
1	The center piece of the new tilt equipment is a 13" diameter manual CNC Tilt Table Assembly
2	Variable Speed Controller manufactured by Boston Controls[h] was added to precisely control the speed of rotation. Limit switches connected back to the main Variable Speed Controller were installed to trigger the end of rotation.
3	For tilt function the manual wheel was replaced by an index wheel connected through a timing belt to a gear motor. The Worm-Gear DC Motor produced by Bodine[i] was selected to allow for variation and control of rotational speed. Gear ratios were selected to achieve a 90 degree tilt in a range of 15 to 60 seconds each to meet the requirements of a typical industrial "HALL" tilt machine produced by CMH[j]. An all electric control system instead of the popular hydraulic system provided a much better control over tilt speeds and accuracy in addition to better

[h] Boston Gear © Boston Gear 2003

[i] Bodine Electric Company Copyright © 2009 Bodine Electric Company.

[j] Hall Machine CMH Copyright © 2009 CMH Manufacturing

	operational safety by eliminating using of hydraulic oil in the presence of molten metal.
4	The opening and closing operations of the die for each cycle were controlled by pneumatic cylinders (Festo[k]) with the necessary peripherals mounted on steel supports.
5	The structure frame was designed and manufactured with welded square tubing.
6	The pouring cup is a standard 3lbs cup from CMH[j]. A custom ceramic heater with temperature control (K-type thermocouple) was built and attached to the standard pouring cup to provide a constant pre-heat temperature.
7	Two sets of electric heating elements (1500W/240V) for each half of the die was installed providing a total heating capacity of 6 kW. A Temperature Control Unit (TCU) containing solid state relays and Set/Reset/Monitor temperature controls as sensed by thermocouples attached to die at a distance of 3mm from the surface of the mould cavity were installed. The heaters were designed to allow preheating of the die to over 400°C form room temperature in about 2 hours.
8	A foot pedal operating switch was installed to enable ease of operation.
9	The Die Mould is mounted by bolts on a support steel structure that allows easy die movement and removal for maintenance.

4.2. Tensile Test Tilt Mould Design and Optimization

A viable metal mould was conceived, designed, manufactured and validated to cast test bars in a tilt-pour casting process for mechanical property assessment.

4.2.1. Design

The ASTM B108/B 108M-08 standard mould design has been traditionally used in the industry to cast test bar samples according to the design specified in ASTM B557 to evaluate mechanical tensile properties. However, this mould design is for gravity permanent mould casting without the use of tilt-pour technology. Industries casting components using tilt-pour technology do not have a standard mould to cast test bars for mechanical property assessment and they have conventionally used the above-mentioned standard mould for gravity casting to ascertain the

[k] Festo Copyright 2000-2008, Festo AG & Co. KG.

properties for the castings obtained by tilt-pour casting. The first phase of this project was dedicated to the design, development, manufacturing and validation of a viable metal mould to be used in tilt-pour casting equipment for casting test bars for mechanical property assessment. Figure 4-4 shows a schematic of the cross-section of the metal mould used in conventional gravity casting (Figure 4-4(a)) as per the ASTM B108/B 108M-08 standard and the newly designed metal mould for tilt-pour casting process (Figure 4-4(b)) designed in this project.

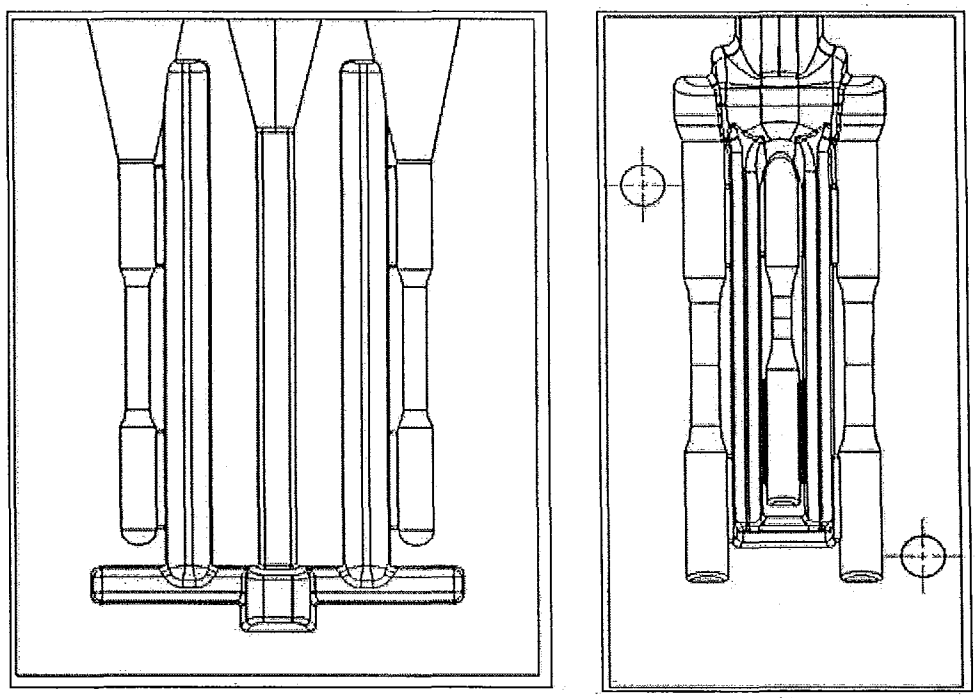

(a) (b)

Figure 4-4. Die Cast Mould a) gravity casting Standard ASTM B108/B 108M-08 and (b) newly designed mould for tilt-pour casting.

The newly designed mould consists of two standard tensile test bars designed according to the ASTM B557 standard and one fatigue test bar designed according to ASTM E466-96 (2002) standard. Figure 4-5 shows the two halves (CAD model) of the ASTM B108/B 108M-08 standard mould used to cast conventional gravity castings. Figure 4-6 shows the two halves (CAD model) of the newly designed mould to cast test bars in a tilt-pour casting process.

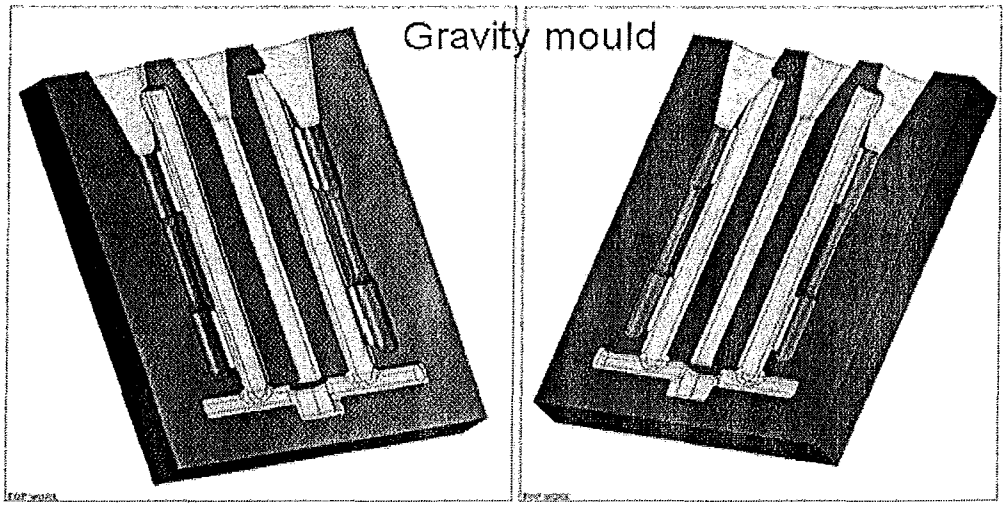

Figure 4-5. Two halves of the mould used for conventional gravity casting.

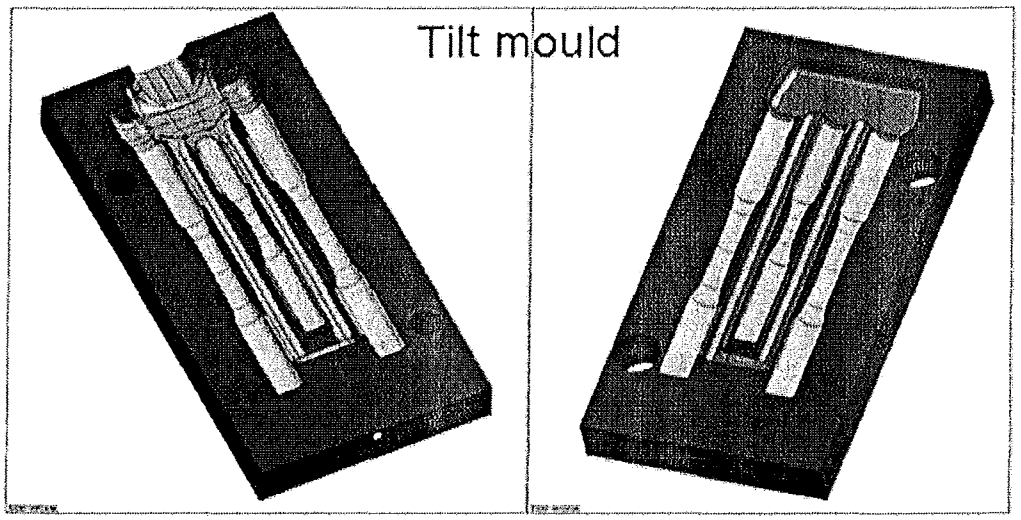

Figure 4-6. Two halves of the mould designed in this project for tilt-pour castings..

Figure 4-7 shows the dimensions of the newly designed mould to cast test bars as shown in Figure 4-6 for the tilt-pour casting process.

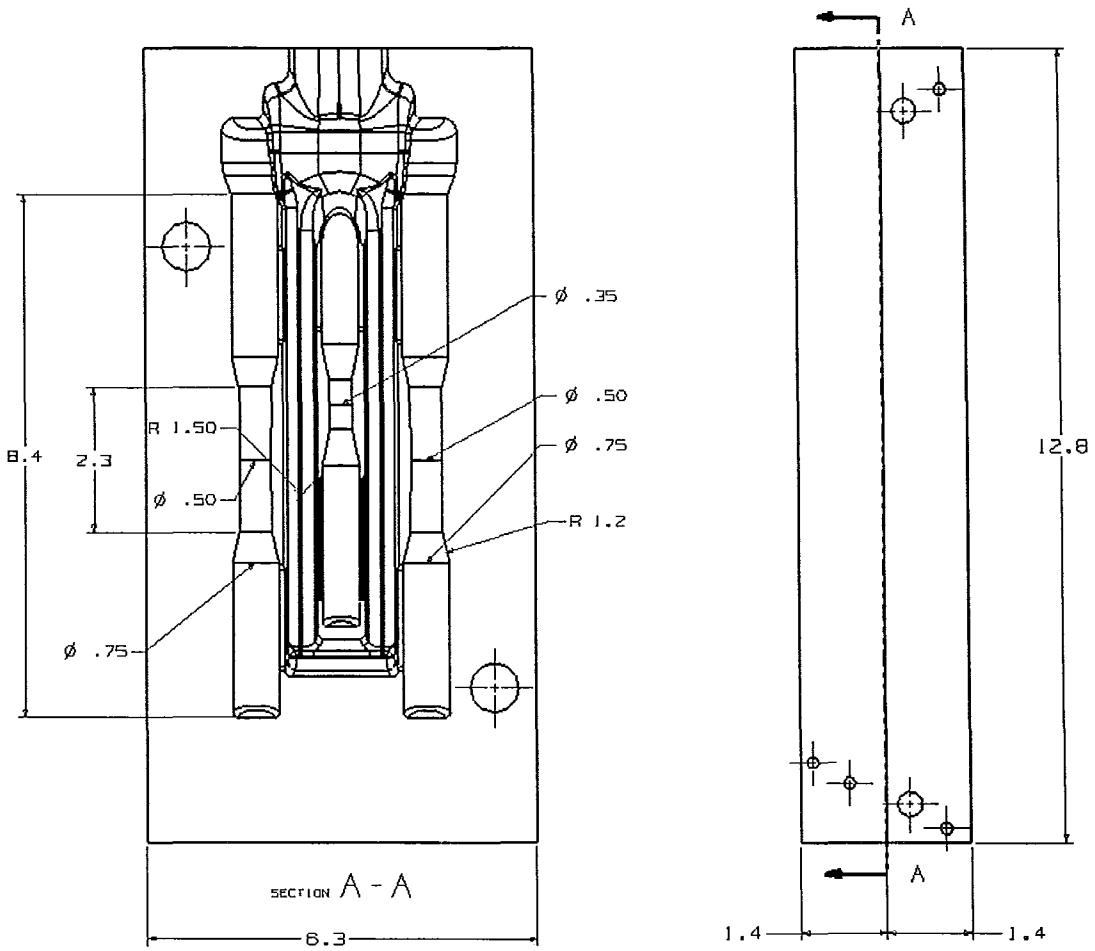

Figure 4-7. Dimensions (inches) of the newly designed mould in Figure 4-6 with various cross-sectional views.

Gravity casting process relies on the reduced cross-section of the tapered sprue to choke the flow of incoming molten metal and minimize the turbulence, metal folding and re-oxidation of the melt. Liquid metal at the initial stage of the process travels through the runner system in the same direction assisted by gravity. Gravity still assists the flow of molten metal to fill the mould cavity in a tilt-pour casting process, the rate of gravity vector increases from zero to the maximum value due to the tilting process. This enables a controlled and nearly laminar stream of molten metal filling the mould cavity. The filling of the mould in this process greatly minimizes the gas entrapment (porosity) in the cast component and results in a high integrity casting. Further, the tilt-pour process also eliminates the use of a sprue and well system and typically, the molten metal directly fills the mould cavity or a runner system. The mould design for a tilt-pour process uses less material and the mould is more compact than that in a gravity casting process. Additionally, the pour weight of the melt for a casting shot is less in the tilt-pour process and hence, the scrap rate is also lower. The feeding system for tilt-pour casting is larger in cross section enabling an increased feed rate. As the mould tilts, the air in the cavity is

slowly replaced by the molten alloy and the volume in the runner system is shared by incoming melt and the escaping air. Hence, the tilt speed and runner/cavity design are critical for optimization to obtain a sound casting. Various design configurations for the mould cavity and tilt speeds were designed, tested and optimized to enable a near-quiescent and laminar flow of the molten metal during filling. Further, the mould dimensions were also optimized for the desired heat transfer conditions during solidification. Flow-3D® software was used optimize the mould design by visualization of the mould filling and solidification of the cast component in the tilt-pour casting process. Further, the simulations enabled the optimization of the tilting parameters such as tilt time, molten metal temperature and mould pre-heat temperatures.

4.2.2. Mould Filling Simulations

Numerical simulations of mould filling and subsequent solidification of the casting was carried out using both Computational Fluid Dynamics (CFD) and solidification models in the Flow-3D commercial software. A pouring cup was added to the die mould design file (CAD) to contain the required amount of liquid alloy to fill the casting mould. The Flow-3D solid material database of H13 was used to define the mould and the pouring cup; and the Al-4.5wt%Cu data from the Flow-3D fluids database was used for the alloy being cast in the simulations. The tilt process simulated was at 6 degrees rotation per second starting from the horizontal position and ending at the vertical position. The mould and pouring cup were given an initial pre-heat temperature of 347 °C and the initial temperature of the liquid alloy in the pouring cup was 727 °C. A coating was not assumed on the inside surface of the mould cavity and to compensate a 50^0C superheat was used for fluid inside the cavity. A mesh of 2 mm side cubic cell was used in the simulation applied to the CAD model for the mould and pouring cup.

The preliminary design for the new metal mould used in the tilt-pour casting process is shown in Figure 4-8, wherein, there was no runner system as shown in the final design (Figure 4-6).

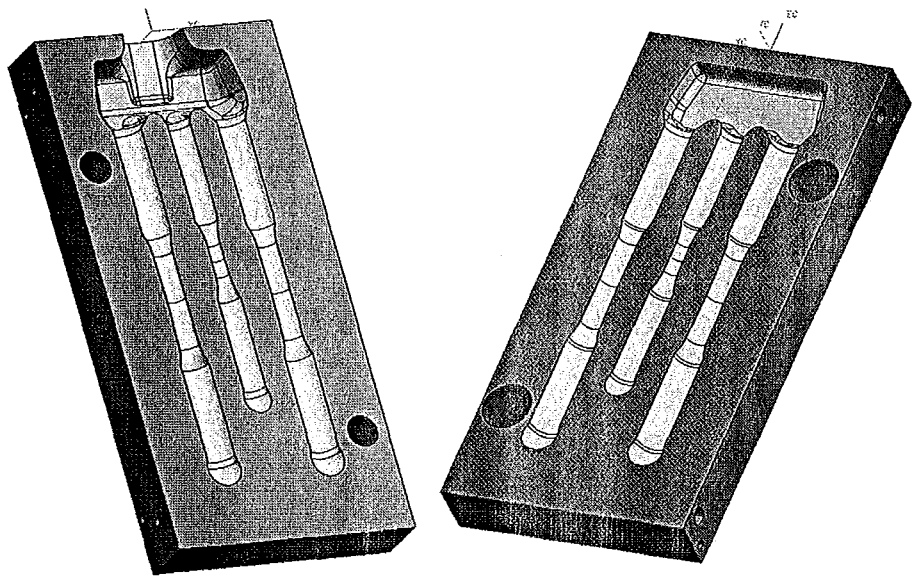

Figure 4-8. Initial design of the test bar mould (two halves) for tilt-pour casting process.

Figure 4-9 (a) to (e) show the snapshots of results of macroscopic energy distribution obtained from the numerical simulations of filling the mould in Figure 4-8 for increasing times of filling from the start of the tilt process. Figure 4-9 (f) shows the visualization scale used to quantify the macroscopic energy during filling in Figure 4-9. These results show that there is significant turbulence in the filling process as seen by voids of air entrapment caused by swirling and/or breakdown of the flowing metal front. These results show that the initial design in Figure 4-8 was not a favourable mould design and needed improvements.

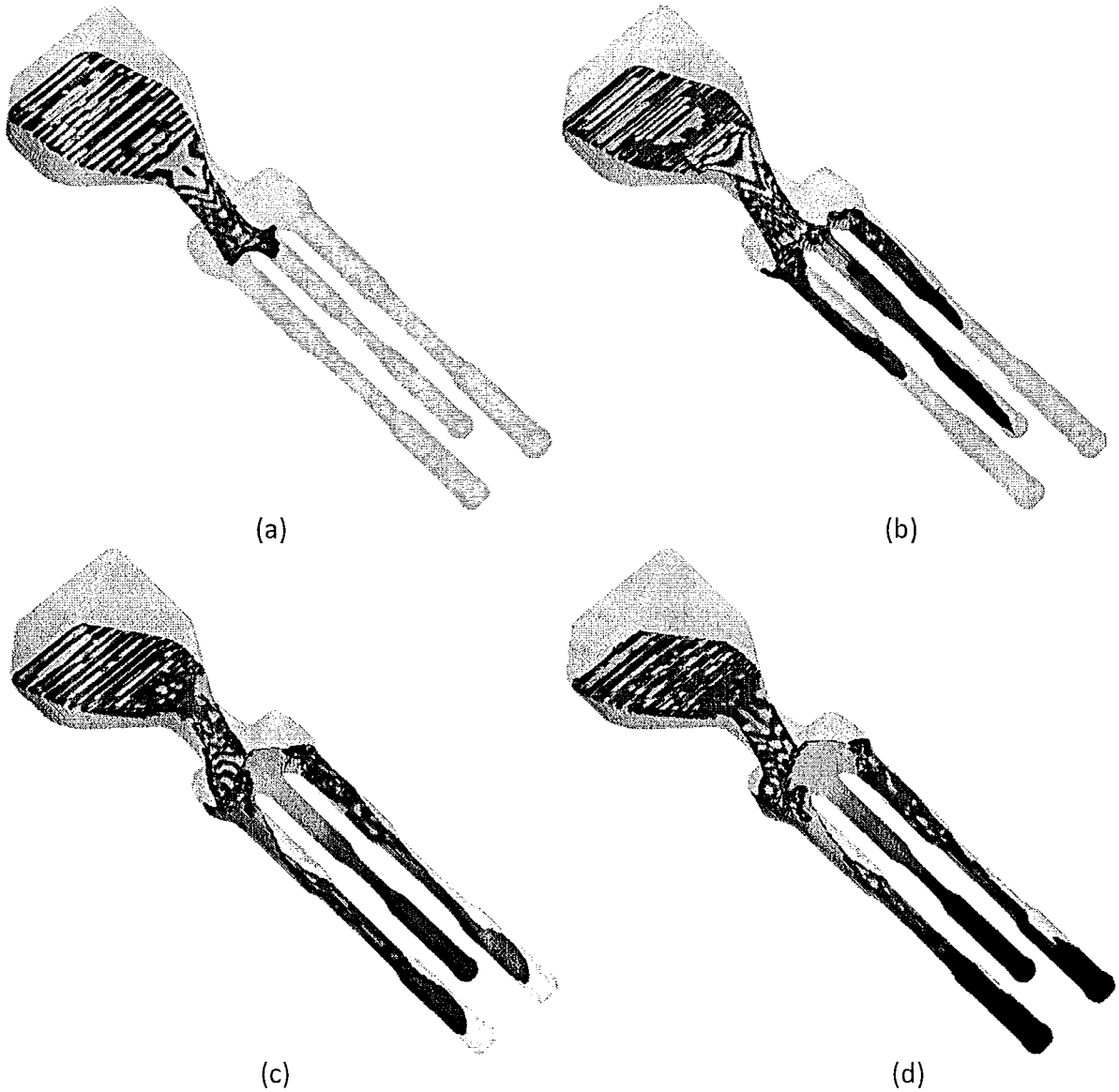

(a) (b)

(c) (d)

(e) (f)

Figure 4-9. Snap shot images of the results of macroscopic energy distribution from numerical simulation of the mould filling during the tilt-pour process with the initial mould design shown in Figure 4-8. (a) to (e) shows increasing times during the filling process and (f) shows the scale used in the visualization.

The mould design in Figure 4-6 shows the improvement to the initial design by the addition of a "U" shaped runner system around the middle of the mould to facilitate a more quiescent and laminar flow during mould filling. Further, the header cavity was re-designed to facilitate a quiescent metal flow while feeding the mould cavity. The new header and runner system also acts as a riser system to absorb all the shrinkages from the test bars during solidification. Figure 4-10 (a) to (e) show the snapshots of results of macroscopic energy distribution obtained from the numerical simulations of filling the mould in Figure 4-6 for increasing times of filling from the start of the tilt process. Figure 4-10 (f) shows the visualization scale used to quantify the macroscopic energy during filling in Figure 4-10. These simulation results show that the melt flow is quiescent and nearly laminar with a nearly undisturbed metal flow front during the entire filling process which shows that the modified mould design in Figure 4-6 was favourable for development.

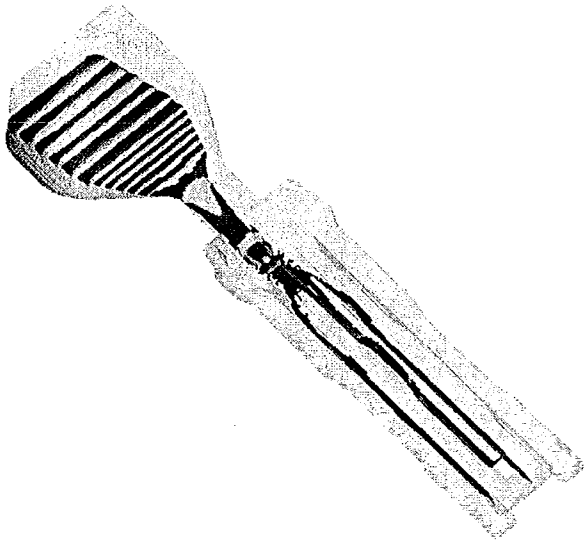

(a)

(b)

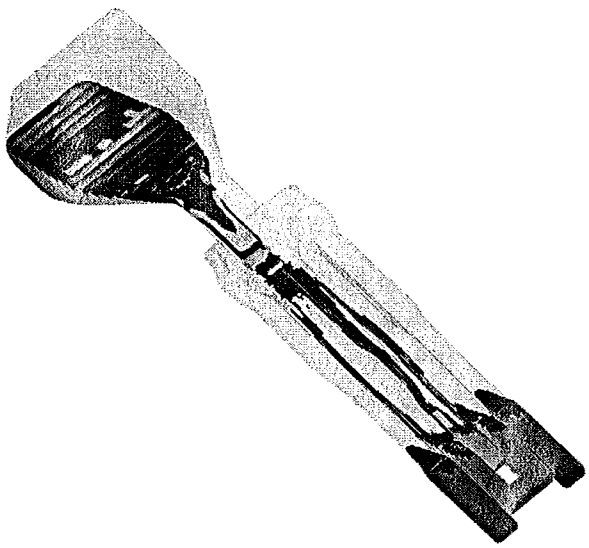

(c)

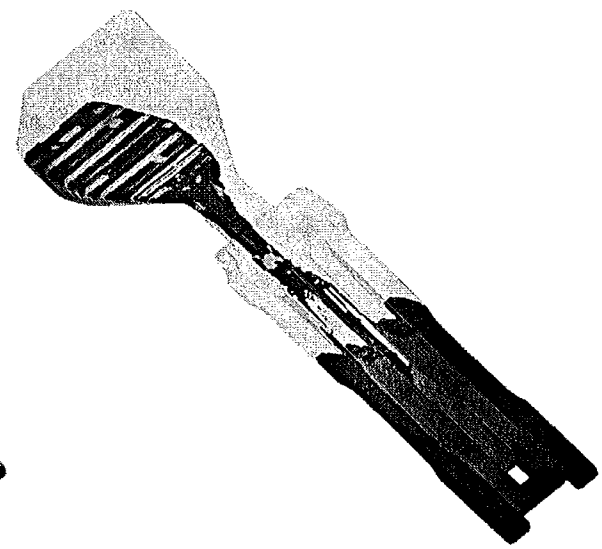

(d)

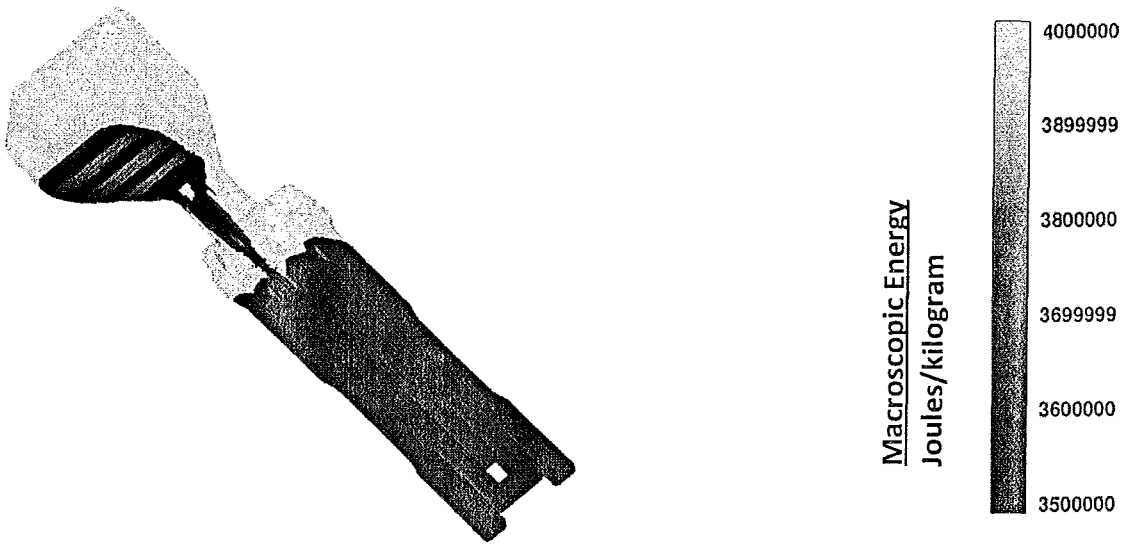

(e) (f)

Figure 4-10. **Snap shot images of the results of macroscopic energy distribution from numerical simulation of the mould filling during the tilt-pour process with the initial mould design shown in Figure 4-6. (a) to (e) shows increasing times during the filling process and (f) shows the scale used in the visualization.**

4.2.3. Tilt-pour Casting Process Optimization

The die mould as shown in Figure 4-6 was manufactured from AISI P20[l] pre-hardened mould steel and mounted on the tilt equipment (Figure 4-3). The die was preheated to 200°C and the surface of the die was coated with Dycote 39[m] to control the solidification by improving the heat retention capacity of the die mould. A thin layer of Dycote 39 was applied by a spray gun onto the die mould surface to provide a favourable smooth surface finish of the final cast component. After the coating process, the temperature of the mould was increased to the 350°C to facilitate the casting process.

The commercially popular aluminium casting alloy A356.2[n] was used for the tilt-pour casting process optimization and validation of the mould design. Table 4-2 shows the average composition of the A356.2 alloy used in this study as measured by a Glow Discharge Spark Spectroscopy (GDOES). The alloy was melt and degassed at 750 °C for 30 minutes at 200 RPM with ultrahigh purity Ar gas at a flow rate of 5 l/min. The alloy pouring temperature was 662 °C into the pouring cup.

---

[l] http://www.matweb.com/search/DataSheet.aspx?MatGUID=1871f21cd5674498adfca966c3d4b87f&ckck=1.

[m] Dycote 39 © FOSECO Metallurgical Inc. 2005

[n] http://www.matweb.com/search/DataSheet.aspx?MatGUID=298c59f174c04575bb9f1c192b2d370f.

Table 4-2. Chemical composition of aluminium A356.2 casting alloy.

Al	Si	Mg	Fe	Sr	Ti	Others
92.074	7.231	0.3797	0.12058	0.0196	0.07834	Balance

Various tilt speeds and pre-heat temperatures for the die were investigates and optimized to produce a sound cast component with no visible porosity in the gauge cross-section of the test bars. The optimum process was found to be a tilt rate of 6 degrees per second for a 90 degree tilt and the die pre-heat was 350 °C.

4.2.4. Validation of the Mould and Process

The validation of the new metal moulds and the tilt-pour casting process were carried out by assessment of the tensile properties of the test bars cast in both the new mould design (Figure 4-6) mounted in the tilt-pour casting equipment (Figure 4-3) and metal mould (ASTM B108/B108M-08) in Figure 4-5 with the gravity permanent mould casting process (ASTM B557), respectively. The gravity permanent mould casting process has been standardized by ASTM. The cast parts were subsequently heat treated to three temper conditions as shown in Table 4-3. The tensile tests were carried out at a strain rate of 1mm/min and the elongation was measured by an extensometer attached to the gauge of the test specimen. Table 4-4 shows the tensile properties of castings at various tempers in the two casting processes: tilt-pour and gravity permanent mould. The results shown in Table 4-4 shows that the properties of the A356.2 alloy in both the conventional gravity permanent mould process and the newly designed metal mould used in the tilt-pour casting process are similar and hence validated the new mould and tilt-pour casting equipment. Further, as envisioned, Table 4-4 shows that the quality index (Q) [23] and the level of standard deviation for the samples obtained from the tilt-pour casting mould and equipment is superior to that of the conventional gravity casting process. Table 4-4 also shows the published standard for the A356.2 casting alloy and the castings obtained in tilt-pour casting process exceeds this standard in all mechanical properties.
Quality index was introduced in 1970 to define the relationship between UTS, YS and El% and it has units of MPa or ksi. Equation (4) [23] presents the formulation for the Quality index, Q.

$$Q = UTS + (K) \log (\%El) \qquad (4)$$

K is selected such that Q is independent of YS and it has different values for different alloys. For heat treated 356 alloy, K=150 [23]. Calculating and monitoring changes of Q for various heat treatment and casting processes options allows an evaluation of the material properties of the resultant alloy.

Figure 4-11 shows the relationship among UTS, YS and Elongation for Al-7Si-Mg alloy and the influence of the casting and heat treatment process on the value of Q. The higher Q values of above 350 suggests that the casting is sound and of high quality.

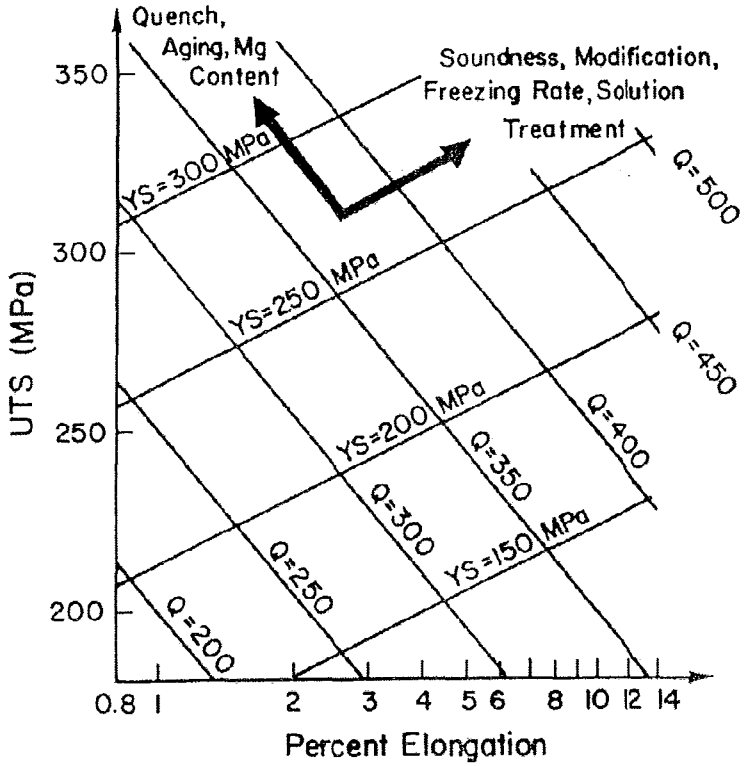

Figure 4-11 Relationship between Ultimate Tensile Strength, Elongation, Yield Strength and Quality Index for Al-7%Si-Mg alloy [23]

Table 4-3. Three temper conditions used for evaluating tensile properties of A356.2 alloy.

Temper	Solutionizing	Natural Ageing	Artificial Ageing
F (As-Cast)	None	None	None
T4	540 °C for 12 hours and quenched in water at 80 °C	10 hours at room temperature	None
T6	540 °C for 12 hours and quenched in water at 80 °C	10 hours at room temperature	155 °C for 5 hours and air cooled.

Table 4-4. Tensile properties of A356.2 alloy in both the tilt-pour and gravity casting processes at various tempers along with the quality index (Q) test results comparison for Gravity pour castings and Tilt pour casting

Sample no.	Temper	UTS	Std. Dev.	YS (0.02%)	Std. Dev.	Elongation	Std. Dev.	Quality Index (Q)
		Mpa (Ksi)	Mpa (Ksi)	Mpa (Ksi)	Mpa (Ksi)	(%)		

Tilt-pour mould and process	F (As-Cast)	199.62 (28.95)	4.20 (0.68)	91.48 (13.27)	2.53 (0.41)	8.95	0.89	342.39
	T4	210.08 (30.47)	9.38 (15.28)	89.63 (13.00)	4.59 (6.53)	15.97	1.90	390.58
	T6	289.07 (41.92)	3.46 (0.86)	210.78 (30.57)	3.46 (0.50)	6.01	0.51	405.90
Conventional Gravity Casting Process	F (As-Cast)	188.10 (27.28)	3.23 (0.52)	90.72 (13.16)	1.48 (0.24)	8.53	0.22	327.74
	T4	222.74 (32.30)	2.71 (13.99)	102.13 (14.81)	2.29 (6.42)	16.61	0.82	405.80
	T6	270.65 (39.28)	12.82 (1.86)	195.50 (28.37)	13.85 (2.01)	7.11	0.78	398.43
	Published Standard T6 [13]	262 (38)	-	186 (27)	-	5	-	

Chapter 5 Phase 2: Laboratory Experiments

This chapter of the thesis presents the work carried out to design and optimize the alloy compositions and temperature of melt for the two pre-cursor alloys used for CDS casting of 2024, 6082 and 7075 Al wrought alloys. The experiments were carried out in a laboratory and the materials and equipment used in this phase of the project are presented in 0 of this thesis.

5.1 Nomenclature

The following presents the description of all the notations used in this chapter.

Alloy 1	Pre-cursor alloy with higher thermal mass (higher temperature and higher mass).
Alloy 2	Pre-cursor alloy with lower thermal mass.
Alloy 3	Resultant mixed alloy.
T_{L1} T_{L2} and T_{L3}	Liquidus temperature of Alloy 1, Alloy 2 and Alloy 3, respectively.
T_1, T_2 and T_3	Melt Temperature of Alloy 1, Alloy 2, and Alloy 3, respectively.
m_1 and m_2	Mass of Alloy 1 and Alloy 2 respectively.
m_r	Mass ratio of Alloy 1 and Alloy 2 (m_1:m_2).

5.2 Experiment Procedure

The purpose of these experiments was to optimize the compositions and temperature of the two pre-cursor alloys used in the CDS process to obtain a non-dendritic morphology of the primary phase in the as-cast microstructure.

Figure 5-1 shows a schematic and photograph of the set up used in the laboratory experiments. As shown in Figure 5-1(a), the Alloy 2 with the lower thermal mass was melted in a crucible to the required temperature T_2 in an electric furnace. A second empty crucible with a 6 mm hole fitted with a spout in the bottom was heated along with Alloy 1 in a third crucible to the required temperature T_1 for Alloy 1. The empty crucible with a hole was fitted above the crucible containing Alloy 2 with a laboratory clamp and the hole in the top crucible was plugged shut with a graphite stopper. The Alloy 1 was poured into the top crucible with a hole and the stopper released so that Alloy 1 can mix into Alloy 2 at a repeatable rate of mixing to produce a CDS casting of the resultant Alloy 3 in the bottom crucible shown in Figure 5-1. K-type Thermocouples were inserted in both the top and bottom crucibles to monitor and record the temperature of Alloy 1 and Alloy 2, respectively. The thermocouple in the bottom crucible

recorded the thermal events during the mixing process as well. Temperature data was recorded at a rate of 100 Hertz with a data acquisition software and hardware.

The alloy compositions and temperature of the two pre-cursor alloys were optimized by analyzing the microstructure of the resultant alloy solidified in the bottom crucible shown in Figure 5-1. A predominantly non-dendritic morphology of the primary phase in the microstructure was considered as favourable.

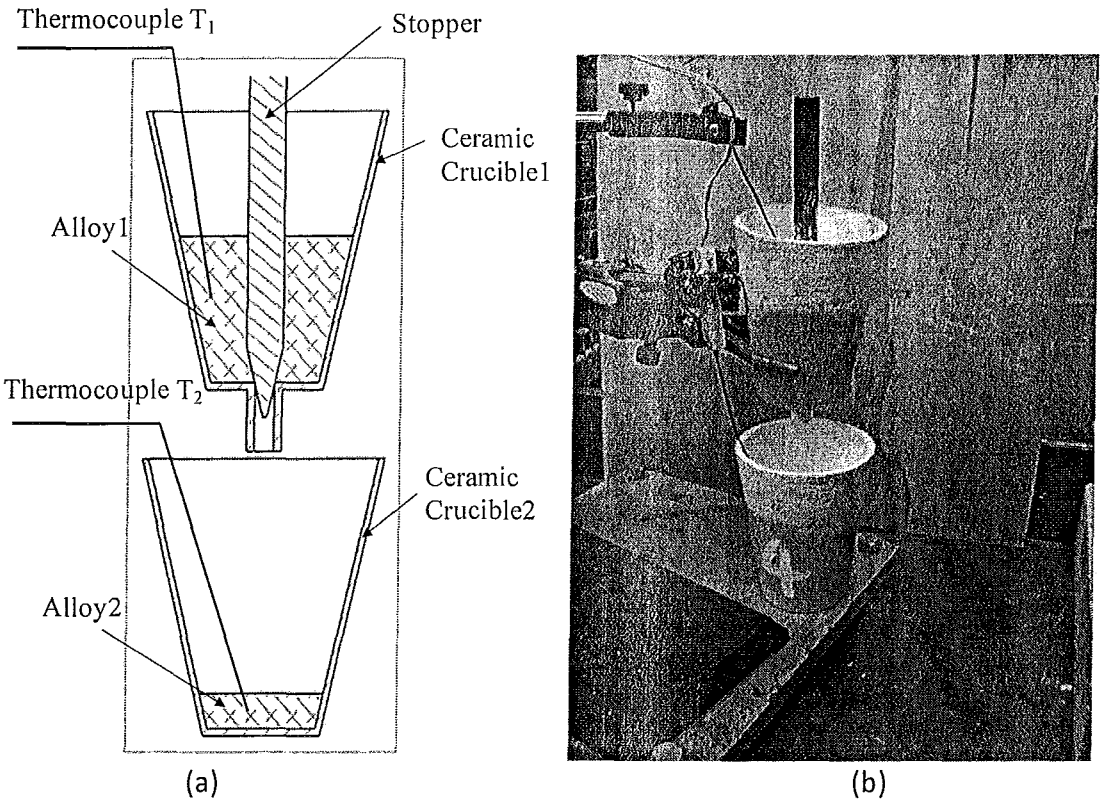

Figure 5-1. Laboratory experiment set up for CDS. (a) Schematic and (b) photograph.

Figure 5-2 shows the procedure to optimize the alloy compositions and melt temperatures for a successful CDS process as reflected by a non-dendritic morphology of the primary phase in microstructure of Alloy 3.

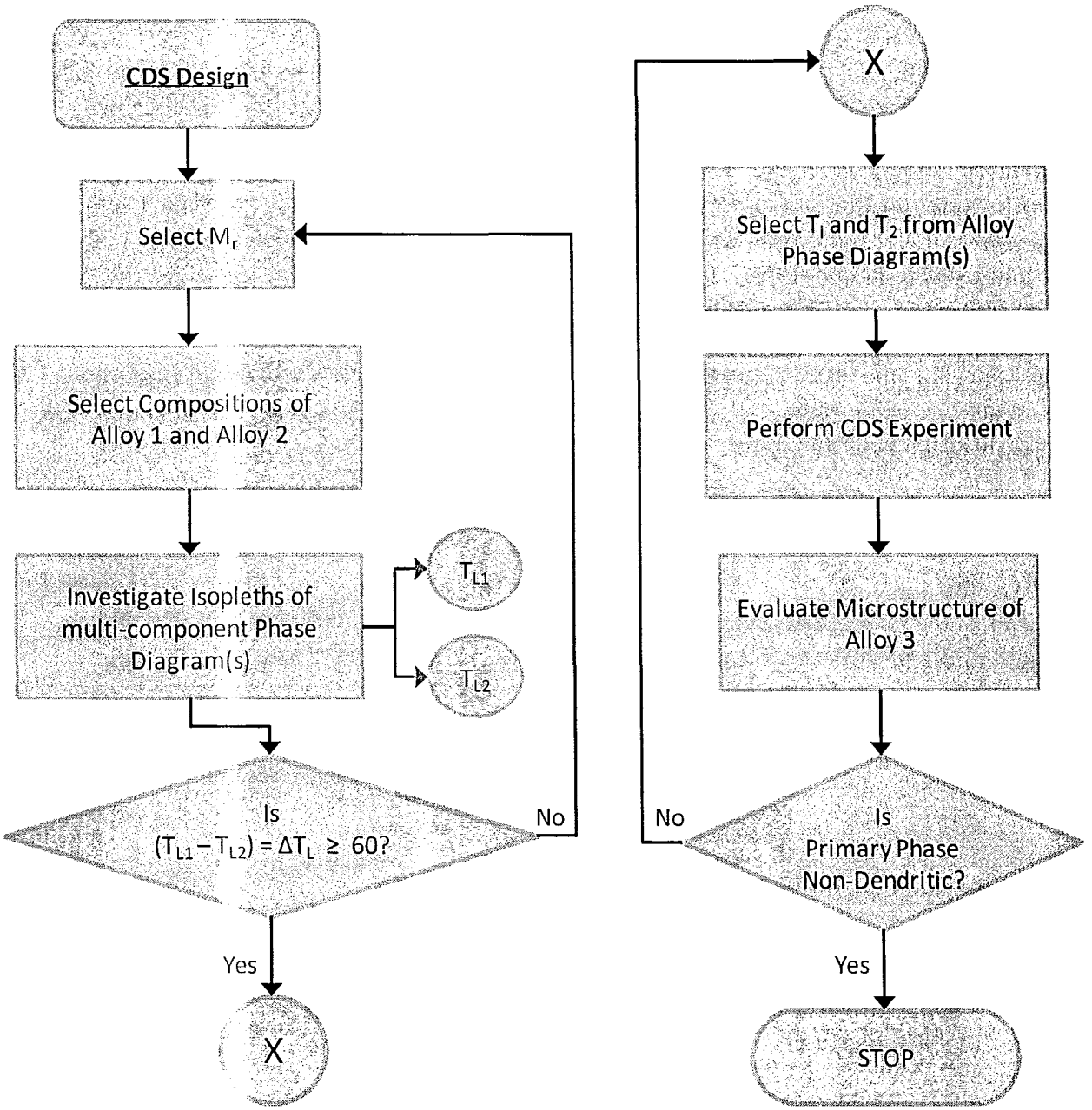

Figure 5-2. **Procedure to optimize alloy compositions and melt temperatures for the two pre-cursor alloys in a CDS process.**

For a specific Alloy 3 needed to be cast using the CDS technology, a mass ratio, m_r is first chosen followed by the compositions of Alloy 1 and Alloy 2 which when mixed will yield the composition of Alloy 3. Various isopleths of multi-component phase diagram(s) containing the elemental additions in Alloy 3 is investigated to evaluate the liquidus temperatures, T_{L1} and T_{L2}. If the difference between T_{L1} and T_{L2}, ΔT_L is greater than 60 °C [24], then we proceed with the selection of suitable melt temperatures, T_1 and T_2. If ΔT_L is less than 60 °C, we re-start the process by selecting a different value of m_r following by different compositions for Alloy1 and

Alloy 2. We carry out the CDS experiments using the setup shown in Figure 5-1 to obtain a casting of Alloy 3. The microstructure of Alloy 3 is investigated to confirm a non-dendritic morphology of the primary Al phase. Further, the thermal data of the thermocouple in the bottom crucible shown in Figure 5-1 is also investigated to verify the similarities with the schematic shown in Figure 1-14. For each alloy, various values of mass ratio, m_r were investigated and the most suitable combination of alloy compositions for Alloy 1 and Alloy 2 was selected and the further experiments were carried out with various values of T_1 and T_2 to optimize these temperatures. It has been previously observed [20,24] that marginal variation in T_2 does not affect the result of the CDs experiments, however, marginal variations in T_1 significantly influences the results.

The following sub-sections presents the optimum conditions for a successful CDS process for three alloys: 2024, 6082 and 7075 Al wrought alloys. Table 5-1 shows the compositions of these three alloys in this study.

Table 5-1. Nominal composition (weight percent) of 2024, 6082 and 7075 alloys.

Alloy	Cu	Si	Mg	Mn	Cr	Zn	Al	Liquidus Temperature (°C)
2024	3.8-4.9	-	1.2-1.8	0.3-0.9	-	-	Bal.	640
6082	-	0.7-1.3	0.6-1.2	0.4-1.0	-	-	Bal.	634
7075	1.2-2	-	2.1-2.9	-	0.2-0.28	5.0-6.0	Bal.	635

5.2.1 2024 Al wrought alloy

A mass ratio, m_r = 6 (m_1:m_2) was selected to cast this alloy. The required weight of Alloy 3 (2024) was 350 grams as dictated by the crucible size and the density of 2024 alloy. Hence, the mass of Alloy 1, m_1 = 300 grams and the mass of Alloy 2, m_2 = 50 grams. A favourable isopleth of the Al-Cu-Mg phase diagram was simulated and shown in Figure 5-3 wherein al the three alloy compositions can be visualized. The values of the liquidus temperatures T_{L1} and T_{L2} were evaluated as 651 °C and 543 °C, respectively. The difference between the two liquidus temperatures, T_{L1} and T_{L2} is 108 °C which is greater than the prescribed 60 °C[4] in Figure 5-2. Three superheat melt temperatures (T_1) above T_{L1} were selected for Alloy 1: 653 °C, 666 °C and 676 °C for optimization. Table 5-2 shows the alloy notations and various process variables used in the CDS experiments of 2024 Al wrought alloy.

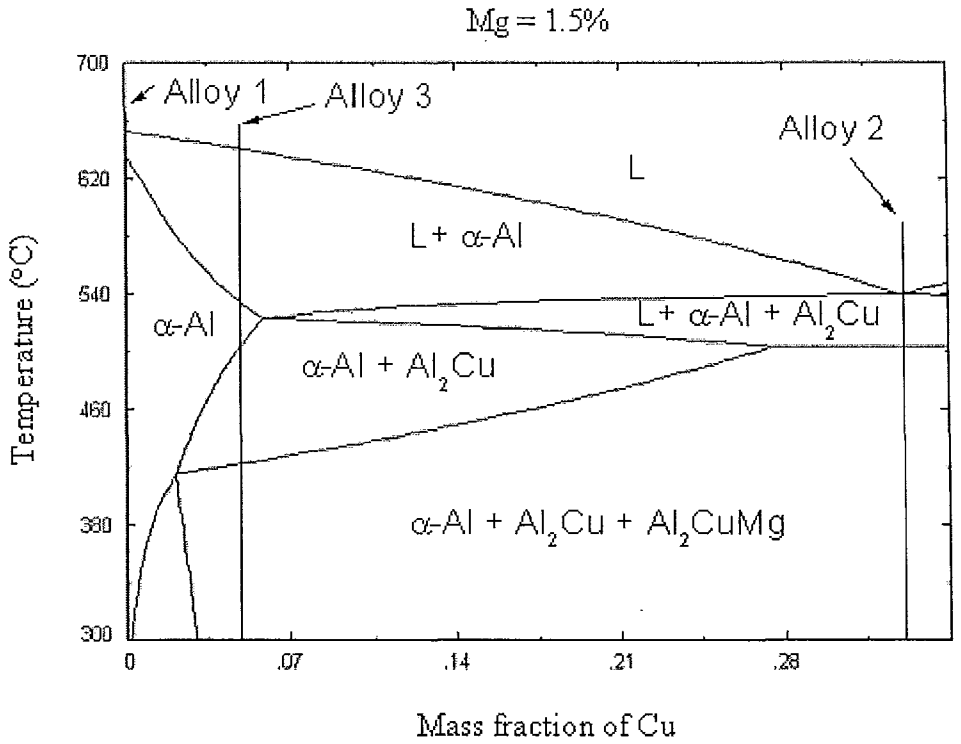

Figure 5-3. Isopleth of Al-Cu-Mg Phase Diagram showing the average compositions of Alloy1, Alloy2 and Alloy 3 (2024).

For conventional casting experiments about 350 grams of 2024 alloy (Alloy3) was melt in a crucible to a temperature of 5 °C above the liquidus temperature of the alloy and poured into the top crucible maintained at the same temperature as the 2024 alloy (Figure 5-1). The bottom crucible in Figure 5-1 was empty and maintained at a temperature of about 5 °C above the liquidus temperature Alloy 2 in Table 5-2. The stopper in the top crucible was instantly lifted and the 2024 alloy was left to fill the bottom crucible and solidify. This sample provided a comparable microstructure data for a conventional cast component from 2024, cast with a low melt superheat temperature. This experiment has the notation 2024 CC (CC stands for Conventional Casting) in Table 5-2.

In Figure 5-4, (a), (b), (c) and (d) are typical microstructures of 2024C1, 2024C2, 2024C3 and 2024CC (Table 5-2), respectively. It can be observed that the 2024C1 and 2024C2 samples show a favourable non-dendritic morphology of the primary Al phase in Figure 5-4 (a) and (b), respectively. Figure 5-4 (c) and (d) show the unfavourable dendritic morphology of the primary phase in 2024C3 and 2024CC alloy samples.

Table 5-2. Notations and Variables used in the CDS experiments to cast 2024 Al wrought alloy. All the temperatures in this table are in degree centigrade.

Notation	Alloy 1	T_1	T_{L1}	Alloy 2	T_2	T_{L2}	m_r	Alloy 3
2024C1	Al-1.5Mg	653	651	Al-33Cu-	548	543	6	Al-4.7Cu-

			1.5Mg				1.5Mg
2024C2	Al-1.5Mg 666	651	Al-33Cu-1.5Mg	555	543	6	Al-4.7Cu-1.5Mg
2024C3	Al-1.5Mg 676	651	Al-33Cu-1.5Mg	553	543	6	Al-4.7Cu-1.5Mg
2024CC	Conventional casting of Al-4.7Cu-1.5Mg						

The thermal data obtained during solidification of the alloys in Table 5-2 is shown in Figure 5-5. It has been hypothesized [20,24] that a successful CDS process is when the point B shown in Figure 1-14 is below the liquidus temperature of Alloy 1, T_{L1}. In Figure 5-5, it can be seen that the point B for 2024C1 and 2024C2 are below T_{L1} and that for 2024C3 is above predicting that conditions for 2024C1 and 2024C2 should be favourable for CDS as confirmed by the microstructures in Figure 5-4. Further, comparing Figure 5-5 and Figure 5-4, it can be hypothesized that the lower the point B in the thermal data obtained during mixing of the pre-cursor alloys, the more equiaxed is the morphology of the primary Al phase in the as-cast microstructure.

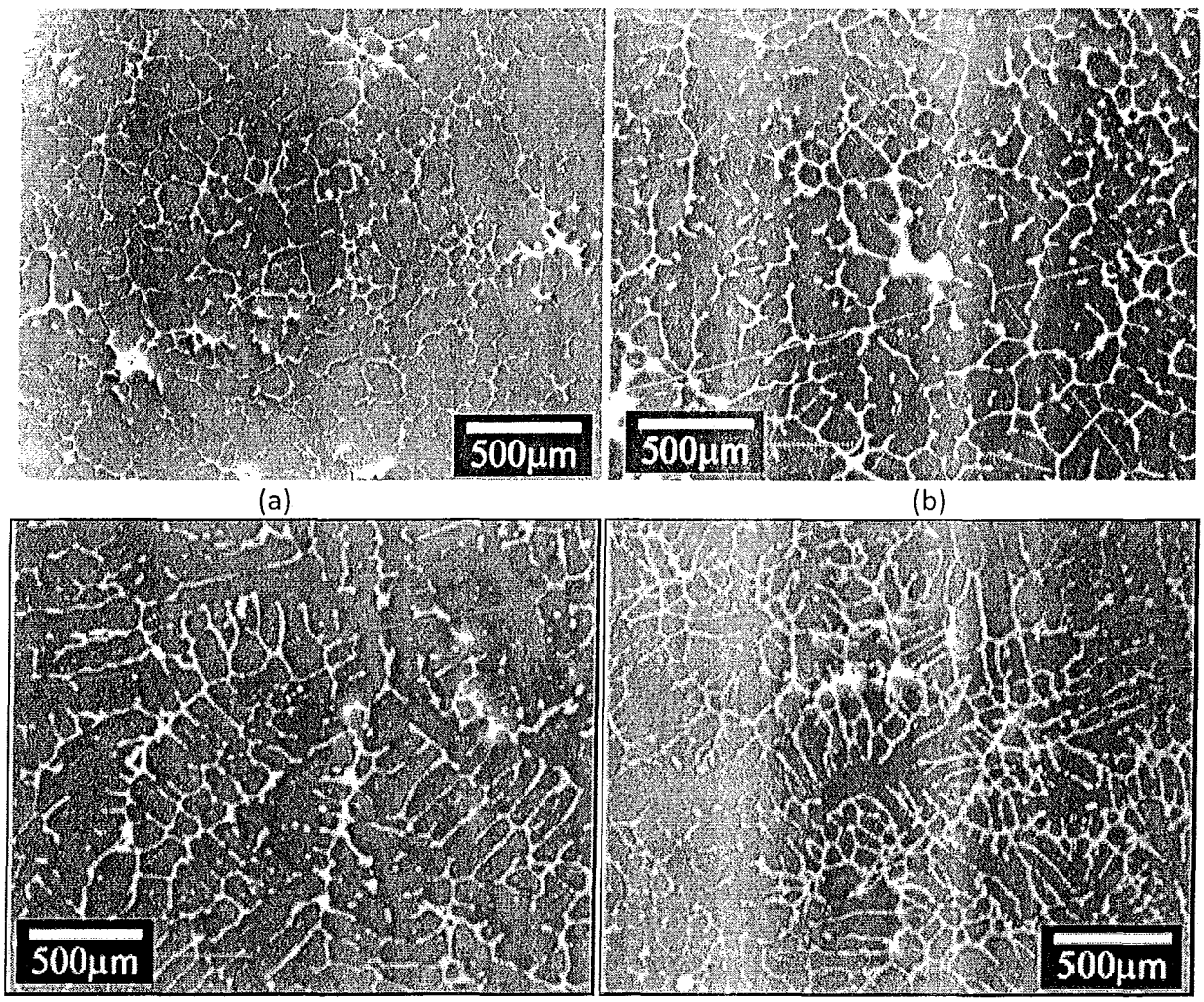

(c) (d)

Figure 5-4. **Typical as-cast microstructures of 2024 alloy (inverted greyscale) at various conditions shown in Table 5-2. (a) 2024C1 (non-dendritic and equiaxed primary phase), (b) 2024C2 (non-dendritic and rosette shaped primary phase, (c) 2024C3 (dendritic primary phase) and (d) 2024CC (dendritic primary phase).**

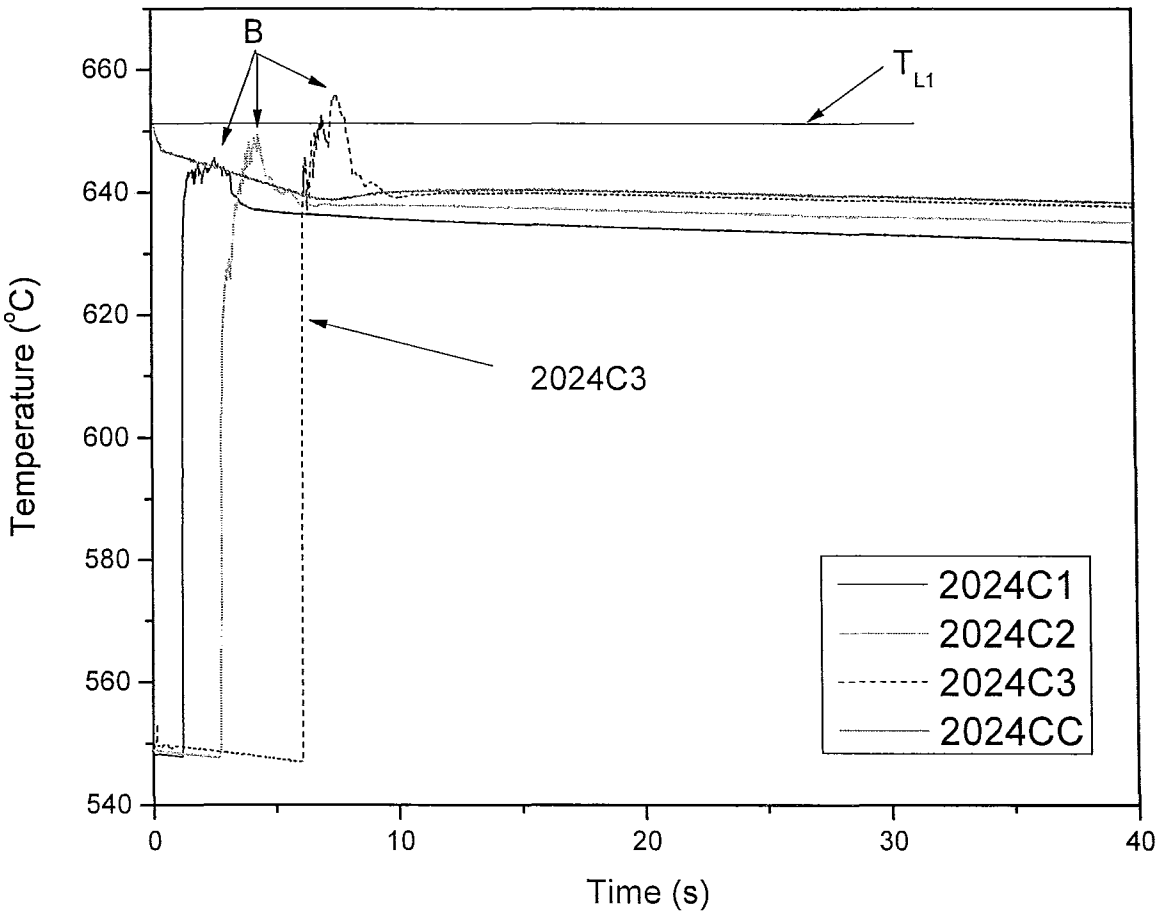

Figure 5-5. **Thermal data obtained during solidification of Alloy 3 (2024) in Table 5-2.**

5.2.2 6082 Al wrought alloy

The procedure for optimization of alloy compositions and melt temperatures for 6082 alloy was similar to that described in Figure 5-2 and that used for optimization of 2024 alloy. A mass ratio, m_r = 6 was initially assumed, however, the ΔT_L (= T_{L1}–T_{L2}) was less than 60 °C. A mass ratio, m_r = 10 proved successful. At this mass ratio, 300 grams of Alloy 1 was mixed into 30 grams of Alloy 2 to obtain 330 grams of Alloy 3 (6082). Visualization of Alloy 1, Alloy 2 and Alloy 3 was not possible in one isopleth of the Al-Mg-Si-Mn phase diagram. Figure 5-6 are three isopleths of various multi-component phase diagrams showing the average compositions of

Alloy 1 (Figure 5-6 (a)), Alloy 2 (Figure 5-6 (b)) and Alloy 3 (Figure 5-6 (c) for 6082 alloy). Table 5-3 shows the alloy notations and values of various variables used for the CDS experiments. A procedure similar to that described in the previous sub-section to cast 2024CC (Table 5-2) was also used to obtain conventional casting sample 6082CC (Table 5-3) as well.

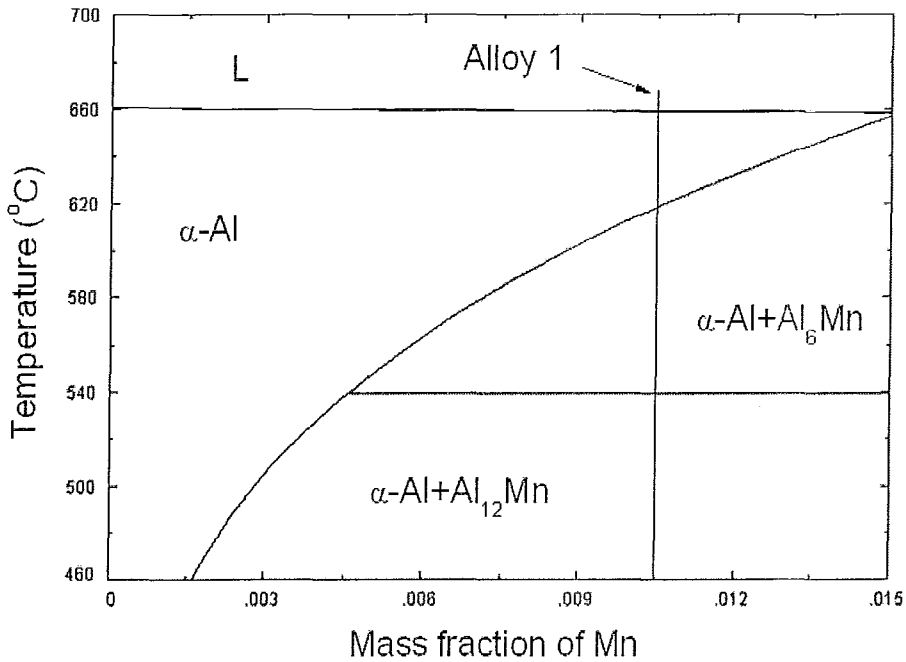

(a)

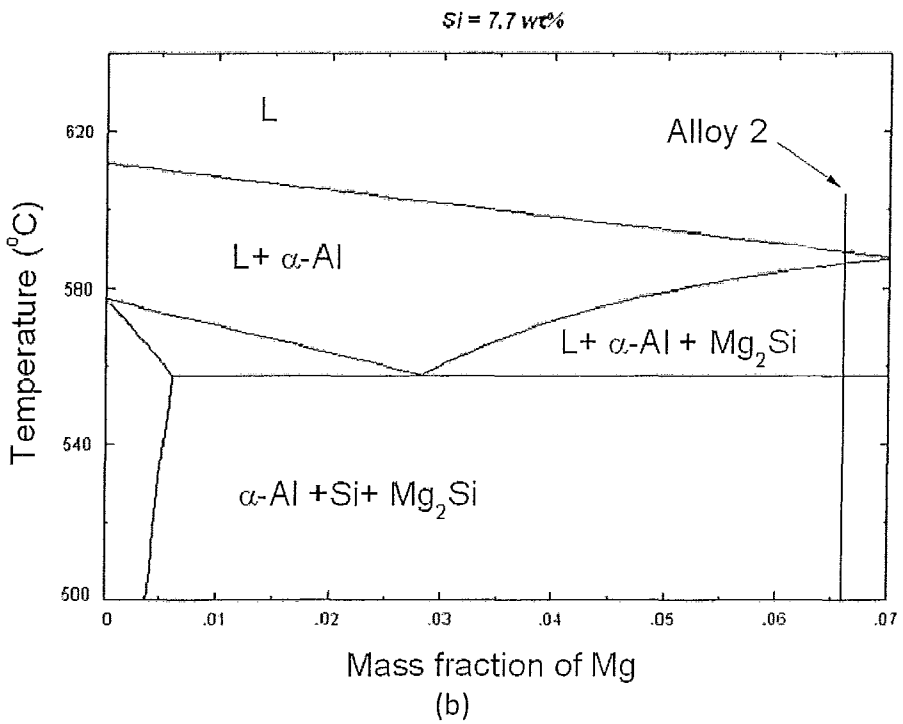

(b)

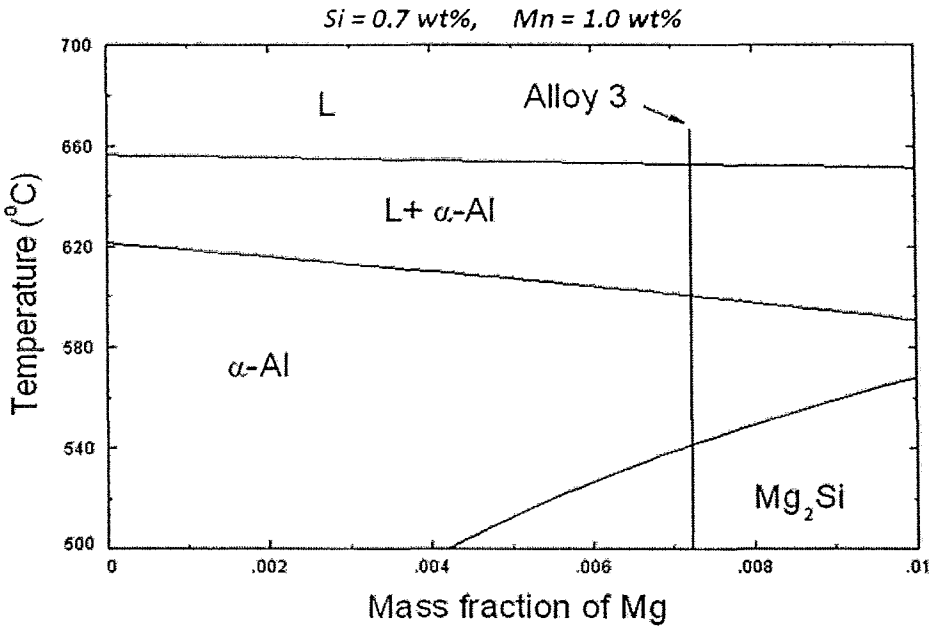

(c)

Figure 5-6. Three Isopleths from the Al-Si-Mg-Mn Phase Diagram showing the average compositions of (a) Alloy1, (b) Alloy2 and (c)Alloy 3 (6082).

Table 5-3. Notations and Variables used in the CDS experiments to cast 6082 Al wrought alloy. All the temperatures in this table are in degree centigrade.

Notation	Alloy 1	T_1	T_{L1}	Alloy 2	T_2	T_{L2}	m_r	Alloy 3
6082C1	Al-1.2Mn	668	659	Al-6.6Mg-7.7Si	619	604	10	Al-1.0Mn-0.6Mg-0.7Si
6082C2	Al-1.2Mn	678	659	Al-6.6Mg-7.7Si	619	604	10	Al-1.0Mn-0.6Mg-0.7Si
6082C3	Al-1.2Mn	686	659	Al-6.6Mg-7.7Si	616	604	10	Al-1.0Mn-0.6Mg 0.7Si
6082CC	Conventional casting of Al-1.0Mn-0.6Mg-0.7Si							

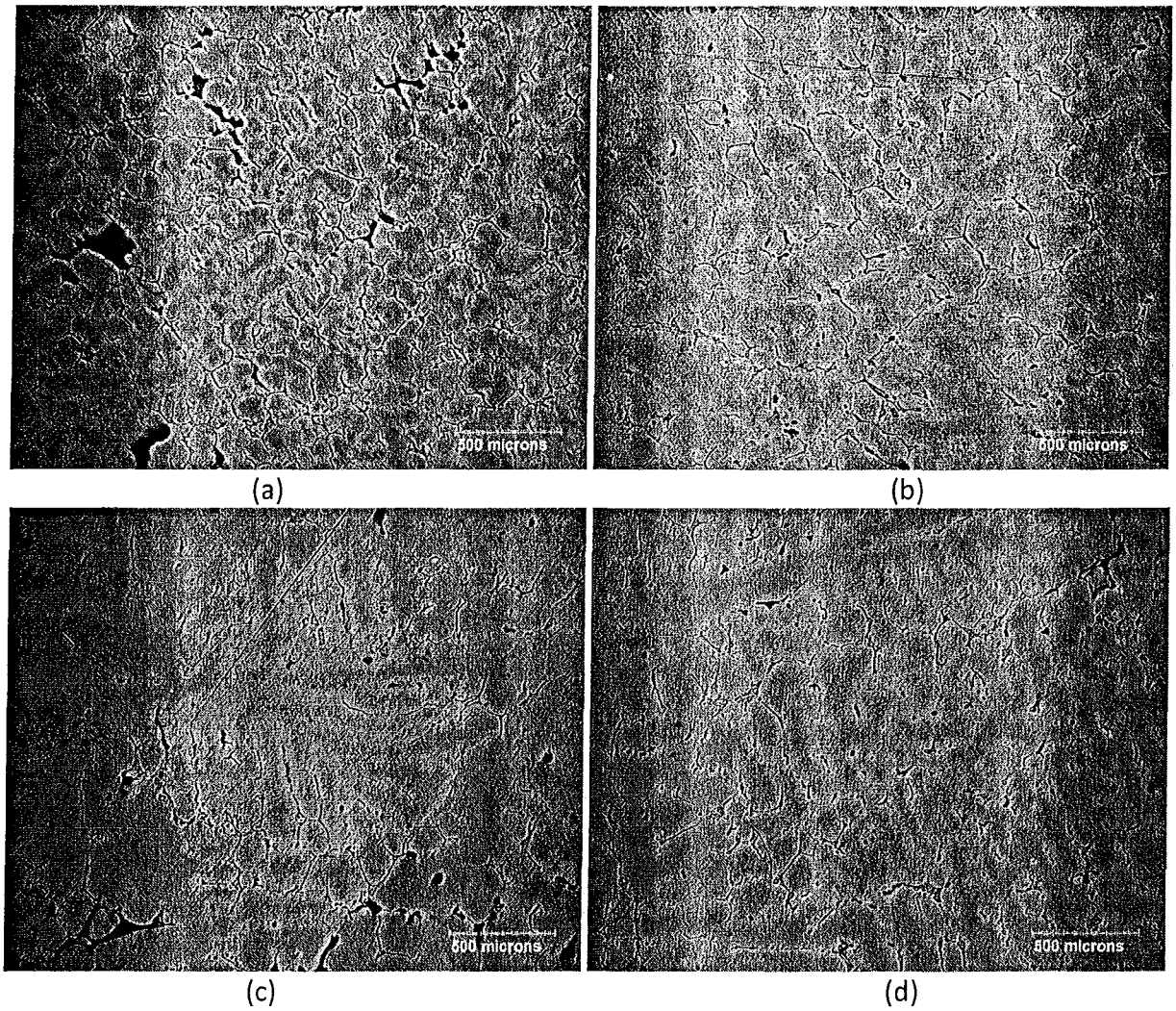

Figure 5-7. **Typical as-cast microstructures of 6082 alloy at various conditions shown in Table 5-3. (a) 6082C1 (non-dendritic and equiaxed primary phase), (b) 6082C2 (partially dendritic primary phase, (c) 6082C3 (dendritic primary phase) and (d) 6082CC (dendritic primary phase).**

Figure 5-7 shows that the most favourable microstructure for CDS process of 6082 alloys is obtained with the conditions for 6082C1. The microstructure of 6082C2 was nearly favourable and those of 6082C3 and 6082CC were unfavourable for a successful CDS process of 6082 alloy. Figure 5-8 shows the thermal data obtained during solidification of Alloy 3 (6082) under various conditions shown in Table 5-3. It can be observed that point B (refer to Figure 1-14) of 6082C1 is below the liquidus temperature, T_{L1} and those for 6082C2, 6082C3 and 6082CC are above. The thermal data in Figure 5-8 predicts that 6082C1 will be the most favourable among the alloys for the CDS process as validated by the microstructures in Figure 5-7.

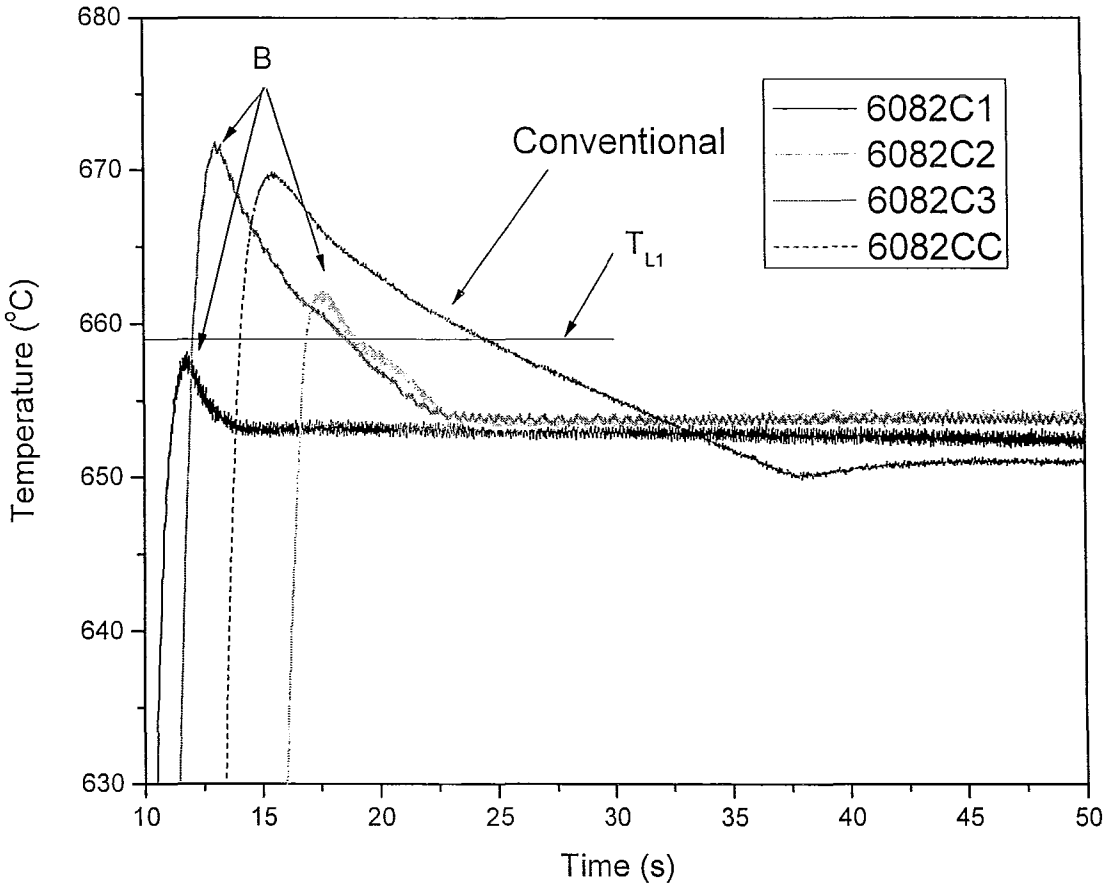

Figure 5-8. Thermal data obtained during solidification of Alloy 3 (6082) in Table 5-3.

5.2.3 7075 Al wrought Alloy

The procedure for optimization of alloy compositions and melt temperatures for 7075 alloy was similar to that described in Figure 5-2 and that used for optimization of 2024 and 6082 alloys. A mass ratio, $m_r = 6$ was chosen and the ΔT_L (= T_{L1}–T_{L2}) was 124 °C which was greater than the stipulated value of 60 °C in Figure 5-2. At this mass ratio, 300 grams of Alloy 1 was mixed into 50 grams of Alloy 2 to obtain 350 grams of Alloy 3 (7075). Visualization of Alloy 1, Alloy 2 and Alloy 3 was not possible in one isopleth of the Al-Zn-Cu-Mg phase diagram. Figure 5-9 are three isopleths of various multi-component phase diagrams showing the average compositions of Alloy 1 (Figure 5-6 (a)), Alloy 2 (Figure 5-9 (b)) and Alloy 3 (Figure 5-9 (c) for 7075 alloy). Table 5-4 shows the alloy notations and values of various variables used for the CDS experiments. A procedure similar to that described in the previous sub-section to cast 2024CC (Table 5-2) and 6082 (Table 5-3) was also used to obtain conventional casting sample 6082CC (Table 5-4) as well.

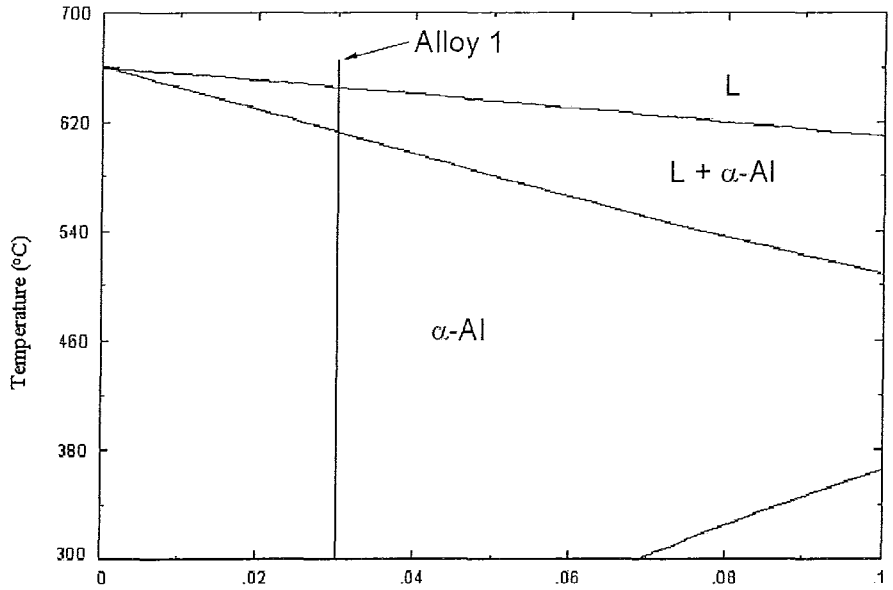
700
620
540
460
380
300
Temperature (°C)
Alloy 1
L
L + α-Al
α-Al
0
.02
.04
.06
.08
.1
Mass fraction of Mg

(a)

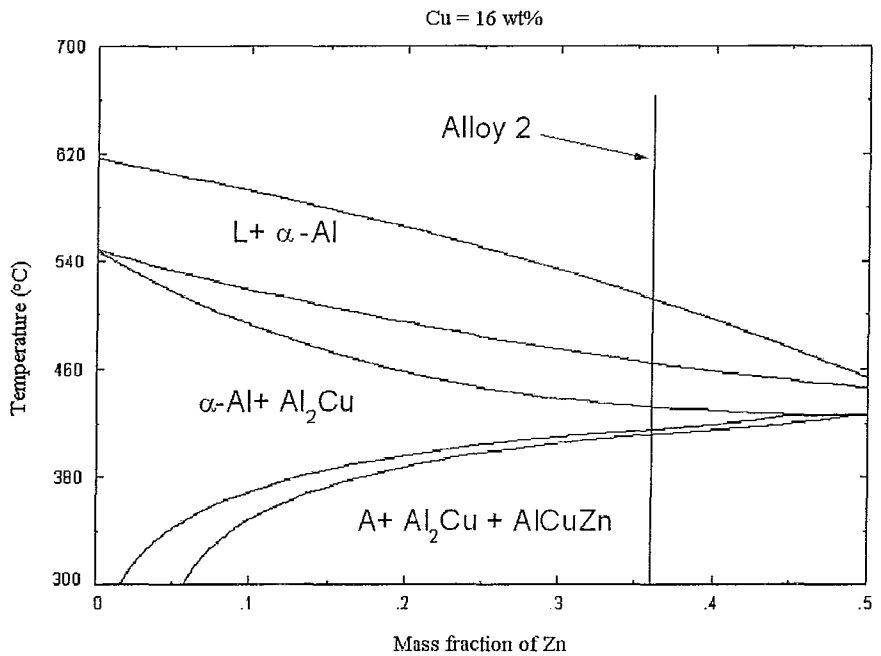
Cu = 16 wt%
700
620
540
460
380
300
Temperature (°C)
Alloy 2
L+ α-Al
α-Al+ Al2Cu
A+ Al2Cu + AlCuZn
0
.1
.2
.3
.4
.5
Mass fraction of Zn

(b)

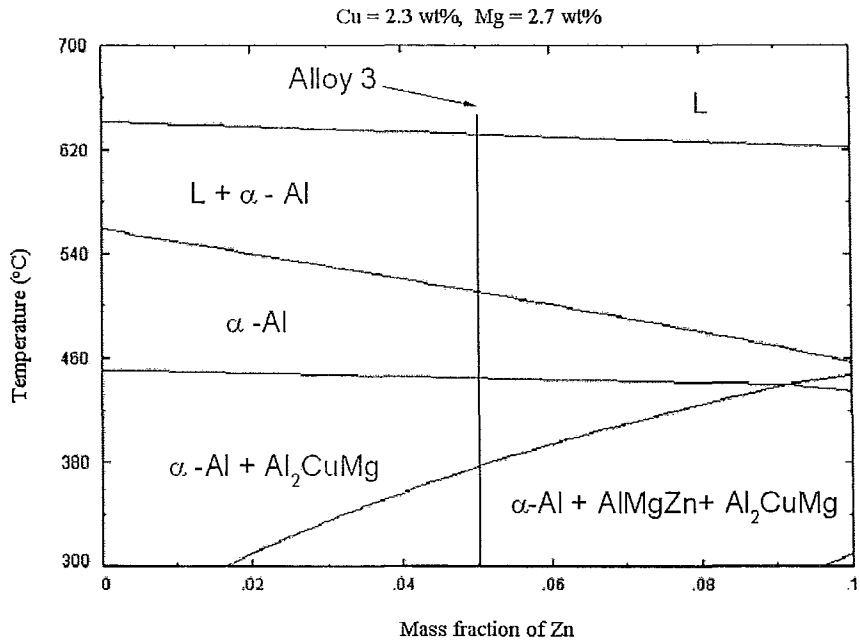

(c)

Figure 5-9. Three Isopleths from the Al-Zn-Cu-Mg Phase Diagram showing the average compositions of (a) Alloy1, (b) Alloy2 and (c)Alloy 3 (7075).

Table 5-4. Notations and Variables used in the CDS experiments to cast 7075 Al wrought alloy. All the temperatures in this table are in degree centigrade.

Notation	Alloy 1	T_1	T_{L1}	Alloy 2	T_2	T_{L2}	m_r	Alloy 3
7075C1	Al-3Mg	647	644	Al-16Cu-36Zn	534	520	6	Al-3.8Cu-5.6Zn-2.7Mg
7075C2	Al-3Mg	655	644	Al-16Cu-36Zn	531	520	6	Al-3.8Cu-5.6Zn-2.7Mg
7075C3	Al-3Mg	673	644	Al-16Cu-36Zn	528	520	6	Al-3.8Cu-5.6Zn-2.7Mg
7075CC	Conventional casting of Al-3.8Cu-5.6Zn-2.7Mg							

In Figure 5-10, (a), (b), (c) and (d) are typical microstructures of 7075C1, 7075C2, 7075C3 and 7075CC (Table 5-4), respectively. It can be observed that the 7075C1 and 7075C2 samples show a favourable non-dendritic morphology of the primary Al phase in Figure 5-10 (a) and (b), respectively. Figure 5-10 (c) shows that 7075C3 is partially dendritic with regions of rosette and dendritic morphologies, respectively in the microstructure. Figure 5-10 (d) shows the unfavourable dendritic morphology of the primary phase in 7075CC alloy samples.

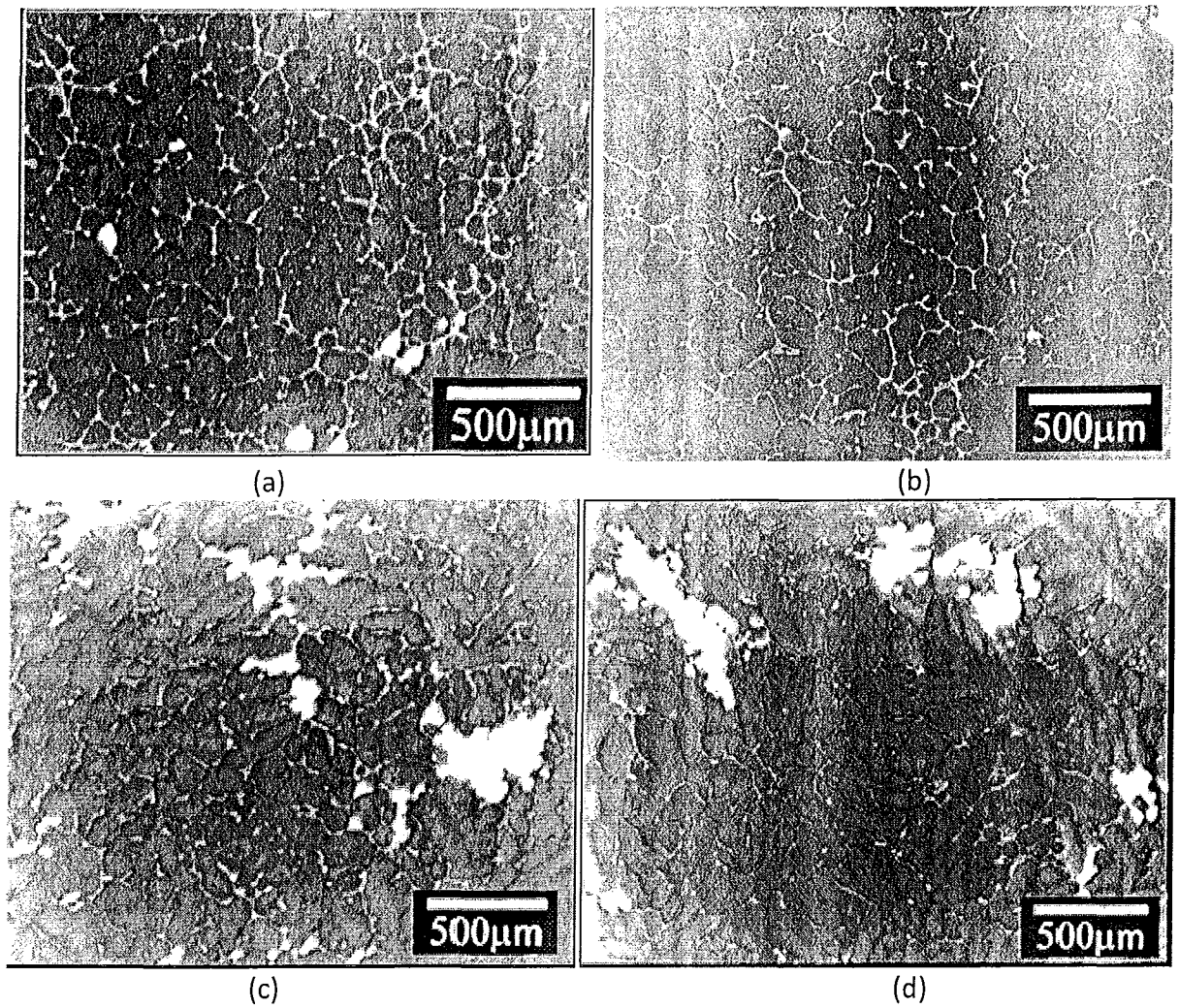

Figure 5-10. **Typical as-cast microstructures (inverted greyscale) of 7075 alloy at various conditions shown in Table 5-2. (a) 7075C1 (non-dendritic and equiaxed primary phase), (b) 7075C2 (non-dendritic and rosette shaped primary phase, (c) 7075C3 (partially dendritic primary phase) and (d) 7075CC (dendritic primary phase).**

The thermal data obtained during solidification of the alloys in Table 5-4 is shown in Figure 5-11. It has been hypothesized [20,24] that a successful CDS process is when the point B shown in Figure 1-14 is below the liquidus temperature of Alloy 1, T_{L1}. In Figure 5-11, it can be seen that the point B for 7075C1 and 7075C2 are below T_{L1} and that for 7075C3 is above predicting that conditions for 7075C1 and 7075C2 should be favourable for CDS as confirmed by the microstructures in Figure 5-10. Further, comparing Figure 5-11 and Figure 5-10, it can be hypothesized that the lower the point B in the thermal data obtained during mixing of the pre-cursor alloys, the more equiaxed is the morphology of the primary Al phase in the as-cast microstructure.

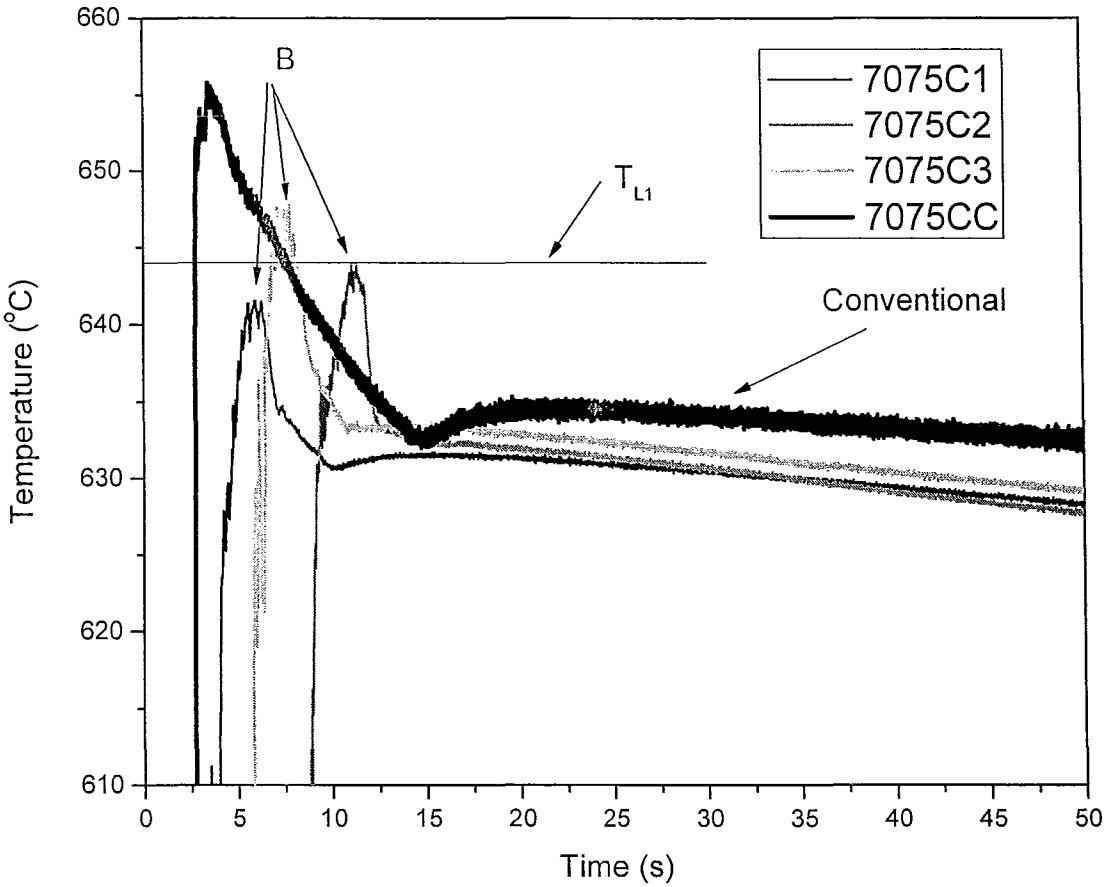

Figure 5-11. Thermal data obtained during solidification of Alloy 3 (7075) in Table 5-4.

5.3 SUMMARY

The following can be summarized from the material presented in this chapter:

- A viable procedure has been formulated to design and optimize the critical parameters in the CDS process such as the alloy compositions and melt temperatures of the two pre-cursor alloys.
- These parameters have been successfully optimized for 2024, 6082 and 7075 Al wrought alloys.
- It can be hypothesized that in the thermal data obtained during the mixing of the two pre-cursor alloys in a CDS process, the temperature of point B (defined in Figure 1-14) should be lower than the liquidus temperature of Alloy 1, T_{L1}.
- A non-dendritic morphology of the primary phase can be repeatedly obtained in the as-cast microstructure of most Al alloys with the CDS technology provided the optimum

conditions of alloy compositions and melt temperatures are used for the two pre-cursor alloys.

The observations and results from the experiments described in this chapter were used to design, optimize and shape cast the 2024, 6082 and 7075 Al wrought alloys into test bars for mechanical property evaluation in a tilt-pour casting equipment. The details and results of these casting trials are elaborated in the subsequent chapter.

Chapter 6 Tilt-Pour Casting of Al Wrought Alloys

This chapter presents the details of Phase 3 (Figure 2-1) of the project where in the 2024, 6082 and 7075 Al wrought alloys were cast into tensile (ASTM B557) and fatigue (ATM E466-96) test bars using the CDS technology for mechanical property assessment. The alloy composition and melt temperatures of the two pre-cursor alloys optimized in the Phase 2 (**Error! Reference source not found.**) of this project were used for the tilt-pour casting trials. The tilt-pour cast component from the three wrought alloys was considered acceptable and sound if the following conditions were met:

- No visual hot-cracking or hot-tearing on the cast component.
- No visual shrinkage or defect feature on the surface of the cast test bars.
- Non-dendritic morphology of the primary Al phase in the microstructure obtained from the cross-section of the gauge in the tensile test bar.
- Reasonably compact features in the optical low magnification micrograph of the fractures cross-section surface of the tensile bars.
- Reasonable tensile properties of the as-cast samples.

6.1 Nomenclature

The following presents the description of all the notations used in this chapter.

Alloy 1	Pre-cursor alloy with higher thermal mass (higher temperature and higher mass).
Alloy 2	Pre-cursor alloy with lower thermal mass.
Alloy 3	Resultant mixed alloy.
T_{L1} T_{L2} and T_{L3}	Liquidus temperature of Alloy 1, Alloy 2 and Alloy 3, respectively.
T_1, T_2 and T_3	Melt Temperature of Alloy 1, Alloy 2, and Alloy 3, respectively.
m_1 and m_2	Mass of Alloy 1 and Alloy 2 respectively.
m_r	Mass ratio of Alloy 1 and Alloy 2 (m_1:m_2).

6.2 Tilt Pour Casting process

The two pre-cursor alloys were melted in two separate electric crucible furnaces and both the alloys were degassed with ultrahigh purity Ar gas passed into the melt by a rotary degasser as explained in Chapter 4 for aluminum A356.2 alloy. The two alloys were held in their respective

crucible furnaces at the prescribed alloy temperatures, T_1 and T_2, respectively. Two ladles were designed to scoop out the prescribed amounts of the individual alloys. The metal mould in the tilt-pour machine was pre-heated to about 350 °C. The prescribed amount of Alloy 2 at temperature, T_2 was poured first into the pouring cup following by the Alloy 1 at temperature, T_1 mixed into Alloy 2 in the pouring cup. Instantly after pouring Alloy 1 in to the cup, the tilt-machine was activated by the foot pedal (Figure 4-3) to begin the tilt process as described in Chapter 4. Subsequent to filling, the alloy was allowed to solidify in the mould for a few minutes. A K-type thermocouple mounted on the mould cavity surface was constantly monitored during solidification. The temperature of this thermocouple continuously increased during solidification and the instant this temperature began to drop, the mould was opened and the cast component ejected. The mould was then sprayed with compressed air to remove any possible debris from the casting and then shut for the next casting. The mould temperature was monitored to reach the prescribed 350 °C for each and every casting. The cast part was subjected to visual inspection after ejection to ascertain the casting quality. The gross weight of the ejected cast component was about 900 grams. Table 6-1 presents the variables used in the tilt-pour casting trials of the three alloys in this study.

Table 6-1. Notations, process and alloy variables used in the tilt-pour casting trials.

Notation	Alloy 1	T_1	T_{L1}	Alloy 2	T_2	T_{L2}	m_r	Alloy 3
2024T	Al-1.5Mg-1Mn	668	658	Al-33Cu-1.5Mg	579	565	6	Al-4.7Cu-1.5Mg-0.85Mn
6082T	Al-1.1Mn	673	657	Al-6.6Mg-7.7Si	594	584	10	Al-1Mn-0.6Mg-0.7Si
7075T	Al-2.5Mg-0.32Cr	670	659	Al-2.5Mg-8.5Cu-35.6Zn	615	605	6	Al-2.5Mg-.27Cr-1.2Cu-5Zn
2024TC								
6082TC	Conventional casting trails (tilt-pour process) with a melt superheat >60°C							
7075TC								

As explained in Chapter 4 for casting aluminium A356.2 alloy, the metal mould was coated with Dycote 39 for improved heat retention in the mould during filling and solidification of the molten alloy.

Figure 6-1 (a) and (b) show an example of visual inspection of a defective casting and sound good quality casting, respectively. Figure 6-1(a) presents photographs of a defective casting obtained by the conventional casting of 2024 Al alloy with about 60 °C melt superheat above the liquidus temperature in the tilt pour process. The conventional casting in this photograph shows a few hot tears and cracking of the as-cast test bars which renders the casting

unsuitable. The same 2024 alloy was cast in the tilt-pour casting process with the CDS technology (Table 6-1) yielding a sound and good quality cast component with no issues of hot tearing/cracking or shrinkages on the test bars as shown in Figure 6-1(b).

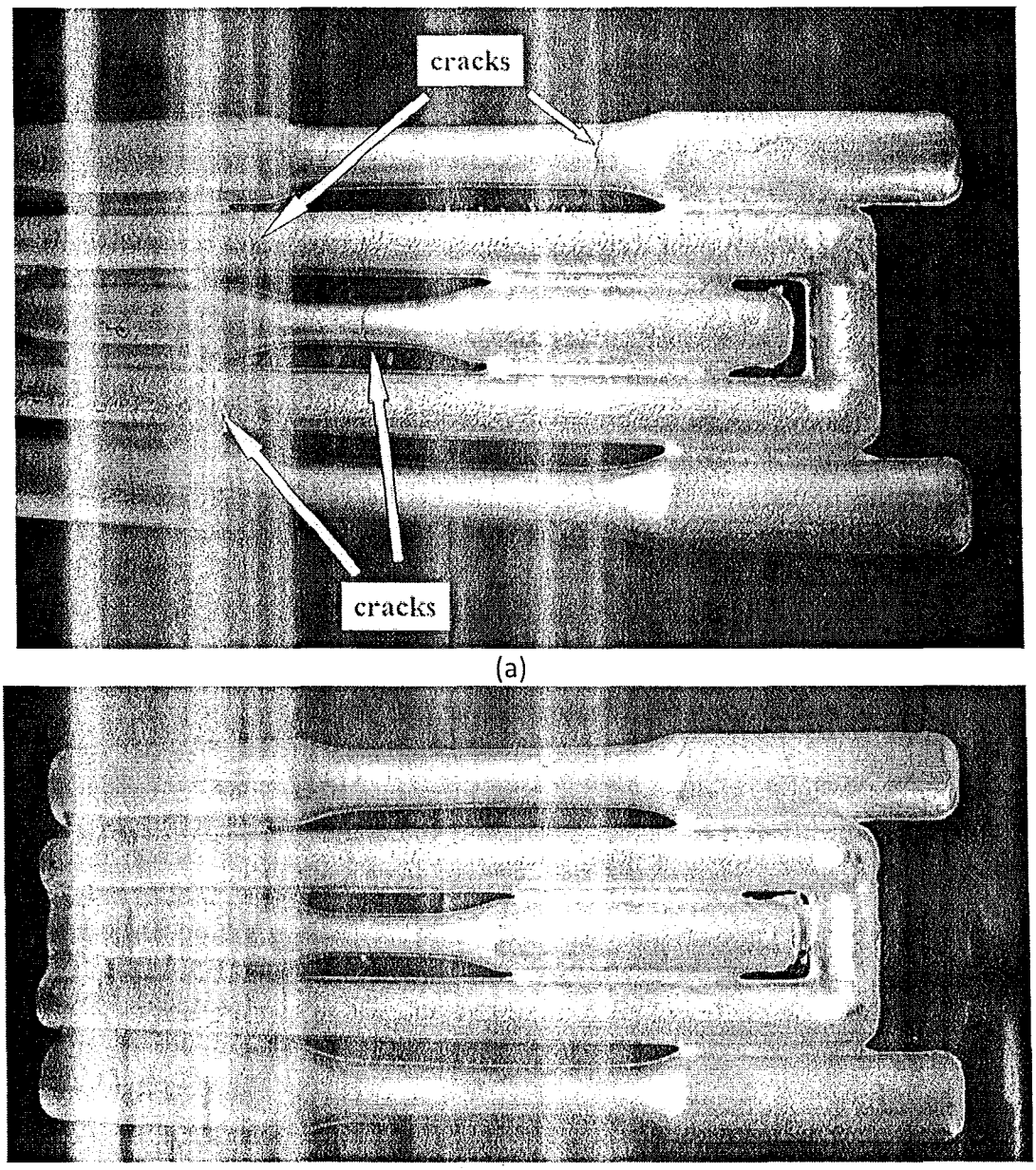

Figure 6-1. Photographs of cast parts produced in the tilt-pour casting trials. **(a)** conventional casting of high superheated 2024 Al alloy showing **hot** tearing/cracking on various critical surfaces **(defective casting) and (b) shape** casting of 2024 Al alloy produced by CDS technology **(sound casting).**

Subsequent to casting the samples, the test bars were machined out of the casting and microstructure analysis was carried out in a sample sectioned from the gauge length in one of

the cast tensile bars. Five samples each were set aside for tensile property assessment in each of the three temper (F, T4 and T6) conditions, respectively.

For each and every tilt-pour casting trial, k-type thermocouples were inserted in the pouring cup to continuously monitor the melt temperatures before, during and after the mixing process in CDS.

In the subsequent sections of this chapter, the results of the tilt-pour casting trials for 2024, 6082 and 7075 Al alloys with the casting parameters shown in Table 6-1 are presented.

6.2.1 2024 Al wrought alloy

Figure 6-2 shows typical optical micrographs showing the microstructure of the cross-section of the cast component obtained from the gauge of an as-cast tensile bar of 2024 Al alloy. Figure 6-2(a) shows the microstructure for 2024T casting with the non-dendritic morphology of the primary Al phase with no discernable casting defect and Figure 6-2(b) shows the dendritic morphology of the primary Al phase in a 2024TC casting with a distinct shrinkage porosity defect as expected in a conventional casting of the wrought alloys. Figure 6-3 shows typical images of the fracture surface obtained on the tensile test bars after testing for 2024T and 2024TC samples. Figure 6-3 (a) and (b) show a reasonable compact structure of 2024T sample with a nearly ductile fracture and no discernable dendritic structure could be observed. Figure 6-3 (c) and (d) show a defective casting of 2024TC sample with several voids (porosity) evident from the clearly defined dendrites in the microstructure. Figure 6-4 shows the typical thermal data obtained from eth pouring cup during the tilt-pour casting trials of 2024T alloy. The data was obtained before, during and after the missing process in the pouring cup. The thermal data shows that the point B (Figure 1-14) lies well below the liquidus temperature, T_{L1} predicting a good CDS process.

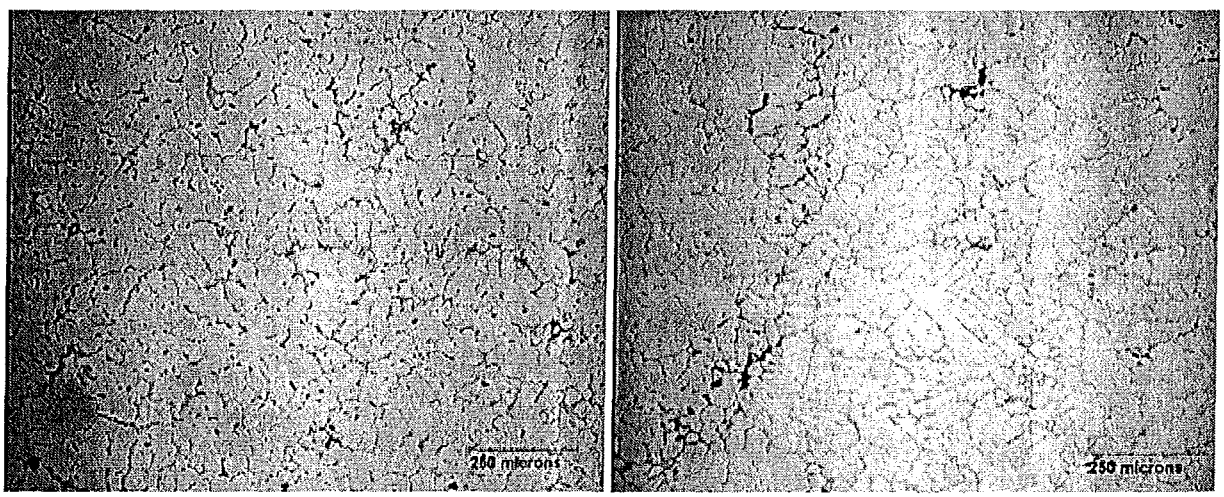

(a) (b)

Figure 6-2. Typical microstructure of the gauge section of tensile bars for 2024 Al alloy. (a) 2024T and (b) 2024TC.

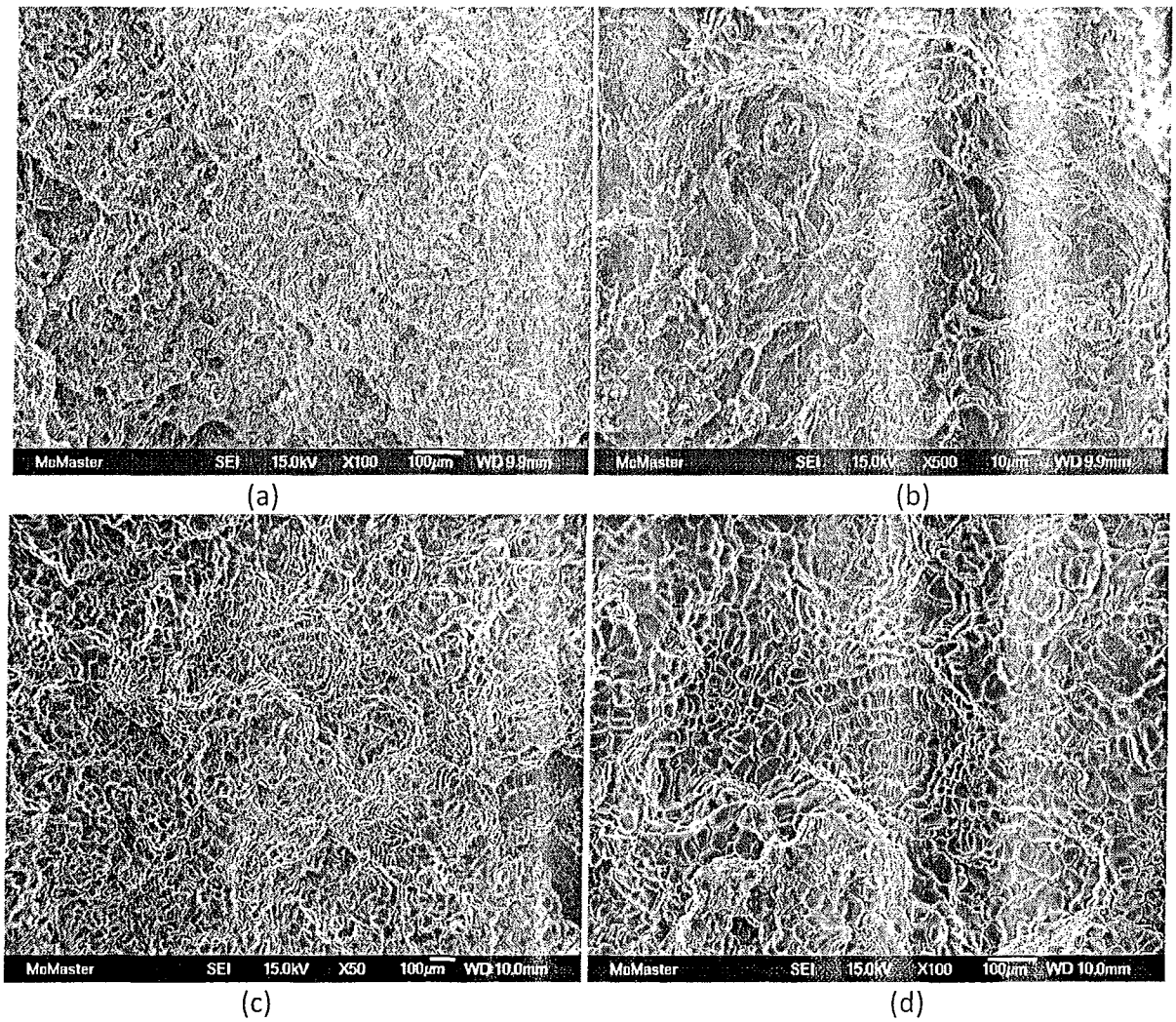

Figure 6-3. Typical Scanning Electron Microscope (SEM) images of fracture surface of the tensile bar cross-section after the testing. (a) low magnification 2024T sample showing a reasonable clean and compact fracture, (b) high magnification 2024T sample showing, (c) low magnification 2024TC sample with numerous voids shown by the definition of the dendrites and lack of soundness and (d) high magnification 2024TC sample.

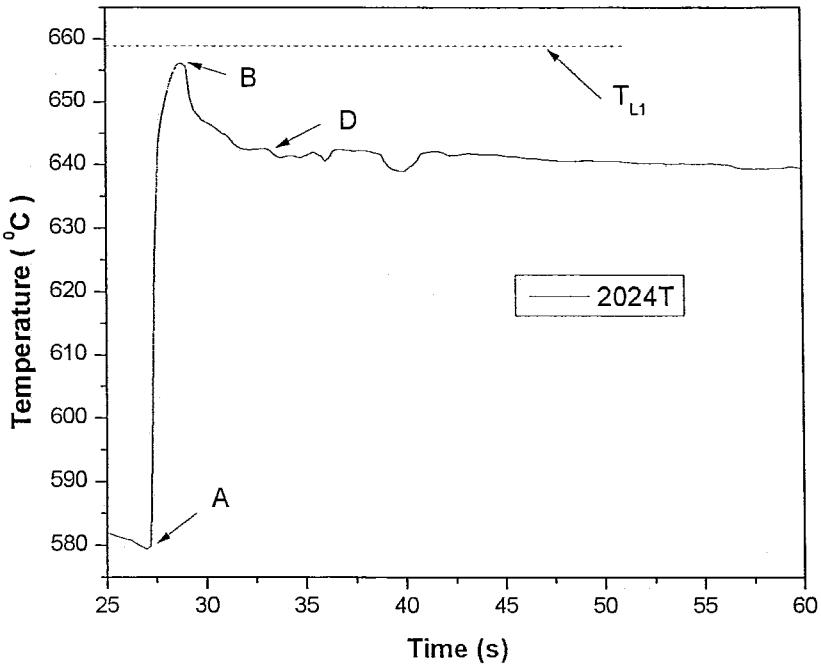

Figure 6-4. **Typical thermal data obtained from the pouring cup during the tilt-pour casting trials of 2024T samples. The data reflects the regions before, during and after the mixing process in CDS for this alloy (Figure 1-14).**

6.2.2 6082 Al wrought alloy

Figure 6-5 shows typical optical micrographs showing the microstructure of the cross-section of the cast component obtained from the gauge of an as-cast tensile bar of 6082 Al alloy. Figure 6-5(a) shows the microstructure for 6082T casting with the non-dendritic morphology of the primary Al phase with no discernable casting defect and Figure 6-5(b) shows the dendritic morphology of the primary Al phase in a 6082TC casting with a distinct shrinkage porosity defect as expected in a conventional casting of the wrought alloys. Figure 6-3 shows typical images of the fracture surface obtained on the tensile test bars after testing for 6082T and 6082TC samples. Figure 6-6 (a) and (b) show a reasonable compact structure of 6082 T alloy with a nearly ductile fracture and no discernable dendritic structure could be observed. Figure 6-6 (c) and (d) show a defective casting of 6082TC sample with several voids (porosity) evident from the clearly defined dendrites in the microstructure. Figure 6-7 shows the typical thermal data obtained from the pouring cup during the tilt-pour casting trials of 6082T alloy. The data was obtained before, during and after the mixing process in the pouring cup. The thermal data shows that the point B (Figure 1-14) lies well below the liquidus temperature, T_{L1} predicting a good CDS process.

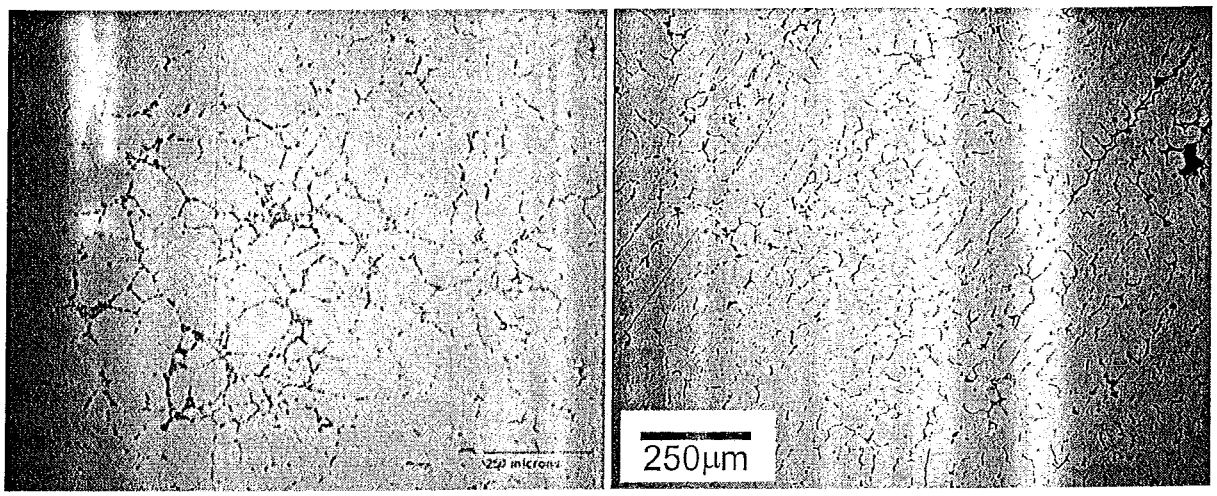

(a) (b)

Figure 6-5. **Typical microstructure of the gauge section of tensile bars for 6082 Al alloy. (a) 6082T and (b) 6082TC.**

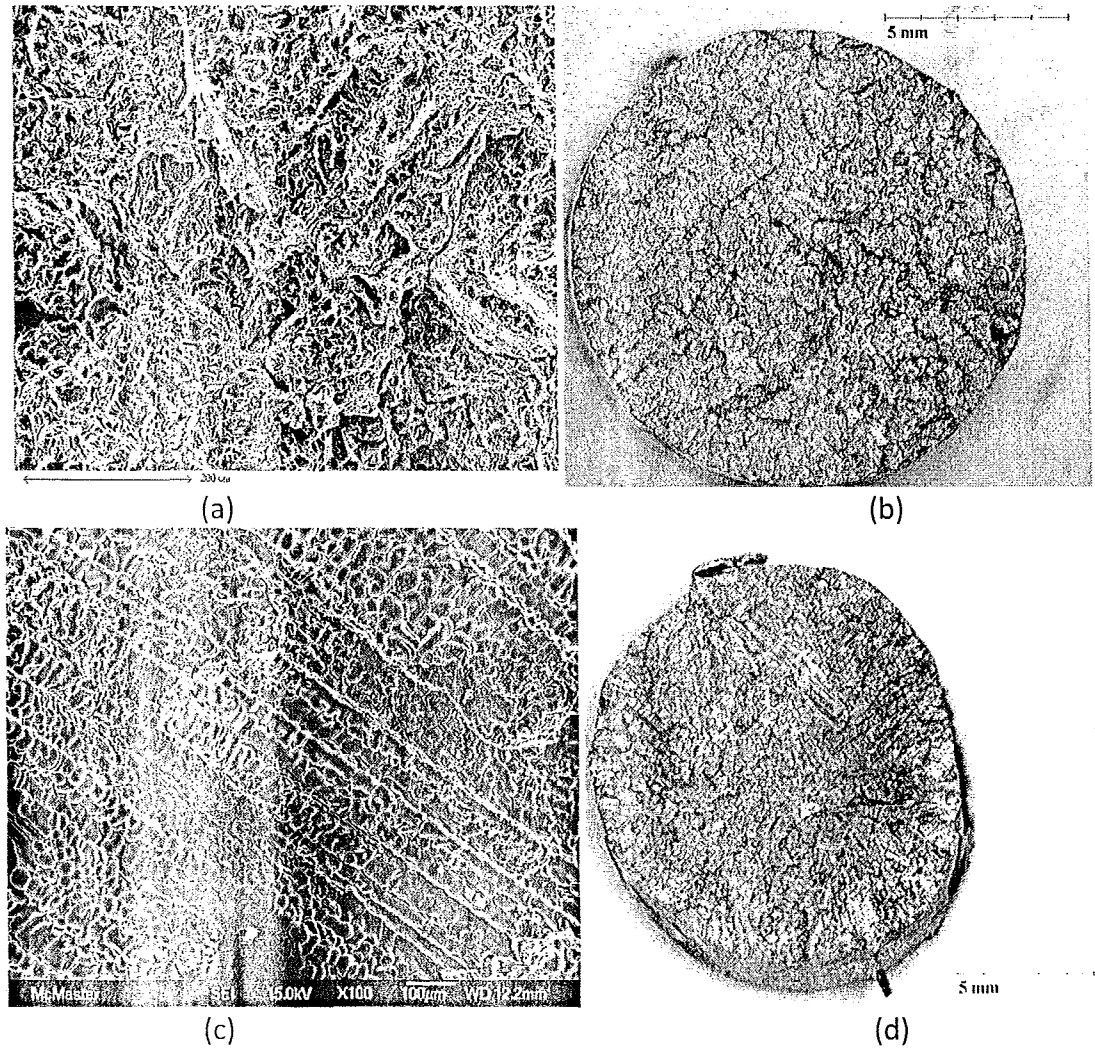

Figure 6-6. Typical images of fracture surface of the tensile bar cross-section after the testing. (a) Scanning Electron Microscope (SEM) image of 6082T sample showing a reasonable clean and compact fracture, (b) low magnification optical image showing a compact relatively defect-free surface, (c) SEM image of 6082TC sample and (d) low magnification image of 6082TC sample with numerous voids shown by the definition of the dendrites and lack of soundness.

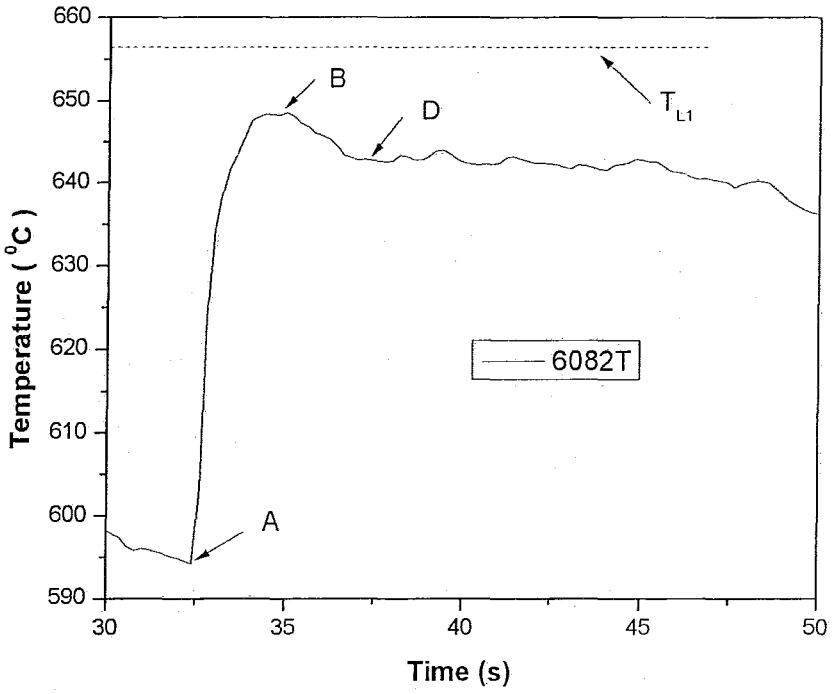

Figure 6-7. Typical thermal data obtained from the pouring cup during the tilt-pour casting trials of 6082T samples. The data reflects the regions before, during and after the mixing process in CDS for this alloy (Figure 1-14).

6.2.3 7075 Al wrought alloy

Figure 6-8 shows typical optical micrographs showing the microstructure of the cross-section of the cast component obtained from the gauge of an as-cast tensile bar of 7075 Al alloy. Figure 6-8(a) shows the microstructure for 7075T casting with the non-dendritic morphology of the primary Al phase with no discernable casting defect and Figure 6-8 (b) shows the dendritic morphology of the primary Al phase in a 7075TC casting with a distinct shrinkage porosity defect as expected in a conventional casting of the wrought alloys. Figure 6-9 (a) and (b) shows typical images of the fracture surface obtained on the tensile test bars after testing for 7075T and 7075TC samples, respectively. Figure 6-9 (a) shows a reasonable compact structure with a nearly ductile fracture and no discernable dendritic structure could be observed. Figure 6-9 (b) shows a defective casting of 7075TC sample with several voids (porosity) evident from the clearly defined dendrites in the microstructure. Figure 6-10 shows the typical thermal data obtained from the pouring cup during the tilt-pour casting trials of 7075T alloy. The data was obtained before, during and after the mixing process in the pouring cup. The thermal data shows that the point B (Figure 1-14) lies well below the liquidus temperature, T_{L1} predicting a good CDS process.

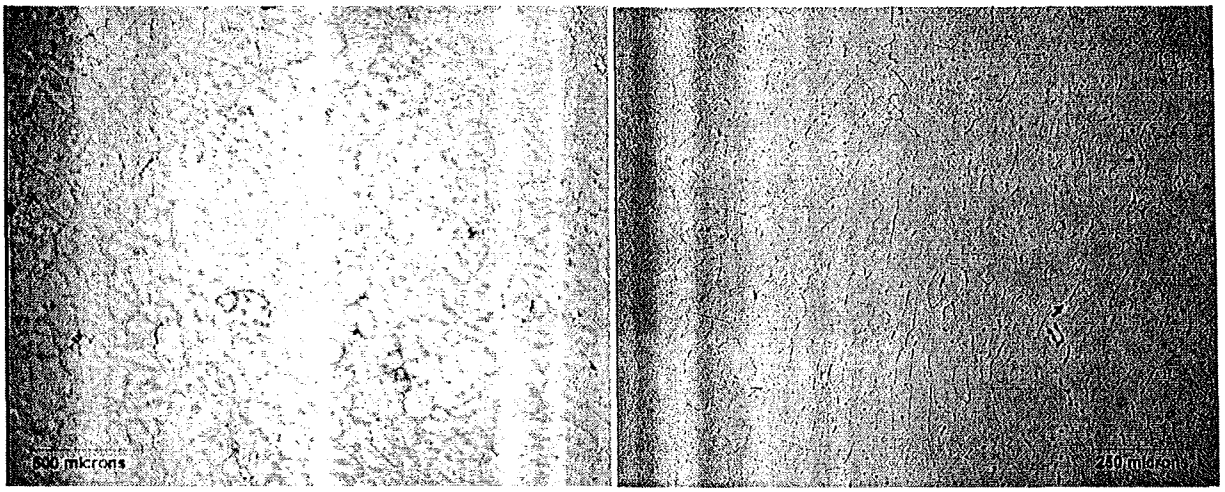

(a) (b)

Figure 6-8. Typical microstructure of the gauge section of tensile bars for 7075 Al alloy. (a) 7075T showing non-dendritic primary phase and (b) 7075TC showing dendritic primary phase.

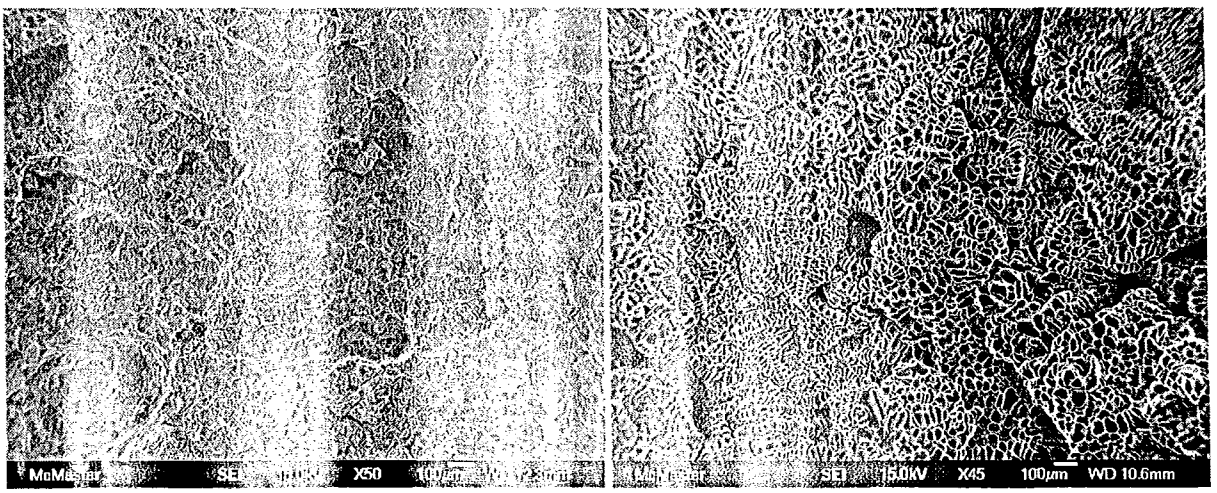

(a) (b)

Figure 6-9. Typical SEM images of fracture surface of the tensile bar cross-section after the testing. (a) 7075T sample showing a reasonable clean and compact fracture, (d) 7075TC sample with numerous voids shown by the definition of the dendrites and lack of soundness.

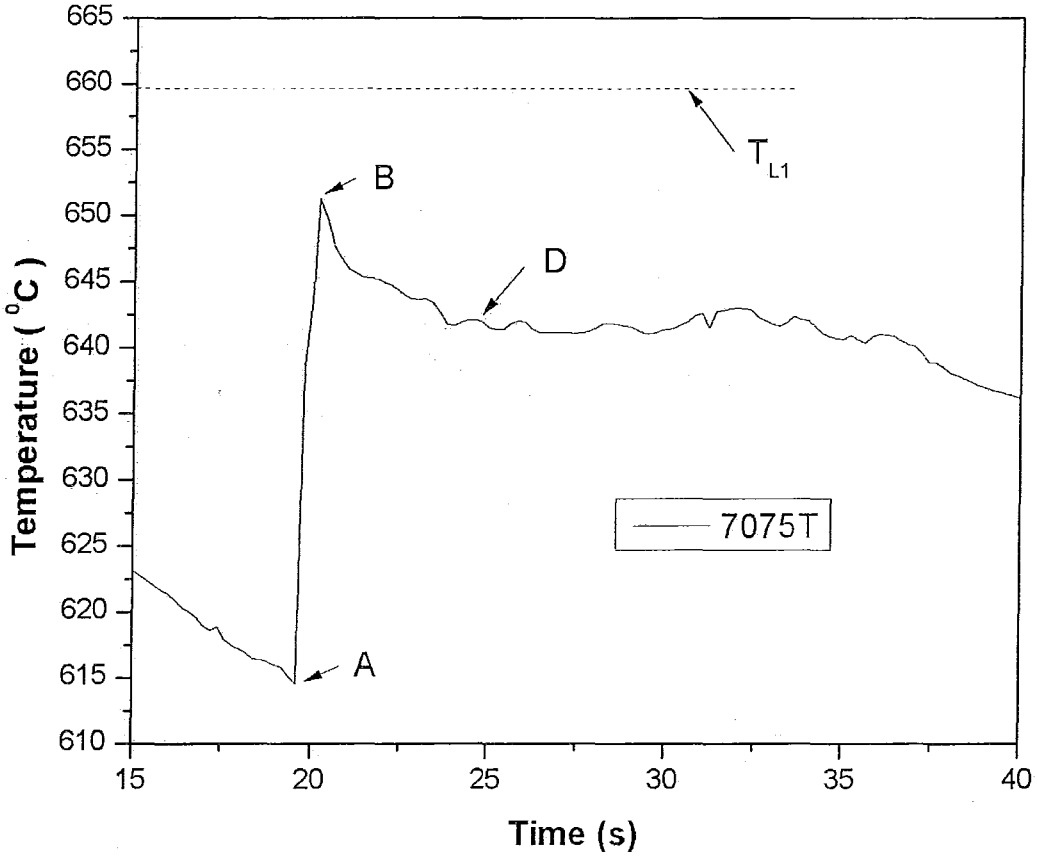

Figure 6-10. Typical thermal data obtained from the pouring cup during the tilt-pour casting trials of 7075T samples. The data reflects the regions before, during and after the mixing process in CDS for this alloy (Figure 1-14).

6.3 Tensile Properties

The tilt-pour casting samples of 2024, 6082 and 7075 were heat treated to three tempers, F (as-cast), T4 and T6, as shown in Table 6-2. Table 6-3 shows the tensile properties of the three alloys cast using CDS technology in the tilt-pour casting trials. The aim of this work is not to maximize or optimize these properties but to demonstrate that the tensile properties are reasonably sound and the castings have a reasonable level of integrity. Improvements to the process will enable significant improvements to these properties. The 2024TC, 6082TC and 7075TC conventional casting samples (Table 6-1) did not exhibit any tensile properties as these samples broke during or instantaneously after loading and starting the tensile test showing that the castings are defective and do not posses any integrity. Further, the heat treatment tempers for these alloys were selected from the literature [[25], [26] of Al wrought alloy processing which may not be suitable for heat treating shape castings because the microstructure and phase formation in a shape cast alloy would be vastly different from those in components that

underwent solid-state processing such as forging, extrusion and rolling. Significant improvements are possible in the CDS process, alloy composition selection and heat treatment cycles and these will enable maximizing the tensile properties of these alloys.

Table 6-2. Heat treatment tempers for the alloys before testing tensile properties. No natural ageing F was carried out and T4 solutionizing and then T6 tempers.

Notation	Temper	Solutionizing	Artificial Ageing
2024T	F (As-Cast)	None	None
	T4	410 °C for 12 hours and quenched in water at 80 °C	None
	T6	410 °C for 12 hours and quenched in water at 80 °C	140 °C for 6 hours and air cooled.
6082T	F (As-Cast)	None	None
	T4	530 °C for 12 hours and quenched in water at 80 °C	None
	T6	530 °C for 12 hours and quenched in water at 80 °C	160 °C for 16 hours and air cooled.
7075T	F (As-Cast)	None	None
	T4	410 °C for 12 hours and quenched in water at 80 °C	None
	T6	410 °C for 12 hours and quenched in water at 80 °C	120 °C for 24 hours and air cooled.

The CDS technology used in these tilt-pour casting trials were crude with minimum control over the melt cleanliness and prevention of inclusions and artifacts during the manual mixing process. Further, the project only aims to demonstrate the feasibility of the CDS casting technology to cast Al wrought alloys and the tilt-pour casting equipment was used for this purpose because this casting process is not pressure assisted and demonstrates the nearly worst case scenario to produce a casting with integrity. The results have amply demonstrated that even in this process the castings possessed reasonable integrity and when compared with the failed attempts to shape cast the three Al wrought alloys by the conventional process, the CDS technology offers realistic hopes to shape cast Al wrought alloys.

The results of this study further show that it will be significantly beneficial to explore casting Al wrought alloys with the CDS technology in a pressure-assisted casting process such as High Pressure Die Casting (HPDC) and/or Squeeze Casting.

Table 6-3. Tensile properties of the alloys cast in the tilt-pour casting trials with CDS.

Sample no.	Temper	UTS	Std. Dev.	YS (0.02%)	Std. Dev.	Elongation (%)	Std. Dev.

		Mpa (Ksi)	Mpa (Ksi)	Mpa (Ksi)	Mpa (Ksi)		
2024T	F (As-Cast)	217.61 (31.58)	11.81	152.5 (22.13)	7.21	1.04	0.01
	T4	212.8 (30.88)	15.62	142.9(20.74)	7.42	1.092	0.43
	T6	212.54 (30.85)	11.73	151.42 (21.98)	3.04	0.9	0.18
6062T	F (As-Cast)	184.96 (26.84)	3.80	99.63 (14.46)	6.61	3.24	0.57
	T4	208.19 (30.21)	7.62	106.00 (15.38)	3.49	3.64	0.70
	T6	287.92 (41.79)	7.62	230.13 (33.40)	3.64	2.34	0.7
7075T	F (As-Cast)	162.34 (23.56)	8.11	109.68 (15.92)	13.5	1.08	13.5
	T4	221.57 (32.16)	3.91	97.35 (14.13)	0.49	9.37	0.49
	T6	324.08 (47.03)	14.59	301.12 (43.70)	10.54	0.79	10.54

6.4 SUMMARY

The Phase 3 of this study has shown that it is viable to shape cast Al wrought alloys, specifically, 2024, 6082 and 7075 alloys by the CDS technology in a tilt-pour casting process. Shape cast components of these alloys by CDS and tilt-pour casting process shows reasonable levels of integrity, no discernable hot-tearing phenomenon and no visual and unusual casting defects. Attempts to shape cast these alloys by conventional means using a superheated melt failed and did not yield any casting with integrity. The study clearly demonstrates that further study to optimize the CDS process for a commercial casting operation is essential to explore shape casting of various Al wrought alloys. Additionally, the heat treatment of shape cast Al wrought alloys would be vastly different from net shaped components made by conventional solid-state transformation processes using these alloys due to the significant differences in microstructure and phase formation in these components. Hence, it will be essential to carry out a thorough and scientific investigation to define new heat treatment cycles for various shape cast Al wrought alloys.

Chapter 7 Scrap Management in CDS Technology

Scrap handling is a critical issue in commercial casting technology. The castings ejected from the die mould typically have many of essential features attached to the cast component such as sprue, runners, risers, in-gates and overflows. These features will have to be cut off from the casting to obtain the cast component. The material in these additional features are typically re-melted and cast again.

In conventional casting process, there is only one alloy melt that is cast and re-melted and hence recycling scrap is not a grave issue. However, in CDS technology the initial pre-cursor alloys are of a different composition than that of the final cast part and hence a viable scrap recycling strategy would have to be conceived and formulated.

This chapter presents a viable scrap recycling strategy for CDS casting of 2024 Al wrought alloys used in this study. The scrap management scheme presented for this alloy can be employed for other Al alloys cast with CDS technology as well.

7.1 Scrap Recycling Strategy

The nomenclature used in this chapter is identical to that presented in Chapter 6.

Typically 20 to 30 percent of the total casting weight is scrap that needs recycling. The compositions of two pre-cursor alloys, Alloy 1 and Alloy 2, are designed such that 20 to 30 percent of the total weight of the cast part can be added directly to Alloy 1 melt and the CDS process carried out as described in previous chapters. To enable scrap addition to Alloy 1, the initial compositions of Alloy 1 and Alloy2 will be accordingly chosen and the alloy melt temperatures determined from various isopleths in the respective alloy phase diagrams.

Examples of Alloy design for CDS casting of 2024 by tilt-pour casting process is presented in Table 7-1. In Table 7-1, three possible scenarios wherein 20%, 30% and 40% by weight of Alloy 1 are made from scrap recycled from the castings of Alloy 3 (2024) are presented. In each case, the composition of Alloy 1, Alloy 2 and Alloy 3 are the same. The mass ratios, m_r, used for the CDS process for 20, 30 and 40% scrap recycled vary as 6.7, 7.66 and 8.94, respectively. The only variable for an industry adopting to cast this alloy by CDS will be the alloy composition the parent ingot used to make Alloy 1 melt as shown by the notation 'Ingot 1' in Table 7-1. This table shows that scrap recycling is viable for CDS process and a table akin to Table 7-1 would have to be constructed for each Al alloy (Alloy 3) intended to be cast into a shaped component.

Table 7-1. CDS process alloy compositions of 2024 Al wrought alloy with three different scrap recycling schemes.

Percentage Scrap Recycled	Alloy Type	Weight % Addition	Weight % element			
			Mg	Mn	Cu	Al
	Ingot 1	80	1.78	0.71	0	92.99
	Alloy 3 (recycled scrap)	20	1.50	0.60	4.40	93.50
20%	**Alloy 1**		1.72	0.69	0.88	**93.09**
	Alloy 2		0	0	28	**96.22**
	Alloy 3		*1.50*	*0.60*	*4.40*	***93.50***
	Mass Ratio			*6.70*		
	Ingot 1	70	1.78	0.71	0	92.99
	Alloy 3 (recycled scrap)	30	1.50	0.60	4.40	93.50
30%	**Alloy 1**		1.70	0.68	1.32	**93.15**
	Alloy 2		0	0	28	**96.22**
	Alloy 3		*1.50*	*0.60*	*4.40*	***93.50***
	Mass Ratio			*7.66*		
	Ingot 1	60	1.78	0.71	0	92.99
	Alloy 3 (recycled scrap)	40	1.50	0.60	4.40	93.50
40%	**Alloy 1**		1.67	0.67	1.76	**93.20**
	Alloy 2		0	0	28	**96.22**
	Alloy 3		*1.50*	*0.60*	*4.40*	***93.50***
	Mass Ratio			*8.94*		

Figure 7-1 shows typical microstructure of 2024 alloy cast with CDS technology (Figure 7-1(a)) and conventional technology with a 60 °C melt superheat for the alloy (Figure 7-1(b)). The CDS process was carried out with Alloy 1 having 30% by weight scrap recycled from the Alloy 3 (2024) castings. Figure 7-1(a) shows that the CDS process yielded a non-dendritic morphology of the primary phase in the microstructure where as the morphology of the conventional cast 2024 sample in Figure 7-1(b) has non-dendritic primary phase.

In order to achieve precise control over Mass Ratio an automated device for mixing is recommended.

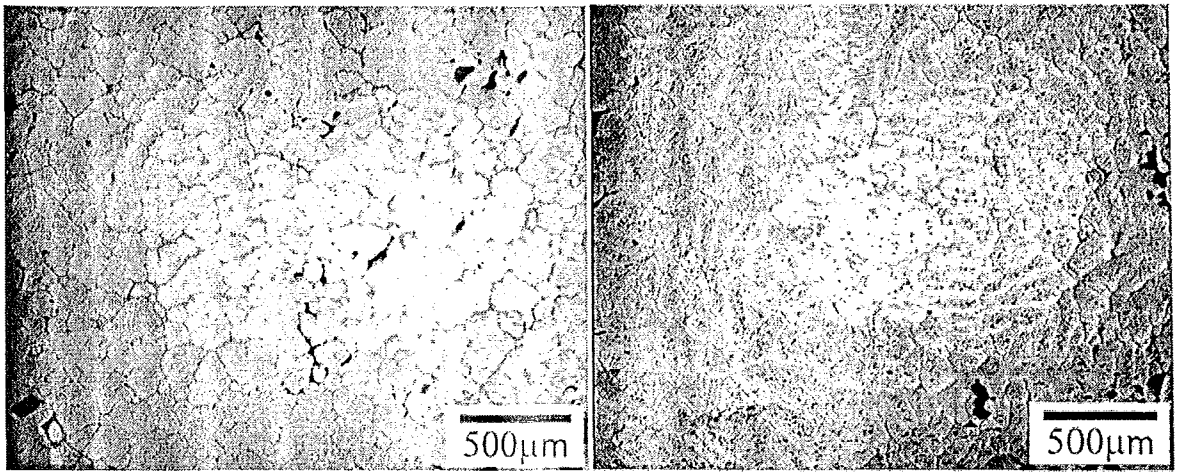

(a) (b)

Figure 7-1. Typical microstructure of 2024 alloy cast in tilt-pour casting trails. The alloy 1 in this case had 30% by weight of scrap recycled from Alloy 3 (2024) castings to verify the scrap recycling scheme presented in Table 7-1. (a) CDS technology showing non-dendritic primary phase and (b) conventional casting of 2024 with 60 °C melt superheat showing dendritic primary phase.

Table 7-1 shows the typical thermal data obtained from the pouring cup during the tilt-pour casting of 2024 alloy with CDS technology and a 30% scrap recycling scheme as shown in Table 7-1. The point B (Figure 1-14) is well below the liquidus temperature, T_{L1} predicting a good CDS process and a non-dendritic morphology of the primary phase in the as-cast microstructure as confirmed by Figure 7-1.

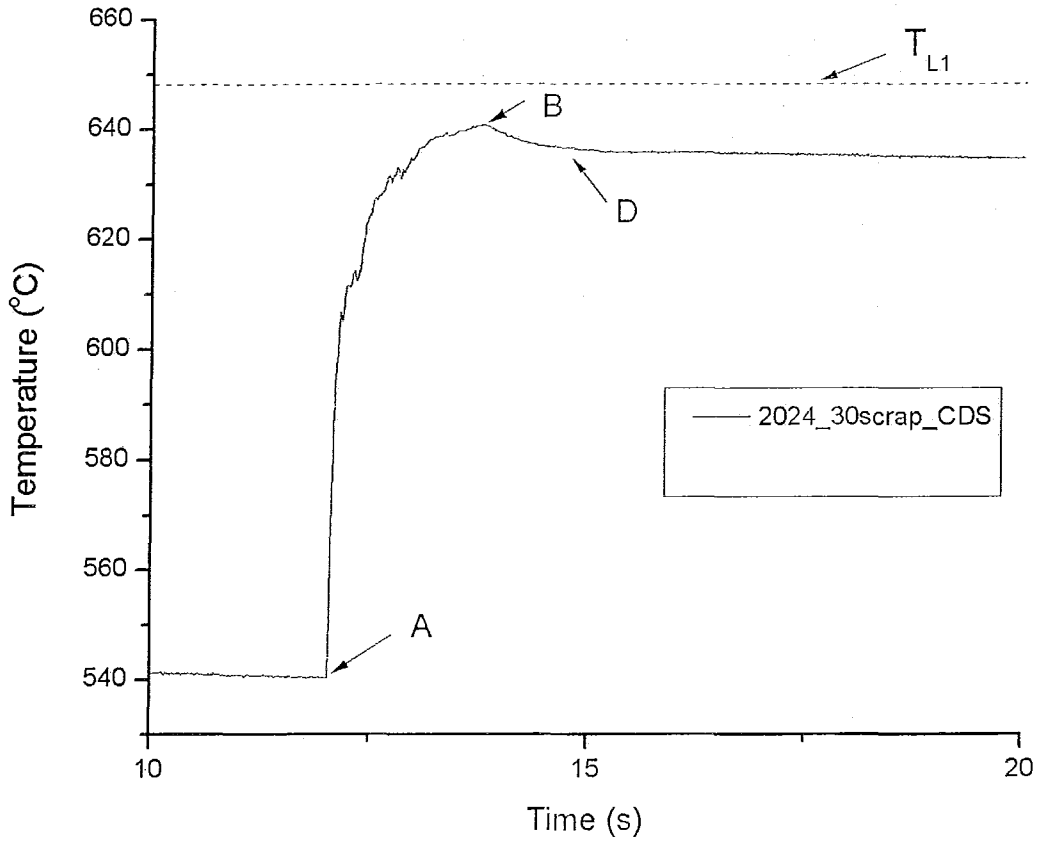

Figure 7-2. **Typical thermal data recorded in the pouring cup during the tilt-pour casting trials of 2024 with CDS technology and 30% scrap recycling scheme (Table 7-1).**

7.2 SUMMARY

Scrap recycling is feasible in the shape casting of Al wrought alloy using the CDS technology. One such recycling scheme was presented in this chapter for casting 2024 Al wrought alloys. There are various other methods to recycle scrap and these may be explored to minimize cost and maximize productivity during commercialization process of this technology.

Chapter 8 Summary of the Project

The following could be summarized from the observations and results in this project:

- A tilt-pour casting setup was successfully designed, manufactured and validated by experiments.
- A new metal mould to enable casting of test bars for as-cast tensile and fatigue property assessments of Al alloys was designed, manufactured and validated by experiments.
- A methodology to enable shape casting of Al wrought alloy using the Controlled Diffusion Solidification (CDS) technology was proposed and validated by sound shape castings of 2024, 6082 and 7075 Al wrought alloys in the tilt-pour casting process.
- The following process parameters were optimized for shape casting three Al wrought alloys: 2024, 6082 and 7075 by CDS process via laboratory and industrial experiments.
    - Pre-cursor alloy compositions.
    - Pre-cursor alloy temperatures.
    - Pre-heat temperatures of mould and pouring cup in the tilt-pour equipment.
    - Tilt-pour process (tilt velocity and filling time).
- The as-cast samples of the three Al alloys were evaluated for cast quality, integrity and ability to heat treat. It was observed that the shape castings of the three Al wrought alloys were sound with good integrity and were heat treatable without the appearance of any discernable defects.
- A viable scrap recycling methodology was proposed and verified by experiments for Al wrought alloys being shape cast with the CDS technology and the 2024 Al alloy was cast for verification.

Chapter 9 Recommendations for Future Work

This project was successful in validating the use of Controlled Diffusions Solidification (CDS) technology in producing near net shaped castings of Al wrought alloys. Although a viable methodology had been proposed to control and optimize certain critical process parameters in CDS, much work is required to enable successful commercial use of this technology in producing high integrity shaped casting. Al wrought alloys in most cases show superior mechanical properties and performances than the cast alloys because of the lower and controlled additions of alloying elements, absence of unwanted alloying elements and the post processing heat treatment and solid-state transformation to obtain near net shaped components. Since, shape casting would not be able to render the component to any further post processing by mechanical operations in solid state, the components can be heat treated and the alloy composition critically controlled to yield superior properties and performance than the Al casting alloys but these properties may not be as good as those in components of Al wrought alloys manufactured by traditional methods. The following areas of research are further encouraged after reviewing the results and observations in this project:

- The time for this project only allowed testing of tensile properties. Fatigue test bars had been cast with the alloys in this project and these could be immediately evaluated for fatigue life and strength under various heat treatment tempers.
- The new metal mould will have to be used to shape cast various Al casting alloys and this mould would have to be standardized by ASTM including the tilt-pour casting parameters that would be used with this mould.
- A new equipment to carry out the controlled mixing of the two pre-cursor alloys is critical to the quality of the cast component.
- The method of mixing the two alloys in CDS will have to critically studied and optimized. There are various possible methods of mixing such as pouring one alloy directly into the other as carried out in this project, mixing one alloy from the bottom of the second alloy, simultaneous mixing of two alloys are respective variable rates and interrupted mixing of two alloys. The mixing method could be optimized by several flow simulations and laboratory experiments.
- CDS technology would have to be validated in casting components in a pressure assisted process such as High Pressure Die Casting (HPDC).
- More alloy compositions for the two pre-cursor alloys would have to explored to attain the most economical and efficient set of pre-cursor alloys.
- This project was aimed at validating the process and hence no special attention was paid to the alloy compositions except that three of the more popular Al wrought alloys were considered as example systems in this project. A thorough and scientific investigation would have to be carried out to design and optimize suitable alloy compositions within each family of Al alloys for shape casting with CDS technology and produce the maximum possible mechanical properties and performances.

- The Al wrought alloys shape cast in this project were heat treated with tempers recommended for these alloys being cast in traditional solid-state transformation processes. These may not be the most appropriate for the microstructure of the shape cast components. An in-depth scientific study would have to be carried out to design and optimize heat treating cycles for the various Al wrought alloys being shape cast by CDS process.

Chapter 10 References

The following are the references used in this thesis manuscript:

1 Canadian Aluminium Transformation Technology Roadmap, 2006 Edition Complete Version, National Research Council Canada and Réseau Trans-Al, Reseau Trans-Al Inc., QC, Canada, 2007.
2 D. Saha, S. Shankar, D. Apelian and M. M. Makhlouf, United States Patent: 7201210.
3 D. Saha, S. Shankar, D. Apelian and M. M. Makhlouf, Metallurgical and Materials Transaction A, July 2004, v.35A, p. 2147.
4 A. Khalaf, P. Ashtari and S. Shankar, Metallurgical and Materials Transaction B, accepted and in-line for print as of July 2009.
5 http://en.wikipedia.org/wiki/Aluminium_alloy.
6 J. Jorstad, High Integrity Die Casting, chapter 3, North American Die Casting Association (NADCA), Rosemont, IL, USA, July 2008.
7 P. Kapranos, http://www.aluplanet.com/documenti/approfondimenti/thixoforming.pdf.
8 S. Chayong, H. V. Atkinson, and P. Kapranos, Material Science and Engineering A, 15 January 2005, v. 390, n.1-2, pp. 3-12.
9 D.G. Eskin, Suyitno, and L. Katgerman, Progress in Materials Science, 2004, v. 49, pp. 629–711.
10 M.C. Flemings: Solidification Processing, Mc Graw Hill, New York, USA 1974.
11 M. Fortier, D.J. Lahaie, M. Bouchard and J. Langlais, Light Metals 2000, eds. J. Kazadi, J. Masounave, Conference of Metallurgists, CASTING AND SOLIDIFICATION I, August 2000, Canadian Institute of Mining, Metallurgy and Petroleum, Montreal, QC, Canada.
12. G. J. Davies, Solidification and Casting, John Wiley & Sons, Canada, 1973.
13 J.G. Kaufman and E.L. Rooy, Aluminium Alloy Castings: Properties, Processes and Applications, ASM International & AFS, Ohio, USA, 2004.
14 NADCA Product Specification Standards for Die Casting Produced by the Semi-Solid and Squeeze Processes, North American Die Casting Assiciation (NADCA), Rosemont, IL, USA, ver. 5, 2009.
15 Ed. A. de Figueredo , Science and Technology of Semi-Solid Metal Processing, (North American Die Casting Association (NADCA), Rosemont, IL, USA, 2001,.
16 D.B. Spencer, R. Mehrabian, and M.C. Flemings, Metallurgical Transaction, July 1972, vol. 3, p.1925.
17 D. Apelian, Worcester Polytechnic Institute (WPI), Worcester, MA, USA, personal communications.
18 H.V. Atkinson, Progress in Materials Science, 2005, v. 50, pp. 341-412.
19 Z .Fan ,X. Fang, S. Ji, Material science and Engineering, A 412, (2005) 298-306.

20 A. Khalaf, P. Ashtari and S. Shankar, Shaped Casting:The 3rd International Symposium, Ed. J. Campbell, P. N. Crepeau, M. Tiryakioglu, TMS (The Minerals, Metals and Materials Society), Warrendale, PA, USA, 2009, pp. 215-222.
21 S. Shankar, D. Saha, M. M.Makhlouf, D. Apelian, , Die Casting Engineer , v.48, n.2, March 2004, pp. 52-57
22 B.K.Dhindaw et al., Materials Science and Engineering A, 2005, v. 413-414, pp. 156-164.
23 J. E. Grusleski, B. M. Closset, Treatment of Liquid Aluminium Alloys, American Foundrymen Socirty (AFS), Des Plaines, IL, USA, 1990, p. 76.
24. P. Ashtari, G. Birsan and S. Shankar, Shaped Casting:The 3rd International Symposium, Ed. J. Campbell, P. N. Crepeau, M. Tiryakioglu, TMS (The Minerals, Metals and Materials Society), Warrendale, PA, USA, 2009, pp. 223-230.
25. M. Cabibbo, E. Evangelista, S Spigarelli and E. Cerri, Materials Technology, 2001, v. 35(1-2), n.9,pp. 9-16.
26. L.B. Ber, Materials Science and Engineering A, 2000, v.280, pp. 91–96.